

A STOCHASTIC APPROACH TO THE SIMULATION OF  
BLOCK CONDUCTIVITY FIELDS CONDITIONED UPON  
DATA MEASURED AT A SMALLER SCALE

A DISSERTATION  
SUBMITTED TO THE DEPARTMENT OF APPLIED EARTH SCIENCES  
AND THE COMMITTEE ON GRADUATE STUDIES  
OF STANFORD UNIVERSITY  
IN PARTIAL FULFILLMENT OF THE REQUIREMENTS  
FOR THE DEGREE OF  
DOCTOR OF PHILOSOPHY

By  
José Jaime Gómez Hernández  
March 1991



© Copyright 1991 by José Jaime Gómez Hernández  
All Rights Reserved



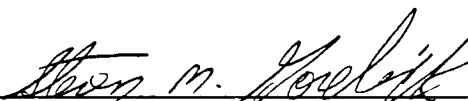
I certify that I have read this thesis and that in my opinion it is fully adequate, in scope and in quality, as a dissertation for the degree of Doctor of Philosophy.



---

André G. Journal  
(Principal Adviser)

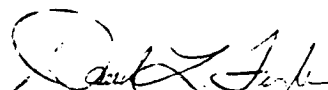
I certify that I have read this thesis and that in my opinion it is fully adequate, in scope and in quality, as a dissertation for the degree of Doctor of Philosophy.



---

Steven M. Gorelick

I certify that I have read this thesis and that in my opinion it is fully adequate, in scope and in quality, as a dissertation for the degree of Doctor of Philosophy.



---

David L. Freyberg  
(Department of Civil Engineering)

Approved for the University Committee on Graduate Studies:

---

Dean of Graduate Studies



*A Inma y Elisa*





# Abstract

Two methods are proposed for the direct generation of block conductivities conditioned upon data measured at a smaller scale. These methods allow Monte-Carlo analyses of aquifer response variables up to 125 times faster than more traditional methods that do not directly generate block conductivities. The first method is analytical, and is limited to two dimensional spaces with small, isotropic variability of the logarithms of hydraulic conductivity and uniform flow in unbounded aquifers. The second method is numerical, and is not restricted by the previous conditions although it is limited to a finite-difference formulation of the groundwater flow equation with blocks of a single size. Both methods call for efficient stochastic conditional simulation algorithms and for accurate methods to scale-up hydraulic conductivities. Regarding conditional simulations, the novel sequential simulation algorithm was fully implemented for the first time for the generation of both Gaussian and non-Gaussian random fields, with direct conditioning to local data. This algorithm was also applied for the first time to the co-simulation of several variables with a joint Gaussian multivariate distribution. Regarding the scaling-up problem, two approaches are proposed, an analytical one under the same aforementioned assumptions and a numerical one not limited by these assumptions. The methodology proposed is applied to a Monte-Carlo analysis of flows in a synthetic aquifer. The results are compared to a reference Monte-Carlo analysis implemented at the smallest scale. In addition, these results are compared with those obtained from the more traditional approach, consisting of generating conductivity fields at the small scale and then scaling-up each block using a within-block flow simulation. The reproduction of the results obtained from the

reference analysis at the smallest scale is shown to be good, with the proposed technique being much faster CPU-wise than either the reference analysis or the traditional methods.

# Acknowledgments

I want to thank my advisor André G. Journel for his guidance and encouragement during these years at Stanford. Without his contagious enthusiasm I would have not entered into Geostatistics. Thanks also to the members of my dissertation committee: professor Steven M. Gorelick, with whom I got my first publication in a major journal and who, so patiently, coached me for my first oral presentation in English; and professor David L. Freyberg who guided me during my first year at Stanford as a Ms. student. Special thanks go to professor Irwin Remson who accepted me to his program some five years ago. Thanks to Yoram Rubin and François Alabert, and again to André Journel, for the enlightening brainstorming sessions from which developed some of the ideas presented in this dissertation. Finally, I also would like to thank Clayton Deutsch for reviewing early drafts of this dissertation and Ana Gómez for spending her summer holidays doing secretarial work for me and helping with the design of the graphics. Financial support was received from the Department of Applied Earth Sciences and the Stanford Center for Reservoir Forecasting (SCRF).



# Contents

<b>Abstract</b>	<b>v</b>
<b>Acknowledgments</b>	<b>vii</b>
<b>1 Introduction</b>	<b>1</b>
1.1 Motivation . . . . .	1
1.2 Dissertation Preview . . . . .	6
<b>2 Literature Review</b>	<b>7</b>
2.1 Stochastic Simulation of Random Fields . . . . .	7
2.2 Block Hydraulic Conductivities . . . . .	12
Effective Hydraulic Conductivity . . . . .	15
Block Hydraulic Conductivity . . . . .	20
2.3 Direct Generation of Block Values . . . . .	32
<b>3 Sequential Simulation</b>	<b>35</b>
3.1 Theory . . . . .	36
General Concepts . . . . .	36
Simulation . . . . .	40
Sequential Unconditional Simulation . . . . .	41
Conditional Simulation . . . . .	43
3.2 Conditional Probabilities . . . . .	44
MultiGaussian Random Functions . . . . .	44

Non-Gaussian Random Functions . . . . .	45
Jointly MultiGaussian Random Functions . . . . .	48
3.3 Implementation . . . . .	50
Markov Paradigm . . . . .	50
Visiting Sequence . . . . .	53
Order Relation Violations . . . . .	53
Programming . . . . .	53
3.4 Advantages of Sequential Simulation . . . . .	59
3.5 Programs . . . . .	60
<b>4 Block Hydraulic Conductivity</b>	<b>61</b>
4.1 Statement of the Problem . . . . .	62
4.2 Analytical approach . . . . .	63
Necessary Assumptions . . . . .	63
Development . . . . .	64
4.3 Numerical Approach . . . . .	67
Starting Point . . . . .	68
Demonstration For Synthetic Aquifers . . . . .	82
Statistically Isotropic Hydraulic Conductivities . . . . .	87
Bimodal Aquifer Hydraulic Conductivities . . . . .	90
Statistically Anisotropic Aquifer Hydraulic Conductivities . . . . .	94
Statistically Anisotropic Aquifer Hydraulic Conductivities (2nd ex.) .	100
Discussion . . . . .	100
<b>5 Direct Generation of <math>K_V</math></b>	<b>107</b>
5.1 The Principle . . . . .	109
5.2 Analytical Approach . . . . .	111
Discussion . . . . .	119
5.3 Numerical Approach . . . . .	120
An Example . . . . .	121
Validation . . . . .	131
Discussion . . . . .	139

<b>6</b>	<b>Conclusions</b>	<b>141</b>
6.1	Suggestions for Further Research . . . . .	144
	Generation of Random Fields . . . . .	144
	Stochastic Modeling of Block $K_V$ . . . . .	147
<b>A</b>	<b>Sequential Simulation Programs</b>	<b>148</b>
A.1	GSIM3D and GCOSIM3D . . . . .	148
A.2	ISIM3D . . . . .	227
<b>B</b>	<b>Finite Differences Code</b>	<b>319</b>
B.1	Numerical formulation . . . . .	319
B.2	Computer code . . . . .	323
B.3	Example input files . . . . .	335
<b>C</b>	<b>Least Squares Formulation</b>	<b>338</b>
	<b>Bibliography</b>	<b>340</b>

# List of Tables

5.1	Conditioning data for Monte-Carlo analysis . . . . .	131
5.2	CPU times . . . . .	139



# List of Figures

1.1	Three Monte-Carlo approaches . . . . .	3
2.1	Discretization of a one-dimensional aquifer . . . . .	13
2.2	Spatial variability of hydraulic conductivity . . . . .	13
2.3	A set of typical boundary conditions . . . . .	25
2.4	Another set of boundary conditions . . . . .	29
3.1	Within-class cdf models . . . . .	47
3.2	Search neighborhood . . . . .	52
4.1	Macroscale discretization . . . . .	68
4.2	Megascale discretization . . . . .	69
4.3	Megahead . . . . .	70
4.4	Megaflow . . . . .	71
4.5	Finite differences discretization . . . . .	73
4.6	Interblock . . . . .	75
4.7	One block from two aquifers . . . . .	78
4.8	Approximate boundary conditions . . . . .	80
4.9	Computing the interface conductivity . . . . .	81
4.10	Field boundary conditions . . . . .	84
4.11	Boundary conditions used in the proposed method . . . . .	85
4.12	Cross-sections for the global comparison . . . . .	86
4.13	A realization of log-hydraulic conductivities (isotropic covariance) . .	88
4.14	Isotropic lognormal aquifer: Local flow comparison . . . . .	91

4.15	Isotropic lognormal aquifer: Total flow comparison . . . . .	92
4.16	Sand/shale aquifer . . . . .	93
4.17	Sand/shale aquifer: Local flow comparison . . . . .	95
4.18	Sand/shale aquifer: Total flow comparison . . . . .	96
4.19	Measuring the impact that one shale may have in determining the block conductivity . . . . .	97
4.20	An aquifer in which the traditional approach cannot be used . . . . .	98
4.21	Anisotropic lognormal aquifer . . . . .	99
4.22	Anisotropic lognormal aquifer: Local flow comparison . . . . .	101
4.23	Anisotropic lognormal aquifer: Total flow comparison . . . . .	102
4.24	Anisotropic lognormal aquifer (2nd ex.) . . . . .	103
4.25	Anisotropic lognormal aquifer (2nd ex.): Local flow comparison . . .	104
4.26	Anisotropic covariance (2nd ex.): Total flow comparison . . . . .	105
5.1	Typical Monte-Carlo analysis of aquifer responses . . . . .	108
5.2	Proposed Monte-Carlo analysis of aquifer responses . . . . .	110
5.3	Expected value of the block conductivity for different variances of point conductivity . . . . .	115
5.4	Expected value of the block conductivity for different variances of point conductivity . . . . .	116
5.5	Variance of the block conductivity for different variances of point con- ductivity . . . . .	117
5.6	Variance of the block conductivity for different variances of point con- ductivity . . . . .	118
5.7	Inferring the statistical model for interface conductivities . . . . .	121
5.8	Macroscale unconditional realization of standardized log-conductivities used to build a training image of interface conductivities . . . . .	123
5.9	Training image for the horizontal interface log-conductivities . . . . .	125
5.10	Training image for the vertical interface log-conductivities . . . . .	126
5.11	Normal and lognormal probability plots of the interface conductivities $K_{V,xx}$ . . . . .	127

5.12	Normal and lognormal probability plots of the interface conductivities	
	$K_{V,yy}$ . . . . .	128
5.13	Input parameters for the co-simulation of interface conductivities . .	129
5.14	Input parameters for the co-simulation of interface conductivities . .	130
5.15	Conditioning data . . . . .	132
5.16	Monte-Carlo analysis of horizontal flows . . . . .	135
5.16	Monte-Carlo analysis of horizontal flows (cont.) . . . . .	136
5.17	Monte-Carlo analysis of vertical flows . . . . .	137
5.17	Monte-Carlo analysis of vertical flows (cont.) . . . . .	138
6.1	Three Monte-Carlo approaches . . . . .	142
B.1	Finite differences discretization . . . . .	320



# Chapter 1

## Introduction

### 1.1 Motivation

The reader may ask: “What is the motivation for stochastic modeling of block conductivities conditioned upon measurements at a smaller scale?”; or more fundamentally: “Why should modeling such conductivities be done in a stochastic framework?”, “Why block conductivities?”, and “Why distinguish between different scales?” This section tries to answer such questions.

An ideal Monte-Carlo analysis of groundwater flow response variables would proceed as depicted in the first row of Fig. 1.1: 1a) data are collected and analyzed; 1b) multiple, equiprobable hydraulic conductivity fields are generated at the measurement scale and conditioned to the data, 1c) groundwater flow is simulated in each field and 1d) a frequency distribution of the response variable is built. Because the discretization of the aquifer at the scale of the measurements generally requires millions of small blocks, repeated simulation of groundwater flow at that scale is impossible at present time. An alternative and feasible Monte-Carlo analysis is depicted in the second row of Fig. 1.1. This Monte-Carlo analysis uses a scaling-up procedure to transform the conductivity values generated at the measurement scale (2b) into

block conductivities at a scale that can be easily handled by current numerical simulators (2c); groundwater flow is then simulated at that scale (2d) and a frequency distribution of the response variable is built (2d). Although feasible, this approach is still too expensive to be used systematically: the generation of multiple hydraulic conductivity fields at the measurement scale, the scaling-up of each individual block and the final simulation of groundwater flow are, all three, expensive steps. A third approach, which is proposed in this dissertation is depicted in the third row of Fig. 1.1. This approach combines steps 2b) and 2c) into a single step, that is, instead of generating conductivity fields at the measurement scale that are going to be averaged later, it is proposed to generate directly the conductivity fields at the numerical simulator gridblock scale conditioned to the data. Step 3b) is the novelty of this approach and requires the integration of geostatistical and scaling-up techniques. This dissertation gradually proceeds towards this integration; it starts with the revision and extension of geostatistical techniques for the generation of random fields; it continues with the development of a new technique for scaling-up conductivities; and it concludes with the merging of geostatistics and the proposed scale-up procedure into a procedure that allows the direct generation of block conductivities conditioned upon data measured at a smaller scale.

The reason why Monte-Carlo analyses are needed is because stochastic modeling of conductivities is necessary. As Freeze (1975) points out, and as was corroborated later by Smith (1981), Hoeksema and Kitanidis (1985a) and Sudicky (1986) field data indicate that hydraulic conductivity most often varies in space in a non-deterministic, unpredictable manner. Because hydraulic conductivity cannot be predicted accurately at unsampled locations, each time a value of hydraulic conductivity is assigned to an element of a numerical model, there is some uncertainty involved. The uncertainty associated with these conductivity values causes uncertainty of the aquifer response variables; namely, hydraulic heads and specific discharges.

One way to model the uncertainty of hydraulic conductivities and its consequent impact on the response variables is by considering hydraulic conductivities as a random function, thus adopting a stochastic approach. From a physical point of view,

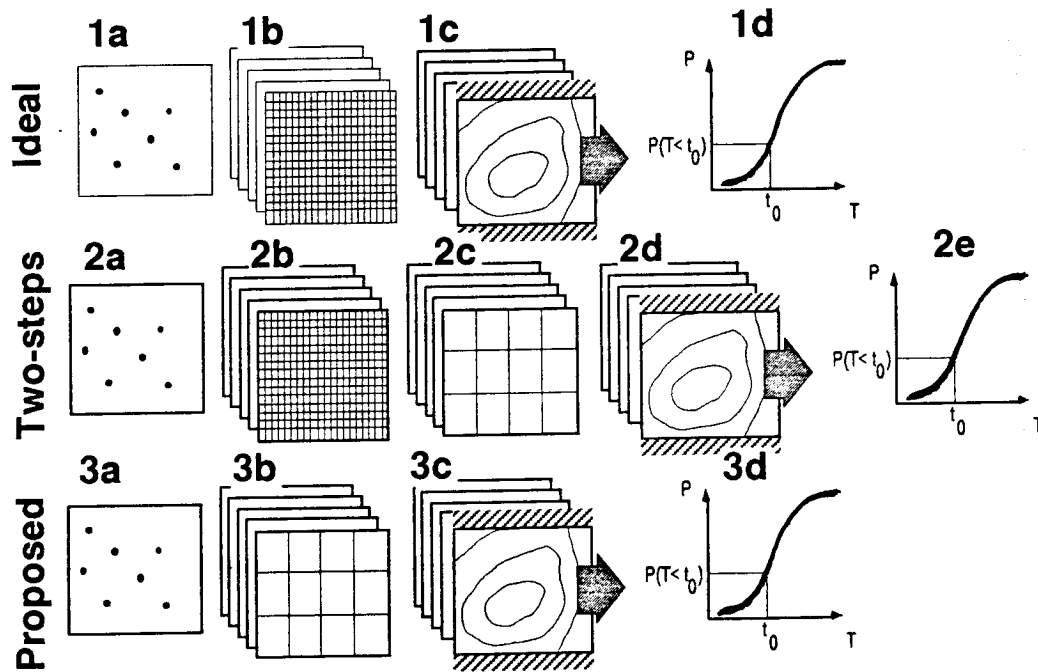


Figure 1.1: **Three Monte-Carlo approaches.** 1) An ideal approach: fields of hydraulic conductivities are generated at the measurement scale (1b) conditioned to the data (1a), groundwater flow is simulated at that scale (1c) and a frequency distribution of the response variables is built (1d). 2) A two-steps approach: fields of hydraulic conductivities are generated at the measurement scale (2b) conditioned to the data (2a), hydraulic conductivity values are scaled-up so that the number of resulting gridblocks can be easily handled by current numerical simulators (2c), groundwater flow is simulated at the gridblock scale (2d) and a frequency distribution of the response variable is built (2e). 3) Proposed approach: fields of hydraulic conductivities are directly generated at the gridblock scale (3b) conditioned to data measured at a smaller scale (3a), groundwater flow is simulated at the gridblock scale (3c) and a frequency distribution of the response variable is built (3d)

the stochastic approach amounts to considering the real aquifer as one of many possible aquifers, all of them honoring the same available data. From the point of view of the modeler, all these aquifers are equally plausible and any one of them could be the real one. However, our inability to discern which one is the real one, forces us to study the entire set of possible aquifers. The statistical analysis of the set of solutions generated by this ensemble of aquifers provides a measure of uncertainty on the response variables.

This statistical analysis can be carried out through a Monte-Carlo approach. Or, it can be done under restrictive conditions by solving, analytically, the stochastic partial differential equation describing steady state saturated flow in porous media

$$\nabla \cdot (\mathbf{K} \nabla h) = 0,$$

where both the hydraulic conductivity ( $\mathbf{K}$ ), and the hydraulic head ( $h$ ) are considered random functions.

Analytical solutions to the stochastic partial differential equation have been obtained for specific multivariate distributions of  $\mathbf{K}$  and for a few geometries and boundary conditions (Matheron, 1967; Gelhar, 1974; Gelhar et al., 1977; Bakr et al., 1978; Gutjahr et al., 1978; Dagan, 1979; Chirlin and Dagan, 1980; Dagan, 1981; Gutjahr and Gelhar, 1981; Mizell et al., 1982; Dagan, 1982a; Dagan, 1982b; Gelhar and Axness, 1983; Dagan, 1985; Naff and Vecchia, 1986; King, 1987; Rubin and Dagan, 1987a; Rubin and Dagan, 1987b; Naff and Vecchia, 1987; Ababou et al., 1988; Dagan and Rubin, 1988; Rubin and Dagan, 1988; Poley, 1988; Rubin and Dagan, 1989; Dagan, 1989). These analytical solutions are limited to the expected value and the two-point covariance (or variogram) of the hydraulic heads; they fall short providing the actual probability distribution of the response variables. In addition, their practical applicability is limited for the following reasons: i) they correspond to very specific geometric configurations; most relate to either unbounded domains, or bounded domains with very simple geometries; ii) most of the analytical solutions are based on perturbation theory and therefore their applicability is limited to small variability of  $\mathbf{K}$  (or of its logarithm); and iii) most of the solutions do not honor local data at their



locations. For these reasons this dissertation adopts the more flexible Monte-Carlo approach.

Monte-Carlo methods have been used in the past with the same objective of quantifying uncertainty of aquifer response variables (Warren and Price, 1961; Freeze, 1975; Delhomme, 1979; Smith and Freeze, 1979a; Smith and Freeze, 1979b; Clifton and Neuman, 1982; El-Kadi and Brutsaert, 1985; Desbarats, 1987a; Desbarats, 1987b; Deutsch, 1987; White, 1987; White and Horne, 1987; Desbarats, 1988; Gómez-Hernández and Gorelick, 1988; Desbarats, 1989; Deutsch, 1989; Gómez-Hernández and Gorelick, 1989; Wagner and Gorelick, 1989). However, none of these studies accounts for the important problem of scales (Lasseter et al., 1986; Haldorsen, 1986; Dagan, 1986; Dagan, 1989). Field data are available at different scales, but infrequently at the scale of the blocks used to discretize the field prior to numerical flow simulations. Haldorsen (1986) discusses this scale problem in detail. Data from a core-plug are representative of volumes that are several billion times smaller than the volume represented by a pumping test. In between these two extremes there are whole core measurements, sonic logs and slug tests, all of which are representative of intermediate volumes. A typical block used in a flow simulator will be much larger than the volume of any field measurement and the variability observed at the data scale needs not prevail at another. Therefore, there is a need for an averaging procedure that converts information from one scale to the next. This need, in turn, brings us to the problem of block conductivities.

Since, in general, there are no measurements of block conductivities as required by the numerical flow simulators, their spatial variability cannot be characterized directly from data. This thesis proposes to use the statistics of the spatial variability of conductivity at the data scale—say, whole-core samples—to derive that of the block values. To link both scales a two-steps approach is proposed, first, a computer algorithm is built to generate block values conditioned on, say, the whole-core measurements taken within and around it, and second, a statistical model is established for the relationship between these block conductivities and the whole-core measurements. Alternatively, a statistical model of block versus point conductivities is obtained analytically under some restrictive conditions.

Once such statistical model is obtained, the stochastic generation of block conductivity values conditioned upon data measured at a smaller scale is possible.

## 1.2 Dissertation Preview

This dissertation is organized as follows. Chapter 2 presents a literature review on relevant work on conditional simulations, block conductivity modeling and the scaling-up of conductivity values. Chapter 3 recalls the theory of sequential stochastic simulation, proceeding with specific implementation algorithms for univariate multiGaussian random fields, random fields with a generic bivariate distribution, and multivariate multiGaussian random fields. Chapter 4 addresses the problem of computing block hydraulic conductivities for heterogeneous blocks sampled exhaustively at a smaller scale. Two methods are proposed. The first method is analytical in nature, and limited to two-dimensional space with small, isotropic variability of the logarithms of hydraulic conductivity. The second method is numerical; it is developed in two dimensions, but can be straightforwardly extended to three, and is not limited to small variability of the hydraulic conductivities. Chapter 5 combines the results of chapters 3 and 4 and proposes two new methods for the stochastic generation of block conductivities. The first is based on the analytical derivations of chapter 4 and provides a closed-form expression for the expected value and covariance of block conductivities under some limiting assumptions. The second method follows the numerical approach adopted in chapter 4 to generate synthetic block conductivity fields from which expected values and covariances can be inferred. Once statistical models are available, stochastic generation of synthetic block conductivity fields can be performed using the sequential simulation algorithms developed in chapter 3 (i.e., block conductivities can be directly generated conditioned upon data at a smaller scale). Chapter 6 recalls the limitations of the various methods proposed, and concludes with recommendations for further research.

# Chapter 2

## Literature Review

This chapter presents a literature review on the three theoretical problems involved in a Monte-Carlo analysis of aquifer responses as described in Fig. 1.1: (1) the stochastic simulation of random functions conditioned to local data, (2) the scaling-up of conductivities into equivalent block values, and (3) the stochastic modeling of the spatial variability of such block values.

### 2.1 Stochastic Simulation of Random Fields

A random field or random function  $Z(\mathbf{x})$ , can be seen as a set of random variables, one for each location  $\mathbf{x}$  within a domain  $\mathcal{D}$  of definition. A random function is characterized by the  $n$ -variate joint probability distributions of all possible  $n$ -tuples,  $\{Z(\mathbf{x}_i), \mathbf{x}_i \in \mathcal{D}, i = 1 \dots n\}$ , with any  $n = 1 \dots \infty$  (Papoulis, 1986). The realizations of a random function are spatial functions  $z(\mathbf{x})$ . The collection of all possible realizations is called the ensemble.

It is important to distinguish between unconditional and conditional realizations. Conditional realizations are those functions  $z(\mathbf{x})$  that take fixed values at specific locations. The set of all conditional realizations for a given set of conditioning points is a subensemble of the larger ensemble of unconditional realizations. We will refer to

any technique that allows one to draw a realization **at random** from the ensemble of possible realizations as a stochastic simulation technique. If the drawing is done from the ensemble of unconditional realizations, we will call it an unconditional simulation technique. If, on the other hand, the drawing is done from the subensemble of conditional realizations, we will call it a conditional simulation technique.

From a practical point of view, conditional simulation techniques are more useful than unconditional ones since there are always data available that we want to honor in some sense. For this reason, this section of the literature review concentrates only on conditional simulation techniques.

There are two basic approaches for the generation of conditional realizations: an indirect approach and a direct one. The indirect approach to conditional simulation is a two-steps process. First, an unconditional realization is generated, and second, it is modified to honor the data at their locations. The procedure described by Journel (1974) and summarized below takes advantage of the fact that kriging errors are uncorrelated with kriging estimates.

Let  $z(\mathbf{x})$  denote a realization conditional to the set of  $n$  data  $\{z(x_1), z(x_2), \dots, z(x_n); x_i \in \mathcal{D}, i = 1, \dots, n\}$ . Let  $z_{SK}^*(\mathbf{x})$  be the field obtained by interpolation of the data using simple kriging (Journel and Huijbregts, 1978, p. 561). Any realization  $z(\mathbf{x})$  can be expressed as the sum of the kriging estimate  $z_{SK}^*(\mathbf{x})$  and the kriging error:

$$z(\mathbf{x}) = z_{SK}^*(\mathbf{x}) + \underbrace{(z(\mathbf{x}) - z_{SK}^*(\mathbf{x}))}_{\text{kriging error}}$$

It can be shown that the expected value through all possible realizations of the product  $Z_{SK}^*(\mathbf{x})(Z(\mathbf{x}) - Z_{SK}^*(\mathbf{x}))$  is zero. This means that the kriging errors and the kriging estimates are orthogonal (uncorrelated). Taking advantage of this result, a conditional simulation ( $z_C$ ) can be generated by replacing the actual unknown kriging error by a simulated kriging error. This simulated error is obtained by applying the same kriging and data configuration pattern to any unconditional realization ( $z_U$ ):

$$z_C(\mathbf{x}) = z_{SK}^*(\mathbf{x}) + (z_U(\mathbf{x}) - z_{U,SK}^*(\mathbf{x}))$$

where  $z_{U,SK}^*$  is the kriging estimate of  $z_U$  using for data the values of  $z_U$  at the same locations as the original data used to obtain  $z_{SK}^*$ .

The steps to obtain a conditional simulation are:

1. Obtain the simple kriging estimate  $z_{SK}^*$  using the original data.
2. Generate an unconditional realization  $z_U(\mathbf{x})$
3. Obtain  $z_{U,SK}^*$  which is the kriging estimate of  $z_U$  using for data the values of  $z_U$  at the same locations as the data used to obtain  $z_{SK}^*$ .
4. Add the kriging errors  $z_U - z_{U,SK}^*$  from the unconditional realization to the kriging estimates  $z_{SK}^*$

The last three steps are repeated for the generation of multiple realizations conditioned to the same data values.

There are many methods for the generation of unconditional simulations (Matern, 1960; Shinozuka and Jan, 1972; Matheron, 1973; Journel, 1974; Journel and Huijbregts, 1978; Journel, 1979; Smith and Freeze, 1979a; Smith and Freeze, 1979b; Mantoglou and Wilson, 1981; Mantoglou and Wilson, 1982; Dagan, 1982a; Clifton and Neuman, 1982; Borgman et al., 1984; Luster, 1985; Brooker, 1985; Mantoglou, 1987; Thompson et al., 1989; Black and Freyberg, 1990). The most efficient algorithm for the simulation of realizations over a very large number of nodes is the turning band method (Matheron, 1973; Journel 1974). It reduces the generation of a two- or three-dimensional realization to the generation of a few one-dimensional realizations that later are combined to provide a 2- or 3-D realization with the correct statistical description. Unfortunately, as with all other methods, it generates realizations from multiGaussian random fields. In addition, the turning band technique tends to generate artifact banding over the realizations.

The major drawback of indirect techniques is the large expense incurred in the conditioning step. The conditioning step amounts to solving a simple kriging system of linear equations for each node in the realization. In most cases, this step is more time-consuming than the already expensive generation of the unconditional realization. Another drawback of indirect methods is that, in the conditioning step, the

substitution of simulated kriging errors for the unknown, actual kriging errors calls for multiGaussianity of the random function model ( $Z(\mathbf{x})$ ); for then, orthogonality between kriging estimates and kriging errors also implies independence.

The direct approach draws the realization directly from the sub-ensemble of conditional realizations. This approach is almost always faster than the indirect approach, at least for Gaussian realizations, because it does not require the expensive kriging step for conditioning. However, and up until the introduction of the sequential simulation algorithm, which is the subject of chapter 3, the only method available for direct generation of conditional simulations was limited to grids of only a few hundred nodes and to realizations from multiGaussian random fields.

A method for the direct generation of Gaussian conditional simulations was suggested by Dagan (1982b) and applied by Neuman and his co-workers to the generation of hydraulic conductivity fields in the Avra valley (Clifton and Neuman, 1982). This method is an extension of the well-known Cholesky decomposition of covariance matrices as used for generating realizations of Gaussian fields (Anderson, 1984). Dagan's contribution is the use of both the conditional covariance matrix and the conditional expectations. This method is referred hereafter as the matricial method. A brief review of it follows.

The problem is to generate a conditional realization of a Gaussian random function  $Z(\mathbf{x})$  over  $N$  nodes. Let  $\mathbf{C}$  be the conditional covariance matrix of the random function, with element  $c_{ij}$  being the covariance between nodes  $x_i$  and  $x_j$  **conditional to the data**. The Cholesky decomposition of  $\mathbf{C}$  in the product of upper and lower triangular matrices is:

$$\mathbf{C} = \mathbf{B} \mathbf{B}^T$$

It can be shown, that the vector

$$\mathbf{z} = \bar{\mathbf{z}}_C + \mathbf{B} \mathbf{u}$$

where  $\bar{\mathbf{z}}_C$  is the conditional expectation of the random field at the  $N$  nodes and  $\mathbf{u}$  is a vector of uncorrelated random numbers with zero mean and unit variance, is a conditional realization of the random field.

In order to apply the matricial method, knowledge of the conditional mean and the conditional covariance is required. If the random field is multiGaussian, the conditional mean and the conditional covariance are given by the solution of a set of normal equations (Luenberger, 1969). Also, the conditional mean and covariance obtained from the solution of the normal equations are the simple kriging estimate and the simple kriging variance commonly used in geostatistics (Journel and Huijbregts, 1978, p.566).

A numerical algorithm that uses the matricial approach was developed by Davis (1987) and applied by Alabert (1987a) to the simulation of soil lead concentration near a smelter in Dallas, Texas. This algorithm is very efficient for the generation of large numbers of small realizations. The conditional mean and the conditional covariance matrix are obtained implicitly rather than through an explicit simple kriging, then the covariance matrix is Cholesky-decomposed, and finally, the generation of multiple realizations is reduced to a series of matrix multiplications, one for each realization. The method can be applied to the generation of conditional simulations over either a regular or an irregular grid, but is limited to a few hundred nodes, because it requires the storage and manipulation of a covariance matrix with as many elements as the square of the number  $N$  of nodes.

The two drawbacks of the matricial method are that it cannot be used for the generation of very large realizations, and that it can only generate realizations from multiGaussian random fields.

Another algorithm for the direct generation of conditional realizations is the sequential simulation proposed by Journel (1985). This technique is based on the recursive application of Bayes' theorem and the assumption of some Markovian properties of the random field. It is described with more detail in chapter 3. The single most important feature of this technique is that it is not limited to the generation of realizations from multiGaussian fields. A second important feature is that it is the fastest technique for conditional simulations of multiGaussian fields over a large number of nodes. As will be explained in chapter 3, Gaussian sequential simulation calls for one single simple kriging at each node being simulated, whereas any indirect method,

as explained earlier, requires one such kriging **in addition** to a prior unconditional simulation.

Sequential simulation was first applied within the framework of indicator functions by Journel and Alabert to generate realizations of a random function with a generic bivariate distribution (Alabert, 1987b; Journel and Alabert, 1988; Journel and Alabert, 1989; Journel and Alabert, 1990). It has been applied also to the generation of realizations from binary random fields not necessarily Gaussian-related (Journel and Gómez-Hernández, 1989a; Gómez-Hernández, 1989; Gómez-Hernández, 1990b; Gómez-Hernández, 1991), and recently to the generation of realizations from multiGaussian random fields (Journel and Gómez-Hernández, 1989b; Isaaks, 1990).

In this dissertation, the sequential simulation technique is applied for the first time to the joint generation of realizations from several random fields which are jointly multiGaussian.

## 2.2 Block Hydraulic Conductivities

To illustrate the problem of block conductivities, consider the groundwater flow equation in one-dimension:

$$\frac{d}{dx} \left( K \frac{dh}{dx} \right) = 0$$

where the hydraulic conductivity tensor degenerates into the scalar  $K$ .

Consider a one-dimensional aquifer discretized into elements of length  $\Delta x$ , as shown in Fig. 2.1. A simple finite difference expression for the hydraulic head at node  $i$  is given by

$$\frac{1}{\Delta x} \left( K_{i+1/2} \frac{h_{i+1} - h_i}{\Delta x} - K_{i-1/2} \frac{h_i - h_{i-1}}{\Delta x} \right) = 0$$

This expression requires values of the hydraulic conductivity between the nodes (i.e., at locations  $K_{i+1/2}$  and  $K_{i-1/2}$ ). If  $K$  is not constant and displays the kind of variability typically encountered in field data (Fig. 2.2), it is unclear which  $K$  value should be assigned to  $K_{i+1/2}$  and which to  $K_{i-1/2}$ . In one-dimensional flow, the



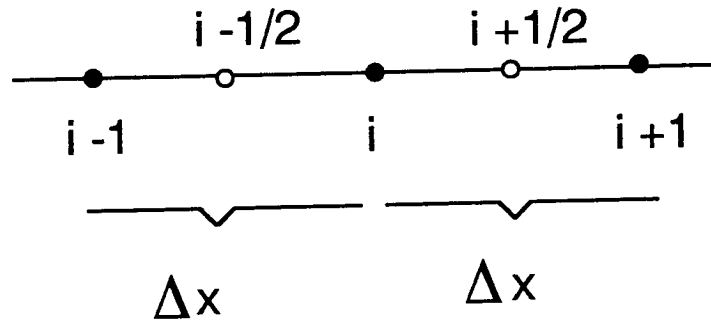


Figure 2.1: Discretization of a one-dimensional aquifer.

hydraulic conductivity value that preserves flows for a given hydraulic head gradient is given by the harmonic mean of the hydraulic conductivities within the nodes (Freeze and Cherry, 1978):

$$K_{i-1/2} = \left( \int_{x=i-1}^{x=i} \frac{dx}{K(x)} \right)^{-1} \quad (2.1)$$

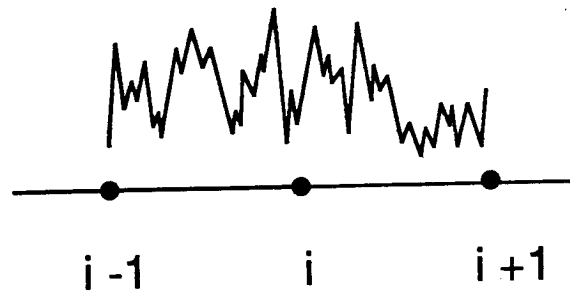


Figure 2.2: **Spatial variability of hydraulic conductivity.** A schematic cross-section displaying the typical kind of spatial variability in hydraulic conductivity

The problem of obtaining equivalent block hydraulic conductivity values is more acute for flow in two and three dimensions because a closed-form expression for the

block conductivity such as (2.1) has been found only for some very specific spatial configurations of the  $\mathbf{K}^1$  values and for relatively large blocks.

The problem of obtaining block conductivities is sometimes mistaken for the problem of obtaining effective conductivities. A block conductivity is an average, in some sense, of the spatial variability of hydraulic conductivity within the block, whereas effective conductivity is a characteristic parameter of the random function used to model  $\mathbf{K}$ .

After solving for flow within a heterogeneous block  $V$  for given boundary conditions, block conductivity can be defined as the conductivity  $\mathbf{K}_V$  of a homogeneous block satisfying

$$\frac{1}{V} \int_V \mathbf{q} dV = -\mathbf{K}_V \frac{1}{V} \int_V \nabla h dV \quad (2.2)$$

where  $\mathbf{q}$  and  $\nabla h$  are the specific discharge and piezometric head gradient, respectively, solution of the flow problem within the heterogeneous block. The block value  $\mathbf{K}_V$  is a tensor relating the spatial average of flow to the spatial average of the hydraulic head gradient. It is a function of both the conductivity values within the block and the boundary conditions.

Effective permeability is defined in terms of the random function used to model the uncertainty of  $\mathbf{K}$ . The most common definition is:

$$E\{\mathbf{q}(\mathbf{x})\} = -\mathbf{K}_{\text{eff}}(\mathbf{x})E\{\nabla h(\mathbf{x})\} \quad (2.3)$$

where the operator  $E\{\cdot\}$  means expected value through the ensemble of realizations and  $\mathbf{K}_{\text{eff}}$  is the effective hydraulic conductivity tensor. In theory  $\mathbf{K}_{\text{eff}}$  would vary with  $\mathbf{x}$ , although, in practice, the random functions chosen for  $\mathbf{K}$  have statistical properties that ensure that the expected values of  $\mathbf{q}$  and  $\nabla h$ , and consequently of  $\mathbf{K}_{\text{eff}}$ , are constant in space.

There is one case in which both  $\mathbf{K}_V$  and  $\mathbf{K}_{\text{eff}}$  coincide. If the block is of infinite extent and the values of  $\mathbf{K}$  within the block can be considered as a realization from a

---

<sup>1</sup>In two and three dimensions,  $\mathbf{K}$  is a tensorial parameter and will be denoted by a capital bold letter

stationary and ergodic<sup>2</sup> random function, then it can be shown that the value of  $\mathbf{K}_{\text{eff}}$  does not depend on  $\mathbf{x}$  and is equal to  $\mathbf{K}_V$ .

## Effective Hydraulic Conductivity

Although in this dissertation we are interested in block values  $\mathbf{K}_V$  and not in effective values  $\mathbf{K}_{\text{eff}}$ , this subsection reviews some relevant results on effective values since they represent a limiting value for  $\mathbf{K}_V$  as  $V$  tends towards infinity.

One of the first studies of effective hydraulic conductivities was Matheron (1967) who solved equation (2.3) for the value of  $\mathbf{K}_{\text{eff}}$ . The basic hypotheses of his analysis were that  $\mathbf{K}$  is a stationary random function and that  $E\{\nabla h\}$  is constant (i.e., the flow is uniform).

One of the most general results of Matheron's (1967, 1984) analysis is that, in two dimensions, the effective permeability is equal to the geometric mean of  $\mathbf{K}$  under the following conditions: i)  $\mathbf{K}$  can be reduced to a scalar  $K$ , ii) the multivariate distribution of  $K$  is invariant under rotation, and iii) the distribution of  $K/E\{K\}$  is the same as the distribution of  $K^{-1}/E\{K^{-1}\}$ , as is the case if  $K$  has a multilognormal distribution with an isotropic covariance. This result is not limited by the magnitude of the variability of  $K$ .

Matheron (1967) also shows that, in  $N$  dimensions, if the flow problem admits the solution  $\nabla h(\mathbf{x}) = \text{"constant vector"}$  over the entire aquifer, the components of the effective conductivity tensor are obtained as the expected value of the corresponding components of  $\mathbf{K}$ :

$$K_{\text{eff},ij} = E\{K_{ij}\}$$

where the subindex  $ij$  is used to indicate a tensor component. This result is a generalization of the well-known result that the effective hydraulic conductivity for perfectly stratified layers of infinite extent in the direction parallel to layering is the arithmetic mean of the individual layers.

---

<sup>2</sup>Definitions of stationarity and ergodicity are given in chapter 3.

Similarly, in  $N$  dimensions, if the flow problem admits the solution  $\mathbf{q}$  = “constant vector” over the entire aquifer, the components of the effective hydraulic conductivity tensor are given by:

$$K_{\text{eff},ij} = \frac{1}{E\{1/K_{ij}\}}$$

Again, this is a generalization of the results obtained for perfectly stratified layers of infinite extent and flow orthogonal to layering.

For the more general case in which the flow problem does not admit any of the two previous solutions, Matheron (1967) carried out a second-order analysis of the flow equation which closely follows Schwydlar’s work (cited in Matheron, 1967). The two constitutive hypotheses of this analysis are that the expected value of the hydraulic conductivity tensor reduces to a scalar  $k_0$ :

$$E\{\mathbf{K}\} = k_0 \mathbf{I}$$

where  $\mathbf{I}$  is the identity matrix and that the hydraulic conductivity  $\mathbf{K}$  can be expressed as

$$\mathbf{K} = k_0(\mathbf{I} + \epsilon \mathbf{K}')$$

where the tensor  $\mathbf{K}'$  has null expected value  $E\{\mathbf{K}'\} = \mathbf{0}$  and the parameter  $\epsilon$  is small enough so that all expansions in terms of  $\epsilon$  can be stopped at  $\epsilon^2$  without loss of accuracy.

Under these hypotheses and after some elaborate manipulations of (2.3), the effective hydraulic conductivity is:

$$\mathbf{K}_{\text{eff}} = k_0(\mathbf{I} - \epsilon^2 \mathbf{S}) \quad (2.4)$$

where  $\mathbf{S}$  is the so-called Schwydlar tensor. The Schwydlar tensor is a weighted spatial average of the covariance of  $\mathbf{K}$ . When the covariance is isotropic, the expression for  $\mathbf{K}_{\text{eff}}$  reduces to:

$$\mathbf{K}_{\text{eff}} = k_0 \left( 1 - \frac{\sigma_K^2}{N} \right) \mathbf{I} \quad (2.5)$$

where  $\sigma_K^2$  is the variance of  $\mathbf{K}$  and  $N$  is the number of space dimensions. This expression can be further manipulated to give the effective hydraulic conductivity as a function of the arithmetic mean, the harmonic mean and the dimension  $N$  of the space:

$$\mathbf{K}_{\text{eff}} = \frac{N+1}{N} E\{\mathbf{K}\} + \frac{1}{N} \left( E\{\mathbf{K}^{-1}\} \right)^{-1} \quad (2.6)$$

Matheron concludes his analysis of effective hydraulic conductivities for uniform flows with the conjecture that a generalization of (2.6) for large values of the parameter  $\epsilon$ , that is, for large variability of  $\mathbf{K}$  would be given by

$$\mathbf{K}_{\text{eff}} = (E\{\mathbf{K}\})^{\frac{N-1}{N}} \left( E\{\mathbf{K}^{-1}\} \right)^{-\frac{1}{N}}$$

which identifies the harmonic mean in one dimension and the geometric mean in two dimensions. An expansion of that last relation retaining terms up to the second order on  $\epsilon$  is none other than (2.6).

Expressions equivalent to (2.5) have also been obtained by other authors for the same range of variability of  $\mathbf{K}$ , but using different approaches.

Gutjahr *et al.* (1978) linearize the logarithm of  $\mathbf{K}$  and use spectral analysis to show that, for lognormally distributed  $\mathbf{K}$  with isotropic covariance, the values of  $\mathbf{K}_{\text{eff}}$  are the harmonic mean in one dimension, the geometric mean in two dimensions and in three dimensions  $\mathbf{K}_{\text{eff}}$  is given by:

$$\mathbf{K}_{\text{eff}} = K_g \left( 1 + \frac{\sigma_{\ln(\mathbf{K})}^2}{6} \right) \mathbf{I}$$

where  $K_g$  is the geometric mean of  $\mathbf{K}$ . Qualitatively this result can be interpreted as the effective hydraulic conductivity in three dimensions is larger than the geometric mean but smaller than the arithmetic mean by an amount equivalent to the one given by Matheron's expression (2.5). Gutjahr *et al.* suggest that their results should not be applied for  $\sigma_{\ln(\mathbf{K})}^2 > 0.25$ .

Dagan (1979, 1981, 1982b) uses an embedding matrix approach to compute effective hydraulic conductivities. Two advantages of this method are: it is not limited to small variability of  $\mathbf{K}$ , or  $\ln(\mathbf{K})$ , and it is based in a physical model. However, it is

limited to slowly varying average properties and slowly changing flow (quasi-uniform flow). The solution of equation (2.3) is sought by considering an aquifer formed by spheres of different radii embedded at random within a matrix of constant hydraulic conductivity. The hydraulic conductivity varies in space although within each sphere is constant and isotropic. Its variability is not correlated with the sphere radius. In the embedding method the perturbation caused by any given sphere is computed by assuming that all surrounding spheres can be substituted by a matrix of constant (and isotropic) permeability. Furthermore, a self-consistent approximation is made assuming that the hydraulic conductivity of this matrix is equal to the effective hydraulic conductivity of the medium. Under these conditions, the effective hydraulic conductivity is a scalar and is given by the following implicit integral expression (see Dagan, 1979, eq. 45).

$$\int_{-\infty}^{\infty} \frac{K_{ef} - K}{(N-1)K_{ef} + 2K} f(K) dK = 0 \quad (2.7)$$

where the tensor notation has been dropped since all hydraulic conductivities are isotropic,  $N$  is the number of dimensions of the space, and  $f(K)$  is the probability density function of  $K$ .

Kirkpatrick (1973, eq. 5.4) obtains the same expression (2.7) in his analysis of effective conductance of random resistor networks. Numerical evaluation of this expression provides an effective hydraulic conductivity equal to the geometric mean of  $\mathbf{K}$  in two dimensions even for large values of the variance of  $\ln(\mathbf{K})$ . In three dimensions, the effective hydraulic conductivity is larger than the geometric mean by an amount that depends on the magnitude of  $\sigma_{\ln(K)}^2$ . Dagan (1979) also shows that, by using a small perturbation approach of the type used by Gutjahr *et al.* (1978), the three-dimensional effective hydraulic conductivity obtained with the self-consistent approach is equal to the value obtained by Gutjahr *et al.* (1978).

Dagan (1989) extended the embedding method approach to the treatment of formations in which the most important characteristic is the presence of a low conductivity medium embedded in a medium of much higher conductivity, as is the case in the sand-shale formations commonly found in petroleum engineering. Both media could

be heterogeneous but the dominant factor is the large conductivity contrast. The self-consistent model is a poor approximation because it presumes that the spheres are distributed in space at random independently of their hydraulic conductivity value, whereas in the case of sand-shale formations the high conductivity medium surrounds the low conductivity one. The values for the effective conductivity obtained by Dagan (1989) with the extended embedding approach compare fairly well with the numerical results obtained by Desbarats (1987b).

Gelhar and Axness (1983) relax the hypothesis of isotropic covariance of  $\mathbf{K}$  and, using a second-order small perturbation approach, obtain the following expression for the effective hydraulic conductivity tensor:

$$\mathbf{K}_{\text{eff}} = K_A(\mathbf{I} - \mathbf{F})$$

where  $K_A$  is the arithmetic mean of the point hydraulic conductivity,  $\mathbf{I}$  is the identity matrix and  $\mathbf{F}$  is a matrix whose components are functions of the log-hydraulic conductivity variance and its spectrum. Note the striking similarity with the result (2.4) obtained by Schwydtler (as quoted in Matheron, 1967). Given that both approaches provide the same values for isotropic covariances, we presume that they should also provide the same values for anisotropic covariances.

Poley (1988) provides the most general results for effective hydraulic conductivity tensors to date. He uses the embedding matrix approach with the self-consistent approximation of Dagan (1979). Ellipsoids with different isotropic hydraulic conductivities are embedded at random within a matrix of constant (but anisotropic) hydraulic conductivity. Poley's results reproduce those of Gelhar and Axness (1983) and generalizes them for large variability of  $\mathbf{K}$ . The components of the effective hydraulic conductivity tensor are given by a complex implicit integral expression of the same type as (2.7) (see eq. (19) of Poley, 1988).

Freeze (1975) and Smith and Freeze (1979b) used Monte-Carlo analysis to evaluate effective hydraulic conductivities. For steady-state flow in one dimension they corroborate that the harmonic mean is the effective value. For two dimensions they find that the geometric mean is a good approximation for the case of isotropic  $\mathbf{K}$ .

In a study on the impact of spatial variability of hydraulic conductivity Gómez-Hernández and Gorelick (1988,1989) use also a Monte-Carlo approach to compute the effective permeability for a complex aquifer system containing pumping wells, recharge ponds and rivers. They define the effective permeability as that constant value that best reproduces (in a least-square sense) the expected value of the hydraulic heads at all nodes within the aquifer. Their analysis studied two cases: first when the hydraulic conductivity realizations are unconditional, and second, when the realizations are conditional to the conductivity values at the well locations. In both cases, it was found that the effective hydraulic conductivity was below the geometric mean with the conditional case being close to it.

## Block Hydraulic Conductivity

Effective conductivity values can be used to provide a check on the procedures used to compute block conductivity values for the limiting case when the block size tends towards infinity. However, in this dissertation we are mainly interested in block values of finite extent.

The determination of the block conductivity  $\mathbf{K}_V$  in (2.2) is posed as a deterministic problem, not as a probabilistic one. We assume that  $\mathbf{K}$  is perfectly known everywhere in  $V$  so that we can solve for heads and flows within the block for any given boundary conditions. Then, the spatial integrals in (2.2) are evaluated and  $\mathbf{K}_V$  is retrieved. This procedure could be applied to all blocks within the aquifer, but would be a very expensive task. Most works dealing with block conductivities seek to replace the detailed flow solution within each block by a simpler solution. Ideally, one would like to obtain the value of  $\mathbf{K}_V$  as some simple function of the values of  $\mathbf{K}$  within the block (such as their geometric mean). The search for such a simpler solution has been carried out both analytically and numerically.

## Analytical Approaches

Sáez *et al.* (1989) use the multiple scale method to find an analytical solution for the value of  $\mathbf{K}_V$ . They consider two distinct observation scales. At the larger scale



the small scale heterogeneity is assumed non-detectable and hydraulic conductivity varies smoothly. At the smaller scale the heterogeneity of the medium is apparent and hydraulic conductivity varies abruptly and erratically. At any particular location, hydraulic conductivity is expressed as the sum of a large scale value plus a perturbation due to the heterogeneity at the smaller scale. Similarly, hydraulic head is expressed as the sum of the large scale value plus a perturbation. After averaging out the small heterogeneities, the only remaining term is the hydraulic head at the large scale. Permeability for a block much larger than the small scale of heterogeneity is defined as the value of  $\mathbf{K}$  for which the large scale component of the hydraulic head satisfies a mass conservation equation,

$$\nabla \cdot (\mathbf{K}_V \cdot h^{(0)}) = 0,$$

where  $h^{(0)}$  is the large scale component of the hydraulic head. A set of partial differential equations is derived by Sáez *et al.* in order to solve for  $\mathbf{K}_V$ . This set of partial differential equations is then solved for the case of a periodic medium with unit period being the block for which the block conductivity is sought. This block is referred to as the unit cell. The following expression for the block conductivity is obtained:

$$\mathbf{K}_V = \mathbf{K}_A + \mathbf{t} \quad (2.8)$$

That is, the block conductivity is the sum of the arithmetic average,  $\mathbf{K}_A$  plus a tortuosity tensor  $\mathbf{t}$  defined by the following spatial average computed within the block:

$$\mathbf{t} = \frac{1}{V} \int_V \mathbf{K} \cdot \nabla \mathbf{g} \, dV,$$

where the vector function  $\mathbf{g}$  satisfies the following boundary-value problem,

$$\nabla \cdot (\mathbf{K} \nabla \mathbf{g}) = -(\nabla \cdot \mathbf{K}), \quad \text{with } \mathbf{g} \text{ periodic in the unit cell.} \quad (2.9)$$

Sáez *et al.* thus provide an analytical solution to the problem of block conductivities. However, their solution is limited to blocks larger than the scale of the erratic variability component of  $\mathbf{K}$ . Furthermore, it requires the permeable medium to be periodic with period equal to the block size.

A different approach is taken by King (1988). He uses a real-space renormalization technique. The idea is to calculate the block hydraulic conductivities over smaller areas first. Consider a two dimensional heterogeneous block that is divided into a large number of smaller blocks within which conductivity could be considered as constant. Each homogeneous small block has isotropic hydraulic conductivities. The small blocks are grouped into blocks of four and the average hydraulic conductivity of each group is computed. This average hydraulic conductivity is defined in the sense of (2.2), that is, a single value that gives the same flow for the same pressure drop. After the first renormalization has been carried out over all groups of four blocks, the procedure is repeated with the new block values. The renormalization procedure is repeated until the renormalized blocks are of the desired size. Hence, the problem of spatial averaging of a large number of small blocks has been reduced to the problem of averaging four contiguous blocks multiple times. This procedure is extremely fast since simple expressions for the block conductivity of groups of four blocks are easy to obtain and there is no restriction on the spatial variability of  $\mathbf{K}$ .

King (1988) proposes an expression for the block conductivity of four smaller blocks based on a resistor network model. The technique was validated for isotropic uncorrelated point conductivities against the results obtained with numerical simulations over very large blocks. The renormalization technique proved to be very accurate in predicting the value obtained by numerical simulation for isotropic cases, when the variance of  $K$  is outside the range of application of traditional small perturbation analysis. For highly anisotropic media, as is the case in sand-shale formations, the method did not perform well due to the poor resolution of the resistor network model around the edges of the shales.

Some criticisms to the renormalization approach are: i) there is no theoretical proof of convergence towards the actual block conductivity, ii) the choice of the basic configuration (such as four blocks in two dimensions) is rather arbitrary, iii) it is not well suited for anisotropic media, and iv) most importantly, the technique has been developed for uncorrelated media, although it is possible that a similar recursive algorithm could be applied to correlated media.

Kitanidis (1990) applies the method of moments, first formulated by Aris (1956)

and later generalized by Brenner (1980), to determine block conductivities for blocks of size much larger than the integral scale of the point conductivity. In the method of moments, the definition of block conductivity differs from that in (2.2). Instead of trying to find the block conductivity that relates average flow to average gradient, the objective is to find a block value that matches the spatial moments of the hydraulic head in the heterogeneous medium as explained below. This definition requires the solution of a transient problem as opposed to the definition in (2.2) which requires the solution of a steady-state problem. The concept is best understood with an example. Consider an infinite aquifer with constant hydraulic conductivity and the following boundary and initial conditions

$$\begin{aligned} h(\mathbf{x}, t) &= 0 \quad \text{for very large } \mathbf{x} \\ h(\mathbf{x}, 0) &= \delta(\mathbf{x}) \end{aligned} \tag{2.10}$$

where  $\delta$  is the Dirac delta function. That is, the hydraulic head field is initially flat then a unit pulse is introduced at  $\mathbf{x} = 0$  and  $t = 0$ . The solution of this problem for constant  $\mathbf{K}$  is given by a Gaussian bell:

$$h(\mathbf{x}, t) = (2\pi)^{-3/2} |2\mathbf{D}t|^{-1/2} \exp[-\mathbf{x}\mathbf{D}^{-1}\mathbf{x}/4t]$$

where  $\mathbf{D} = \mathbf{K}/S$  is called the diffusivity tensor,  $S$  is the specific storage coefficient. The second moment of the function  $h(\mathbf{x}, t)$  with respect to the origin is the moment of inertia and is given by

$$\Delta(t) = \int \mathbf{x} \cdot \mathbf{x} h(\mathbf{x}, t) d\mathbf{x} = 2\mathbf{D}t \tag{2.11}$$

Note that half the rate of change of the second moment is given by  $(1/2)d\Delta(t)/dt = \mathbf{D}$ . In the method of moments the idea is to solve the same boundary-value problem (2.10) for the heterogeneous aquifer for the rate of change of the second moment of the hydraulic head. This rate is then identified to the diffusivity tensor of a homogeneous medium.

The rate of change of the second moment of  $h$  can be obtained under some hypotheses. First, the aquifer is assumed periodic with period much larger than the

scale of variability of  $\mathbf{K}$ . Second, the moments are defined at two scales—similarly to Sáez *et al.* (1989)—and only the moments at the larger scale are of interest. The rate of change at the second moment at the larger scale is the one identified to the diffusivity tensor of an homogeneous medium. And third, only slowly varying flow is considered.

Under these hypotheses, the resulting expression for  $\mathbf{K}_V$  is very similar to the expression obtained by Sáez *et al.* (1989). The block hydraulic conductivity tensor is equal to its arithmetic spatial average plus an integral term equivalent to the tortuosity term in (2.8). This integral term is written in terms of a function  $g$  that must satisfy a boundary value problem equivalent to (2.9).

Explicit expressions for  $K_V$  have been obtained only for small variance of  $\mathbf{K}$  and agreement was found with previous results for effective hydraulic conductivities.

Kitanidis' (1990) method has the same drawbacks as the one by Sáez *et al.*: it is limited to large blocks and it requires the assumption that the medium is periodic with period equal to the block size.

### Numerical Approaches

Besides the analytical approaches to determining block conductivities, there is a large body of literature that describes numerical approaches to the problem of block conductivities. The heterogeneous and rectangular block of size  $V$  is discretized into a number of smaller homogeneous blocks. The partial differential equation of groundwater flow is solved numerically for given boundary conditions and the block conductivity value is retrieved using equation (2.2).

Except for the works of Kasap and Lake (1989), and White (1987) that will be discussed later, all numerical attempts to obtain block conductivities have assumed that the principal directions of the block conductivity tensor are known so that the block sides can be oriented parallel to them. Consequently, the conductivity tensor is diagonal and the number of components to be determined is reduced to two (in 2-D) or three (in 3-D).

The procedure commonly used to obtain the  $x$ -component of the block conductivity tensor of a two-dimensional block is as follows: (1) solve for flows and heads

within the block for the boundary conditions in Fig. 2.3, (2) evaluate the total flow  $Q$  through any cross-section parallel to the  $y$ -axis, and (3) the block conductivity in the  $x$ -direction is obtained:

$$K_{V,xx} = - \left( \frac{Q}{y_1 - y_0} \right) / \left( \frac{h_1 - h_0}{x_1 - x_0} \right). \quad (2.12)$$

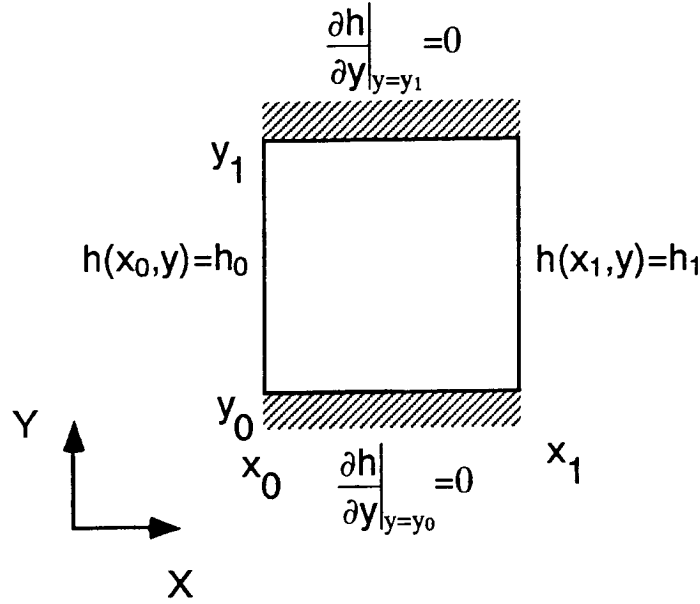


Figure 2.3: **A set of typical boundary conditions.** They are used to obtain the component  $K_{xx}$  of the block conductivity tensor

The value of  $K_{V,yy}$  is obtained similarly after solving for flows and heads with the boundary conditions in Fig. 2.3 rotated  $90^\circ$ .

It is interesting to note that expression (2.12) can be obtained from (2.2), which is the definition used in this dissertation for block conductivity, subject to the boundary conditions in Fig. 2.3. Indeed, Eq. 2.2 can be rewritten as

$$\begin{Bmatrix} \frac{1}{V} \int_V q_x dV \\ \frac{1}{V} \int_V q_y dV \end{Bmatrix} = - \begin{Bmatrix} K_{V,xx} & 0 \\ 0 & K_{V,yy} \end{Bmatrix} \begin{Bmatrix} \frac{1}{V} \int_V (\partial h / \partial x) dV \\ \frac{1}{V} \int_V (\partial h / \partial y) dV \end{Bmatrix}$$

Under the assumption that the principal components of the block conductivity are parallel to the block sides, both the average flow and the average gradient in the  $y$

direction are close to zero for the boundary conditions in Fig. 2.3. Therefore, the estimate of  $K_{V,yy}$  deduced from the previous expression would be unreliable. The estimate for  $K_{V,xx}$  is given by:

$$K_{V,xx} = -\frac{\frac{1}{V} \int_V q_x dV}{\frac{1}{V} \int_V (\partial h / \partial x) dV} \quad (2.13)$$

Both the average gradient and the average flow in the  $x$  direction are extremely simple to obtain from the solution of the boundary-value problem in Fig. 2.3. The average flow in the  $x$  direction is equal to the total flow crossing the block divided by its width. The average gradient is equal to the difference of the constant head values on both sides of the block divided by the length of the aquifer. Substitution of these values in (2.13) results in (2.12).

If a set of boundary conditions different from those in Fig. 2.3 were used, expression (2.2) could still be evaluated but it would result in a value for  $K_{V,xx}$  different from that in (2.12). Therefore, the block values provided by this numerical method are dependent on the boundary conditions used to solve the flow equation. However, as the block becomes much larger than the scale of variability of  $\mathbf{K}$ , the effect of the boundary conditions on the solution for flows and heads within the block becomes smaller, thus the block values are less dependent on the boundary conditions considered.

To check the assumption that the principal directions of  $\mathbf{K}_V$  are parallel to the block sides the magnitude of the average flow in the direction orthogonal to the mean gradient can be computed ( $1/V \int_V q_y dV$  in the previous case). A value significantly different from zero indicates that the off-diagonal terms are not zero.

This conceptually simple method has been applied to obtain block hydraulic conductivities since the early 1960s with the objective of finding a simple function relating  $\mathbf{K}_V$  to the values of  $\mathbf{K}$  within the block.

Both Warren and Price (1961) and Bouwer (1969) find that the geometric mean of the point conductivities within the block is a good approximation for the block conductivity. In a 3-D study, Warren and Price (1961) use uncorrelated isotropic permeability values drawn from four different probability distributions (lognormal, exponential, uniform and discontinuous). In 2-D, Bouwer (1969), uses an analog

simulation with uncorrelated isotropic conductivities drawn from either a uniform distribution or a binary one.

Journel *et al.* (1986), Desbarats (1987a, 1987b, 1988), and Deutsch (1987, 1989) have considered the problem of block permeabilities for three dimensional sand-shale formations using the numerical approach discussed above. The hydraulic conductivity distribution is characterized by the proportion of shale and the covariance of a shale indicator. The shale indicator is a binary variable that takes a value of 1 for shale locations and 0 for sand locations. The covariance of the indicator variable is directly related to the orientation and width-to-length ratio of the shales. These authors find the block conductivity to be a function of the shale proportion, the block size relative to the indicator covariance correlation length, and the conductivity contrast between sand and shale. They propose a power average law to describe the block conductivity for shale proportion below the percolation threshold

$$\begin{aligned} K_{V,xx} &= (p K_{sh}^{w_x} + (1-p) K_{ss}^{w_x})^{1/w_x} \\ K_{V,yy} &= (p K_{sh}^{w_y} + (1-p) K_{ss}^{w_y})^{1/w_y} \\ K_{V,zz} &= (p K_{sh}^{w_z} + (1-p) K_{ss}^{w_z})^{1/w_z} \end{aligned}$$

where  $p$  is the proportion of shales,  $K_{sh}$  and  $K_{ss}$  are the conductivities of the shale and sand respectively, and  $w_x, w_y$  and  $w_z$  are coefficients to be determined empirically depending on the indicator covariance. The block sides are assumed to be parallel to the principal components of  $K_V$ .

An application of this method has been carried out by Bachu and Cuthiell (1990) who analyze the block conductivities of a number of core samples from a Canadian reservoir. After digitizing the geometry of the shales in the core samples, that geometry is discretized using a very detailed finite element mesh used for the solution of groundwater flow. Since their study is limited to 2-D, only horizontal and vertical hydraulic conductivities are computed on several core samples with different proportions of shale and assuming different conductivity contrasts. For each core sample analyzed, the values of  $w_x$  and  $w_z$  were obtained. Bachu and Cuthiell's paper contains

a fairly exhaustive analysis of the variation of the power values ( $\omega$ ) for different shale proportions and different conductivity contrasts.

There are several limitations to this power average approach: first, it requires that the principal directions of the block conductivity tensor be known; second, the boundary conditions in Fig. 2.3 may not be the most representative of the actual boundary conditions prevailing around the block within the aquifer.

A slightly different approach was used by Long and co-workers (Long et al., 1982; Long and Witherspoon, 1985) to analyze flow in fractured media. Their concern is whether a fractured medium can be analyzed as a continuous porous medium using an equivalent anisotropic permeability tensor. Their objective is to check whether the concept of a representative elementary volume (REV; Bear, 1979) can be used in fractured media. With this objective they developed a procedure that might be used to determine block conductivities. In two dimensions, the procedure is as follows. First, select a size for the possible (circular) REV and center it at any given point in the fractured medium. Second, compute the apparent conductivity in the direction of the gradient as explained below, for a large number of square blocks inscribed within the REV. Third, if an equivalent porous medium exists, the inverse of the square root of the apparent permeability should plot as an ellipse that uniquely determines the equivalent anisotropic conductivity tensor.

For any square block inscribed in the REV, the apparent permeability in the direction of the gradient needs to be computed. This is done by solving flow within the block for constant head boundary conditions along the four sides of the block as given in Fig. 2.4. If the block acts as an anisotropic homogeneous porous medium, the flow entering through side 2 should be equal to the flow leaving through side 4, and similarly with sides 1 and 3. The apparent permeability in the direction of the gradient is given by the ratio of the inflow through side 2 to the overall gradient (as given by the uniform heads at sides 2 and 4).

Long's conclusions were that an REV might be difficult to find. When it exists, its size is a function of the fracture density and the average fracture length. The fracture configuration within the block changes as the square block rotates within the REV. Sometimes these changes could be quite dramatic, resulting in very discontinuous



changes on the apparent conductivities, as Long recognizes. A better approach is to solve flow within the entire REV for different flow gradients. In this way the geometry of the fractures remains constant and any change on apparent conductivity is due to the anisotropy of the medium.

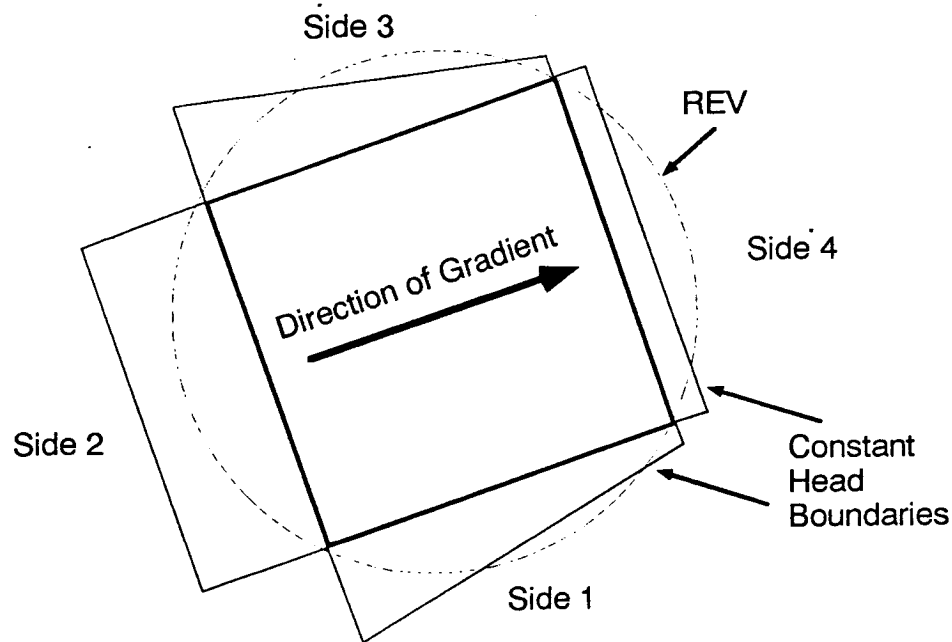


Figure 2.4: **Another set of boundary conditions.** It was used by Long *et al.* (1982) to determine the apparent conductivity in the direction of the gradient.

Haldorsen and Lake (1982) and Haldorsen and Chang (1986) propose a different numerical approach to determining block conductivities in sand-shale formations. The component of the hydraulic conductivity tensor orthogonal to the orientation of shales is computed using a stream-tube approach instead of using a numerical simulation of fluid flow. This component is related to the length of flow paths across the medium. Flow path lengths are equal to the block height plus the horizontal distance traveled to bypass the shales. Begg and King (1985), and Begg *et al.* (1985, 1989) find a functional relation relating the vertical block permeability to the shale proportion and the statistics of shale width and shale length. This functional relation makes it possible to obtain a block vertical conductivity without the need to know the exact

geometry of the shales within the block.

The implicit assumption of the stream-tube approach is that the shales are spaced far apart enough so that the perturbation in the flow field caused by one shale does not affect the flow field around any other neighboring shale. This assumption limits their results to relatively low proportion of shales (15% according to Desbarats, 1987b).

From numerical analysis of resistor networks, Kirkpatrick (1973) proposes a power law that is a function of three coefficients to approximate the block conductance of random resistor networks in which a certain portion of the resistors have been set to zero conductance. This empirical expression has been evaluated for flow in sand-shale formations by Deutsch (1989) who always found a set of parameters that provided a good fit to his numerical results.

In all the previous works concerning block conductivities it is assumed that the block conductivities are either isotropic or anisotropic but with principal components oriented parallel to the block sides. The possibility that the blocks may not be oriented in the same direction as the principal components of the block conductivity tensor has been considered only recently. Two methods for determining block conductivities assuming an arbitrary orientation of the principal components have been proposed in the past few years.

White (1987) and White and Horne (1987) propose the inversion of equation (2.2) without assuming that the off-diagonal terms of the block tensor  $\mathbf{K}_V$  are zero. The entire aquifer, rather than just a single block, is discretized at two scales. First, it is discretized into large heterogeneous blocks which then are discretized in small homogeneous cells. Using the small scale discretization, flow is solved numerically over the entire aquifer, not just over an individual block, using the small scale discretization. To obtain the block hydraulic conductivity tensor of any given block, both the average flow and the average gradient over the block are computed from the solution of groundwater flow over the entire aquifer for a given set of boundary conditions. Equation (2.2) can be rewritten, in two dimensions as:

$$\begin{Bmatrix} \overline{q_x} \\ \overline{q_y} \end{Bmatrix} = - \begin{Bmatrix} K_{V,xx} & K_{V,xy} \\ K_{V,xy} & K_{V,yy} \end{Bmatrix} \begin{Bmatrix} \overline{(\partial h / \partial x)} \\ \overline{(\partial h / \partial y)} \end{Bmatrix}$$

where the overbar is used to indicate spatial averages.

From the previous system of two linear equations the values of the three components of  $\mathbf{K}_V$  are undetermined. To resolve this undetermination, White solves the groundwater flow equation for a different set of boundary conditions. Thus, two more equations relating average flows and average gradients are written for each block. The new expanded system becomes overdetermined (four equations, three unknowns). White suggests solving the flow problem over the entire aquifer for at least two other sets of boundary conditions to end up with eight linear equations per block that can be solved for the three unknowns by least-squares.

Computing block hydraulic conductivities using White's method is very expensive, if not infeasible, since it requires prior solving the flow problem over the entire aquifer at the smallest scale. This expense could be justified if block conductivities are to be used in a numerical simulation of multiphase flow at the block scale. It would not be justified for single phase flow because, if flow has been solved for at the smallest scale, there is no more need for block values.

Kasap and Lake (1989) propose an analytical method to compute the block conductivity tensor for the case of anisotropic point conductivity tensor. Their method is based on the recurrent use of the block conductivity values obtained for a block composed of two layers of homogeneous but anisotropic conductivity, under the assumption that flow lines are parallel. Their basic results can be summarized as follows: the component in the direction parallel to the layers is the arithmetic average of the components of each layer in that direction minus a term which is a function of the off-diagonal components of both layers; the component orthogonal to the layers is equal to the harmonic mean of the components of each layer in that direction; and the off-diagonal component is a function of all the components of both layer conductivity tensors; it is equal to zero if the layers are isotropic.

This dissertation explores both the analytical and the numerical approaches to computing block conductivities. The analytical approach proposed provides block conductivities for block sizes which could be larger than the integral scale of the point conductivity (Rubin and Gómez-Hernández (1990) and Rubin *et al.* (1991)). However,

it requires the point conductivity to have an isotropic covariance with small variance. The numerical approach (Gómez-Hernández, 1990a; Gómez-Hernández and Rubin, 1990; Gómez-Hernández and Journel, 1990) lies between White's (1987) method and the more traditional approach of Warren and Price (1961). It does not require the solution of the flow problem over the entire aquifer. It borrows White's idea of using least squares to determine the coefficients required by a finite-difference formulation of the flow equation. But, instead of solving for flow over the entire aquifer, only a small area is considered. Which boundary conditions should be used is studied.

## 2.3 Direct Generation of Block Values

Determining block conductivity values requires the prior assumption that the block has been exhaustively sampled at a smaller scale. This will rarely be the case. For this reason, block conductivities are uncertain, with that uncertainty being modeled by a random function concept. Through stochastic modeling of block values, this random function model is built and the statistics of the random function determined. The final objective of such stochastic modeling is the generation of realizations of block values for their use in the Monte-Carlo analysis of aquifer response variables, see Fig. 1.1.

While conductivity values obtained from core-plug samples or slug tests are average values over centimeters or meters of aquifer, the blocks used in the numerical simulators require average values representative of tens to thousands of meters. Values of conductivity cannot be measured at the scale of the simulator block (except possibly for some very long pump tests) and, therefore, statistical inference from measured values is not possible. One cannot expect that the statistics of the variability observed in the measurements are going to be the same as the block statistics, although some kind of relation is warranted.

The general problem of how to deduce block variability from smaller scale measurement variability is known as the change of scale (or change of support). The change of scale problem has received much attention from mining engineers (Journel

and Huijbregts, 1978). Mining engineers need to predict the ore grade of the mining units (scale of meters) from the statistics of blastholes grades (scale of centimeters). Their problem is simpler because block grades are exactly equal to the arithmetic average of point grades. Several references provide the expression of the block covariance as a function of the point covariance (Journel and Huijbregts, 1978; Vanmarcke, 1983).

In groundwater flow, however, the problem is much harder for two reasons: first, the functional relation between point and block values has only been established for infinite blocks under very specific hypotheses, and second, in the cases in which that functional relation is known, the function is nonlinear, thus traditional change of scale formulas cannot be used (except in very specific cases that will be explained later).

Two different approaches have been taken commonly in the Monte-Carlo analysis of groundwater flow for the generation of fields of block conductivities. The first consists of generating realizations of conductivity fields at the scale of the measurements. These realizations are then block-averaged, to yield the block value required by the numerical flow simulator: for each block, a small flow simulation is carried out with the objective of evaluating expression (2.2) and determining the block conductivities. The block values are then assembled together, and flow solved over the entire aquifer. For an application of this approach in the oil industry see Begg *et al.* (1989).

A second approach was considered for two-dimensional simulations of statistically isotropic point conductivities. For sufficiently large blocks, the block conductivity is assumed a scalar equal to the geometric mean of the point values within the block. Noting that the geometric mean of a variable  $x$  is the anti-log of the arithmetic average of  $\log(x)$ , the traditional change of support formulas can be applied to determine the covariance of the arithmetic mean of  $\log K$ . In other words, the change of support problem is solved in the log space. First, take the logarithms of the point values. Second, obtain the covariance of  $\log K$ . And third, apply the change of support formulas to obtain the covariance of the arithmetic average of  $\log K$  for the block size considered. This covariance can then be used to generate realizations of the logarithm of the block conductivities. Taking the anti-log of such a realization will result in a realization of block conductivities, with the same statistics as would have

obtained by taking geometric averages over a realization of point conductivities. This approach, which is valid only in two dimensions and for sufficiently large and isotropic blocks, has been discussed in the hydrology literature by Dagan (1982b,1985), Clifton and Neuman (1982) and Hoeksema and Kitanidis (1984,1985b).

For the particular case of one-dimensional flow, the block conductivity is exactly equal to the harmonic mean of the point conductivities within the block. This relation is not linear and the standard change of support formulas cannot be applied. However, Desbarats (1989) uses a Taylor series-type for small variance of  $K$  to provide formulas for the expected value and the variance of 1-D block conductivities as a function of their length.

There appears to be a need for techniques that allow the stochastic characterization of block conductivities without direct inference. Only when the block value is a scalar equal to the geometric mean (in 2-D) or the harmonic mean (in 1-D) of the points within the block, explicit expressions have been obtained for the expected value and covariances of the block values. In response to this need, both an analytical and a numerical method are proposed in order to extend the previous, rather limited results. The analytical method provides the expected value and covariance of an isotropic two-dimensional block without any restriction on the functional relationship between point and block conductivities, although it does require the conditions for a small-perturbation analysis. The numerical method does not require the block to be isotropic or with small variability, it can be applied to small blocks, and it does not assume any specific functional relationship between point and block values.

## Chapter 3

# Sequential Simulation

This chapter describes and implements the algorithm of sequential simulation for the generation of realizations of random fields. The theory of sequential simulation is reviewed first. Then, the specifics of its application to multiGaussian random fields, then to random fields with a generic bivariate distribution, and, finally to multivariate multiGaussian random fields are discussed. Finally, implementation problems of the technique are addressed.

As explained in the introduction, the ability to generate realizations from random fields with given multivariate distributions is key to Monte-Carlo analyses. In this dissertation realizations of single variable random fields are required for the numerical approach to the problem of scaling-up. Next, the joint realizations of multiple variable random fields are required for the direct generation of block conductivities conditioned upon small scale data. This last step can be accomplished only after determining the point-point and the point-block conductivity covariances.

The author's contribution in this chapter consists of the practical implementation of the different simulation algorithms.

### 3.1 Theory

This section starts by reviewing some general probabilistic concepts (a good reference is Papoulis, 1986) then presents the theory of sequential simulation closely following Journal (1983a, 1983b, 1985, 1987, 1989).

#### General Concepts

A random field or random function (RF)  $Z(\mathbf{x})$  can be defined as a rule that assigns a function  $z(\mathbf{x}, \theta)$  to the outcome  $\theta$  of an experiment  $\mathcal{S}^1$  (Papoulis, 1986). Thus, a RF is a set of spatial functions, also called realizations, depending on the parameter  $\theta$ . The set of all possible realizations  $\{z(\mathbf{x}, \theta), \text{ for all } \theta \in \mathcal{S}\}$  is called the ensemble.

Capital letters will be used to refer to the random function and small letters to refer to the realizations. For convenience of notations, the dependence of the realizations on the parameter  $\theta$  will be omitted unless necessary.

For a specific location  $\mathbf{x}$ ,  $Z(\mathbf{x})$  is a random variable with distribution

$$F(z, \mathbf{x}) = P\{Z(\mathbf{x}) \leq z\}$$

This function depends on  $\mathbf{x}$  and represents the probability of the event  $\{Z(\mathbf{x}) \leq z\}$  consisting of all outcomes  $\theta_i$  such that the realizations  $z(\mathbf{x}, \theta_i)$  are less than  $z$  at the specific location  $\mathbf{x}$ . The notation  $F_Z(z, \mathbf{x})$  may be used to explicitly denote that we are referring to the random function  $Z(\mathbf{x})$ .

The function  $F(z, \mathbf{x})$  will be called the first-order cumulative distribution function (cdf) of the RF  $Z(\mathbf{x})$ . When referring to a specific  $\mathbf{x}$ , it may also be called the marginal distribution of the random variable  $Z(\mathbf{x})$ . Its derivative with respect to  $z$ , when it exists,

$$f(z, \mathbf{x}) = \frac{\partial F(z, \mathbf{x})}{\partial z}$$

is the first-order probability density function (pdf) of  $Z(\mathbf{x})$ .

---

<sup>1</sup>For an axiomatic definition of an experiment see (Papoulis, 1986). As an example, the simplest experiment would be tossing a coin, the outcomes of which are heads and tails.



Similarly, the second-order cdf of  $Z(\mathbf{x})$  is given by the joint distribution

$$F(z_1, z_2; \mathbf{x}_1, \mathbf{x}_2) = P\{Z(\mathbf{x}_1) \leq z_1, Z(\mathbf{x}_2) \leq z_2\}$$

of any two random variables  $Z(\mathbf{x}_1)$  and  $Z(\mathbf{x}_2)$ . The corresponding pdf is

$$f(z_1, z_2; \mathbf{x}_1, \mathbf{x}_2) = \frac{\partial^2 F(z_1, z_2; \mathbf{x}_1, \mathbf{x}_2)}{\partial z_1 \partial z_2}$$

The  $n$ th-order cdf also referred as the multivariate cdf of  $Z(\mathbf{x})$  is the joint distribution  $F(z_1, z_2, \dots, z_n; \mathbf{x}_1, \mathbf{x}_2, \dots, \mathbf{x}_n)$  of any  $n$  random variables  $Z(\mathbf{x}_1), Z(\mathbf{x}_2), \dots, Z(\mathbf{x}_n)$ .

It can be shown that a RF is fully characterized by the multivariate cdfs  $F(z_1, z_2, \dots, z_n; \mathbf{x}_1, \mathbf{x}_2, \dots, \mathbf{x}_n)$  for all choices of  $z_i, \mathbf{x}_i$  and  $n$ .

Ideally, we would like to know the multivariate cdf of  $Z(\mathbf{x})$ . For practical limitations, we content ourselves with the first and second-order distributions of  $Z(\mathbf{x})$ ; or simply with a few moments, generally, the expected value, variogram or covariance of  $Z(\mathbf{x})$  as defined next.

**Expected Value.** The mean or expected value  $m(\mathbf{x})$  of  $Z(\mathbf{x})$  is given by, when the integral is defined,

$$m(\mathbf{x}) = E\{Z(\mathbf{x})\} = \int_{-\infty}^{\infty} z f(z, \mathbf{x}) dz$$

**Variogram.** The variogram  $2\gamma(\mathbf{x}_1, \mathbf{x}_2)$  of  $Z(\mathbf{x})$  is defined as the expected value of the square difference  $(Z(\mathbf{x}_1) - Z(\mathbf{x}_2))^2$

$$2\gamma(\mathbf{x}_1, \mathbf{x}_2) = \int_{-\infty}^{\infty} \int_{-\infty}^{\infty} (z_1 - z_2)^2 f(z_1, z_2; \mathbf{x}_1, \mathbf{x}_2) dz_1 dz_2$$

**Covariance.** The covariance  $C(\mathbf{x}_1, \mathbf{x}_2)$  of  $Z(\mathbf{x})$  is the expected value of  $[Z(\mathbf{x}_1) - m(\mathbf{x}_1)][Z(\mathbf{x}_2) - m(\mathbf{x}_2)]$

$$C(\mathbf{x}_1, \mathbf{x}_2) = \int_{-\infty}^{\infty} \int_{-\infty}^{\infty} [z_1 - m(\mathbf{x}_1)][z_2 - m(\mathbf{x}_2)] f(z_1, z_2; \mathbf{x}_1, \mathbf{x}_2) dz_1 dz_2$$

Practical considerations again limit our analyses to RF models which are stationary in some sense (Myers, 1989).

Strict-sense stationarity means that the distributions of the RF remain invariant under translation, that is,  $Z(\mathbf{x})$  has the same distributions as  $Z(\mathbf{x} + \mathbf{c})$  for any vector  $\mathbf{c}$ . Similarly, the  $n$ th-order pdf of a strict-sense stationary RF is such that,

$$f(z_1, z_2, \dots, z_n; \mathbf{x}_1, \mathbf{x}_2, \dots, \mathbf{x}_n) = f(z_1, z_2, \dots, z_n; \mathbf{x}_1 + \mathbf{c}, \mathbf{x}_2 + \mathbf{c}, \dots, \mathbf{x}_n + \mathbf{c})$$

for any vector  $\mathbf{c}$ .

Second-order stationarity is less restrictive than strict-sense stationarity. A RF  $Z(\mathbf{x})$  is second-order stationary if its second-order pdf is invariant under translation,

$$f(z_1, z_2; \mathbf{x}_1, \mathbf{x}_2) = f(z_1, z_2; \mathbf{x}_1 + \mathbf{c}, \mathbf{x}_2 + \mathbf{c}) = f(z_1, z_2; \mathbf{r})$$

where  $\mathbf{r} = \mathbf{x}_1 - \mathbf{x}_2$ .

An even less restrictive definition of stationarity is that of wide-sense stationarity, also known as weak second-order stationarity. A RF is wide-sense stationary if its mean is constant,

$$E\{Z(\mathbf{x})\} = m,$$

and its covariance depends only on the separation vector  $\mathbf{r} = \mathbf{x}_1 - \mathbf{x}_2$

$$C(\mathbf{x}_1, \mathbf{x}_2) = C(\mathbf{r})$$

Under wide-sense stationarity, the variogram also depends only on the separation vector and the following relationship is true,

$$C(\mathbf{r}) = C(0) - \gamma(\mathbf{r}).$$

Furthermore, we will restrict our analysis to mean-ergodic and covariance-ergodic RFs and in some cases to distribution-ergodic RFs. A RF  $Z(\mathbf{x})$  is mean-ergodic if its mean is constant

$$E\{Z(\mathbf{x})\} = m$$

and the spatial average of any particular realization

$$m_V = \frac{1}{V} \int_V z(\mathbf{x}) d\mathbf{x}$$

satisfies,

$$\lim_{V \rightarrow \infty} m_V = m$$

where  $V$  is some volume of integration.

Similarly,  $Z(\mathbf{x})$  is covariance-ergodic if its covariance is only a function of the separation vector

$$C(\mathbf{r}) = E\{(Z(\mathbf{x}) - m)(Z(\mathbf{x} + \mathbf{r}) - m)\}$$

and the spatial integral over any particular realization

$$C_V(\mathbf{r}) = \frac{1}{V} \int_V \int_V (z(\mathbf{x}) - m)(z(\mathbf{x} + \mathbf{r}) - m) d\mathbf{x} d\mathbf{x}$$

satisfies

$$\lim_{V \rightarrow \infty} C_V(\mathbf{r}) = C(\mathbf{r})$$

Finally, prior to giving the conditions for  $Z(\mathbf{x})$  to be distribution-ergodic we have to define the indicator RF  $I(z; \mathbf{x})$  for threshold  $z$

$$I(z; \mathbf{x}) = \begin{cases} 0 & \text{if } Z(\mathbf{x}) > z \\ 1 & \text{if } Z(\mathbf{x}) \leq z \end{cases} \quad (3.1)$$

Note that the expected value of the indicator RF is the first-order cdf of  $Z(\mathbf{x})$

$$\begin{aligned} E\{I(z; \mathbf{x})\} &= 0 \times P\{Z(\mathbf{x}) > z\} + 1 \times P\{Z(\mathbf{x}) \leq z\} \\ &= P\{Z(\mathbf{x}) \leq z\} \\ &= F_Z(z; \mathbf{x}) \end{aligned}$$

The RF  $Z(\mathbf{x})$  is first order distribution-ergodic if all indicator RFs for all possible thresholds  $z$  within the range of variability of  $Z(\mathbf{x})$  are mean-ergodic.

The decisions of stationarity and ergodicity are critical if one wishes to represent the experimental statistics of a unique data set with a RF model. There is no choice but to consider a RF model which is both stationary and ergodic, at least with regard to those moments that one wishes to reproduce.

Stationarity and ergodicity are, thus, model decisions rather than hypotheses or assumptions that are susceptible of a later refutation. This confusion between “decision” and “assumption” has misled many practitioners to believe that there is an actual RF behind what they observe.

## Simulation

We shall consider two different types of simulations: unconditional and conditional.

Unconditional simulation of  $Z(\mathbf{x})$  refers to a technique that allows drawing equiprobable realizations from the ensemble  $\Theta = \{z(\mathbf{x}, \theta), \theta \in \mathcal{S}\}$  of all possible realizations.

To understand the meaning of conditional simulation, we first define the subensemble of conditional realizations given some conditioning values as follows. Let  $\{z_i; \mathbf{x}_i : i \in (N_0)\}$  represent a set of  $N_0$  conditioning data and their locations<sup>2</sup>. The subensemble of conditional realizations is defined as the subset of  $\Theta$

$$\Theta|(N_0) = \{z(\mathbf{x}, \theta), \theta \text{ such that } z(\mathbf{x}_i, \theta) = z_i, i \in (N_0)\}$$

It can be shown that this subensemble defines a new RF, denoted  $Z(\mathbf{x})|(N_0)$ , the statistics of which are defined by the conditional cdfs of  $Z(\mathbf{x})$ . For instance, its second-order cdf is given by

$$F(z_1, z_2; \mathbf{x}_1, \mathbf{x}_2 | Z(\mathbf{x}_i) = z_i, i \in (N_0)) = \frac{F(z_1, z_2, z_i, i \in (N_0); \mathbf{x}_1, \mathbf{x}_2, \mathbf{x}_i, i \in (N_0))}{F(z_i, i \in (N_0); \mathbf{x}_i, i \in (N_0))}$$

---

<sup>2</sup>Hereafter, the notation  $(n)$  will be used to refer to a set of  $n$  integers. This set will be generally, but not necessarily, the set of integers  $\{1, \dots, n\}$ . To unburden notation and without ambiguity,  $(n)$  may be used as a subindex to refer to the entire set of conditioning data

Conditional simulation of  $Z(\mathbf{x})$  given  $\{z_i, \mathbf{x}_i : i \in (N_0)\}$  refers to any technique that allows drawing realizations at random from the ensemble of conditional realizations  $\Theta|(N_0)$ . We will say that conditional realizations honor the conditioning values.

Since a stochastic process is completely characterized by its statistics, more precisely, by its multivariate cdf or pdf, we can conceive simulation as a technique which is equivalent to directly drawing at random from the multivariate pdf of  $Z(\mathbf{x})$ , in which case the statistics of  $Z(\mathbf{x})$  are reproduced by construction. The sequential simulation technique that is described next, takes this direct approach. Hence, the statistics of the random field, whether it is unconditional  $Z(\mathbf{x})$  or conditional  $Z(\mathbf{x})|(N_0)$ , will be reproduced by construction.

## Sequential Unconditional Simulation

We shall first consider the problem of drawing realizations at random from the ensemble of unconditional realizations  $\Theta$ . In general, the realizations  $z(\mathbf{x}) \in \Theta$  cannot be given as an explicit functional expression of  $\mathbf{x}$ , so a non-parametric approach is used. Any realization is specified by its values at a finite number of locations. Instead of drawing a function  $z(\mathbf{x})$  we shall talk about drawing a set of  $N$  values  $\{z(\mathbf{x}_i), i \in (N)\}$  whose  $N$ th-order pdf is given by the RF  $Z(\mathbf{x})$ . The locations represented by  $(N)$  need not be on a regular grid or be ordered in a special manner.

The joint pdf of two random variables  $Z(\mathbf{x}_1)$  and  $Z(\mathbf{x}_2)$  can be written (Papoulis, 1986) as the product of the conditional pdf of  $Z(\mathbf{x}_1)$  given  $Z(\mathbf{x}_2)$  times the pdf of  $Z(\mathbf{x}_2)$

$$f(z_1, z_2; \mathbf{x}_1, \mathbf{x}_2) = f(z_1; \mathbf{x}_1 | z_2; \mathbf{x}_2) f(z_2; \mathbf{x}_2)$$

This expression is obtained by using the definition of random variable plus the axiom of conditional probability (Papoulis, 1986). The axiom of conditional probability can be recursively used to write the  $N$ th-order pdf of  $\{Z(\mathbf{x}_i) : i \in (N)\}$  as

$$f_{(N)}(z_i; \mathbf{x}_i, i \in (N)) = \tag{3.2}$$

$$\begin{aligned}
&= f_{N|(N-1)}(z_N; \mathbf{x}_N | z_i; \mathbf{x}_i, i \in (N-1)) f_{(N-1)}(z_i; \mathbf{x}_i, i \in (N-1)) \\
&= f_{N|(N-1)}(z_N; \mathbf{x}_N | z_i; \mathbf{x}_i, i \in (N-1)) f_{N-1|(N-2)}(z_{N-1} | z_i; \mathbf{x}_i, i \in (N-2)) \\
&\quad f_{(N-2)}(z_i; \mathbf{x}_i, i \in (N-2)) \\
&= (\dots) \\
&= f_{N|(N-1)}(z_N; \mathbf{x}_N | z_i; \mathbf{x}_i, i \in (N-1)) f_{N-1|(N-2)}(z_{N-1} | z_i; \mathbf{x}_i, i \in (N-2)) \\
&\quad \dots f_{2|1}(z_2; \mathbf{x}_2 | z_1; \mathbf{x}_1) f(z_1; \mathbf{x}_1)
\end{aligned}$$

where the subscript to  $f$  is used to indicate whether conditional or unconditional pdfs are used and, in the case of conditional pdfs, to indicate also the conditioning variables; for instance,  $f_{(n)}$  represents an  $n$ th-order unconditional pdf and  $f_{n|(n-1)}$  is the conditional probability of  $Z(\mathbf{x}_n)$  given the set of  $(n-1)$  values. The joint statistics of  $\{Z(\mathbf{x}_i), i \in (N)\}$ , which are fully determined in terms of the joint pdf  $f_{(N)}(z_i; \mathbf{x}_i : i \in (N))$ , are also determined by the pdf of  $Z(x_1)$  and the  $N-1$  conditional pdfs introduced in the previous expression. Consequently, and at least in theory, a realization of  $Z(\mathbf{x}_i), i \in (N)$  can be generated by sequentially drawing from the density of  $Z(\mathbf{x}_1)$  and the  $N-1$  **univariate** conditional pdfs in Eq. (3.2).

**Sequential Simulation Algorithm.** A sequential simulation proceeds as follows:

1. Draw at random  $z_1$  from the marginal density of  $Z(\mathbf{x}_1)$
2. Determine the conditional density of  $Z(\mathbf{x}_2)$  given  $Z(\mathbf{x}_1) = z_1$ . Then draw from it  $z_2$
3. Determine the conditional density of  $Z(\mathbf{x}_3)$  given  $Z(\mathbf{x}_1) = z_1$  and  $Z(\mathbf{x}_2) = z_2$ . Then draw  $z_3$  from it
- $\vdots$
- N. Determine the conditional density of  $Z(\mathbf{x}_N)$  given  $Z(x_i) = z_i, i \in (N-1)$ . Then draw  $z_N$  from it

This procedure is completely general and can be used for the simulation of **any** RF.

For the generation of a second realization simply repeat steps 1 through  $N$ .

## Conditional Simulation

The extension of the previous discussion to drawing generations from the subensemble  $\Theta|(N_0)$  conditioned to the data  $\{z_j; x_j : j \in (N_0)\}$  is straightforward. The statistics of the conditional RF  $Z(\mathbf{x})|(N_0)$  are fully determined in terms of the conditional pdf  $f_{(N)|(N_0)}$ . This pdf can be expressed as a product of univariate conditional pdfs as follows

$$\begin{aligned}
 f_{(N)|(N_0)}(z_i; \mathbf{x}_i, i \in (N)) &= f_{N|(N-1) \cup (N_0)}(z_N; \mathbf{x}_N | z_i, z_j; \mathbf{x}_i, \mathbf{x}_j, i \in (N-1), j \in (N_0)) \\
 &\quad f_{N-1|(N-2) \cup (N_0)}(z_{N-1}; \mathbf{x}_{N-1} | z_i, z_j; \mathbf{x}_i, \mathbf{x}_j, i \in (N-2), j \in (N_0)) \\
 &\quad \dots \\
 &\quad f_{2|1 \cup (N_0)}(z_2; x_2 | z_1, z_j; \mathbf{x}_1, \mathbf{x}_j, j \in (N_0)) \\
 &\quad f_{1|(N_0)}(z_1; x_1 | z_j; \mathbf{x}_j, j \in (N_0))
 \end{aligned}$$

The sequential simulation algorithm remains the same, but instead of drawing the first value  $z_1$  from the marginal pdf of  $Z(\mathbf{x}_1)$  it is drawn from the conditional pdf of  $z(x_1)$  given the original  $N_0$  data. One proceeds from there by including the original  $N_0$  data in the computation of all conditional probabilities, e.g., the second step of the algorithm will be: determine the conditional pdf of  $Z(\mathbf{x}_2)$  given  $Z(\mathbf{x}_1) = z_1$  and  $Z(\mathbf{x}_j) = z_j, j \in (N_0)$ .

**Exactitude Property.** The sets  $(N)$  and  $(N_0)$  may have a non-null intersection in which case at some particular step  $k$ , the random variable to be simulated  $Z(x_k)$  may coincide with the location of one datum, i.e.,  $z_k, \mathbf{x}_k, k \in (N_0)$ . In such a case the conditional pdf

$$f_{k|(k-1) \cup (N_0)}(z; \mathbf{x}_k | z_i, z_j; \mathbf{x}_i, \mathbf{x}_j : i \in (k-1), j \in (N_0)) = \delta(z - z_k)$$

is equal to a Dirac delta function at  $z_k$ , that is, the simulated value is necessarily equal to the datum value  $z_k$ .

It is said that the conditional realization  $\{z_i, x_i, i \in (N)\}$  honors the data values.

### 3.2 Conditional Probabilities

This section will discuss how the conditional probabilities in Eq. (3.2) can be obtained for three cases. The first case corresponds to a RF  $Z(\mathbf{x})$  stationary in the strict-sense with a Gaussian  $n$ th-order pdf. The second case corresponds to a second-order stationary RF  $Z(\mathbf{x})$ , with any generic second-order pdf. The third case is an extension of the first one to the joint simulation of two random functions  $Y(\mathbf{x})$  and  $Z(\mathbf{x})$ , both of them strict-sense stationary and with a joint Gaussian  $n$ th-order density pdf.

We will further consider ergodic models  $Z(\mathbf{x})$  and  $Y(\mathbf{x})$  so that their respective means and covariances can be inferred from the data of a single realization. However, ergodicity is not required for the determination of the conditional probabilities, since they are not inferred from data.

#### MultiGaussian Random Functions

If  $Z(\mathbf{x})$  is strict-sense stationary and its  $n$ th-order pdf is Gaussian, then  $Z(\mathbf{x})$  is fully characterized by its mean  $m$  and its covariance  $C(\mathbf{r})$  (Anderson, 1984). The mathematical congeniality of the multivariate Gaussian density function makes multiGaussian-related RFs the preferred choice among stochastic models, in particular, for modeling uncertainty due to spatial variability of hydraulic conductivity.

It can be shown (Anderson, 1984) that the conditional density function of  $Z(\mathbf{x})$  given any set of data  $\{z_i; \mathbf{x}_i : i \in (n)\}$  is a Gaussian distribution with expected value given by

$$E\{Z(\mathbf{x})|Z(\mathbf{x}_i) = z_i : i \in (n)\} = \left(1 - \sum_{i \in (n)} \lambda_i(\mathbf{x})\right) m + \sum_{i \in (n)} \lambda_i(\mathbf{x}) z_i$$

and variance given by

$$\text{Var}\{Z(\mathbf{x})|Z(\mathbf{x}_i) = z_i : i \in (n)\} = C(0) - \sum_{i \in (n)} \lambda_i(\mathbf{x}) C(\mathbf{x} - \mathbf{x}_i)$$

where the coefficients  $\lambda_i(\mathbf{x})$  are the solution of the following system of normal equations (Luenberger, 1969) also known as simple kriging equations (Journel and Huijbregts, 1978).



$$\sum_{i \in (n)} \lambda_i(\mathbf{x}) C(\mathbf{x}_i - \mathbf{x}_j) = C(\mathbf{x} - \mathbf{x}_j) \quad \forall j \in (n)$$

Note that the coefficients  $\lambda_i(\mathbf{x})$  are functions of the location  $\mathbf{x}$  of the point being estimated.

### Non-Gaussian Random Functions

If the RF  $Z(\mathbf{x})$  is second-order stationary with a non-Gaussian second-order density function the conditional pdfs in (3.2) are not any more Gaussian. In such a case, we can use a non-parametric approach to estimate the conditional probabilities in (3.2). Instead of estimating the parameters of the conditional distribution, we will estimate its value for a selected number of thresholds  $\{z_k, k = 1, \dots, K\}$ .

The definition (3.1) of the indicator RF for threshold  $z_k$  is repeated here:

$$I(z_k; \mathbf{x}) = \begin{cases} 0 & \text{if } Z(\mathbf{x}) > z_k \\ 1 & \text{if } Z(\mathbf{x}) \leq z_k \end{cases}$$

**Note.** For inference reasons we will consider  $Z(\mathbf{x})$  as distribution-ergodic, we will also consider all indicator RFs for all possible values of  $z_k$  within the range of variability  $Z(\mathbf{x})$  as covariance-ergodic.

The conditional expected value of  $I(z_k; \mathbf{x})$  given the set of values  $\{z_i; \mathbf{x}_i : i \in (n)\}$  is

$$\begin{aligned} & E\{I(z_k; \mathbf{x}) | z_i; \mathbf{x}_i : i \in (n)\} \\ &= 0 \times P\{Z(\mathbf{x}) > z_k | z_i; \mathbf{x}_i : i \in (n)\} + 1 \times P\{Z(\mathbf{x}) \leq z_k | z_i; \mathbf{x}_i : i \in (n)\} \\ &= P\{Z(\mathbf{x}) \leq z_k | z_i; \mathbf{x}_i : i \in (n)\} \end{aligned}$$

Therefore, we can estimate the value of the conditional probabilities  $P\{Z(\mathbf{x}) \leq z_k | z_i; \mathbf{x}_i : i \in (n)\}, k = 1, \dots, K$  by estimating the corresponding indicator conditional expectation  $E\{I(z_k; \mathbf{x}) | z_i; \mathbf{x}_i : i \in (n)\}, k = 1, \dots, K$ .

The exact derivation of these conditional expectation is usually very demanding. An approximation that is easier to compute (Journel and Alabert, 1989) is the expected value of the indicator RF at location  $\mathbf{x}$  for threshold  $z_k$  given the indicator transforms of the nearby data for the same threshold:  $E\{I(z_k; \mathbf{x}) | i(z_k; \mathbf{x}_i) : i \in (n)\}, k = 1, \dots, K$  where  $i(z_k; \mathbf{x}_i)$  is the indicator transform of the datum  $z_i; \mathbf{x}_i$  for threshold  $z_k$ . The estimation of these conditional expected values is obtained by the following linear combination (Journel, 1986)

$$\begin{aligned} F_{Z|(n)}^*(z_k; \mathbf{x} | z_i, \mathbf{x}_i : i \in (n)) &\approx E\{I(z_k; \mathbf{x}) | i(z_k; \mathbf{x}_i) : i \in (n)\} \\ &\approx (1 - \sum_{i \in (n)} \lambda_i(z_k; \mathbf{x})) F_Z(z_k) + \sum_{i \in (n)} \lambda_i(z_k; \mathbf{x}) i(z_k; \mathbf{x}_i), \\ &\quad k = 1, \dots, K \end{aligned}$$

where the superscript asterisk indicates an estimated value,  $F_Z(z_k)$  is the marginal cdf of  $Z(\mathbf{x})$ ,  $i(z_k; \mathbf{x}_i)$  is the indicator transform of the sample value  $z_i$  at location  $\mathbf{x}_i$  for threshold  $z_k$  and  $\lambda_i(z_k; \mathbf{x})$  is the corresponding simple kriging weight. Note that the weights are function of both the threshold  $z_k$  and the location  $\mathbf{x}$  at which the conditional distribution function is to be estimated. The weights are obtained by solving an indicator kriging system using the corresponding stationary indicator covariance function  $C_I(z_k; \mathbf{r})$ :

$$\begin{aligned} \sum_{i \in (n)} \lambda_i(z_k; \mathbf{x}) C_I(z_k; \mathbf{x}_i - \mathbf{x}_j) &= C_I(z_k; \mathbf{x} - \mathbf{x}_j) \quad \forall j \in (n) \\ &\quad k = 1, \dots, K \end{aligned}$$

Once an estimate of the conditional cdf at a few carefully chosen thresholds  $\{z_k, k = 1, \dots, K\}$  has been obtained, the  $(K + 1)$  within-class distributions can be interpolated by some within-class distribution, e.g., uniform for all classes and Pareto for the last one (Journel, 1987). Fig. 3.1 shows an example of such an interpolated cdf. The estimated values are represented by stars, a uniform distribution is assumed between estimated values for the first  $K$  classes

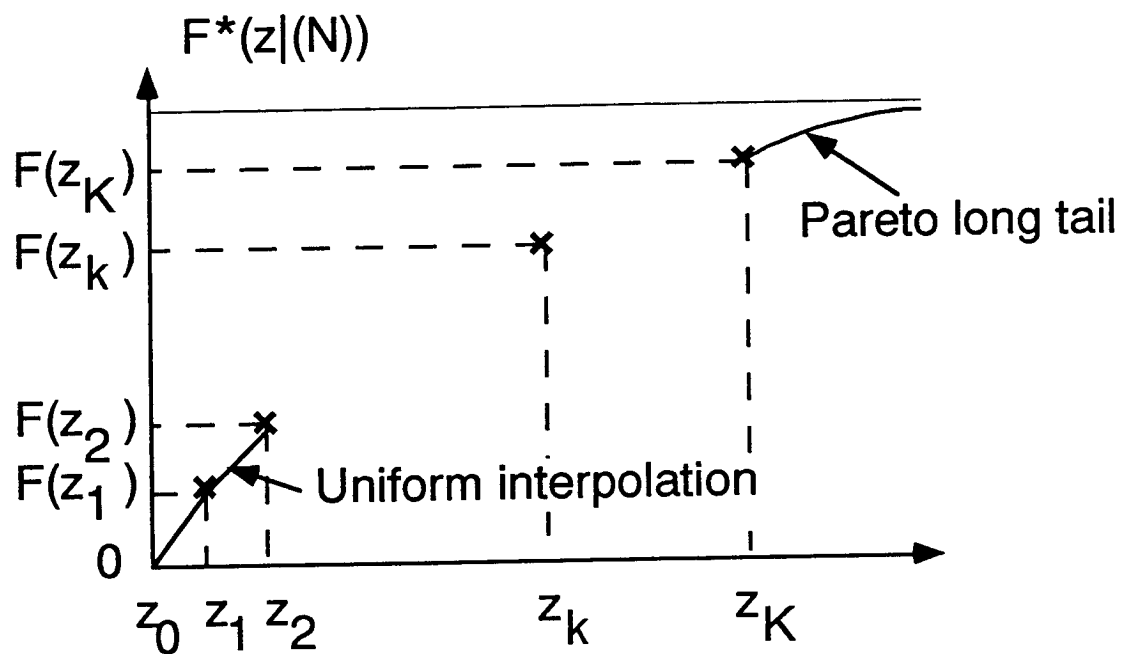


Figure 3.1: **Within-class cdf models.** After estimating a cdf at a selected number of thresholds  $\{z_k, k = 1, \dots, K\}$ , the cdf is interpolated within the  $K + 1$  classes determined using a uniform distribution for the first  $K$  classes and a Pareto distribution for the last one

$$F(z) = (z - z_{k-1}) \frac{F(z_k) - F(z_{k-1})}{z_k - z_{k-1}} \quad \forall z \in ]z_{k-1}, z_k] \\ \forall k = 1, \dots, K \\ \text{with } z_0 = z_{\min}$$

and a Pareto distribution for the last class

$$F(z) = 1 - \frac{z_K[1 - F(z_K)]}{z} \quad \forall z \geq z_K$$

The choice of the uniform and Pareto distributions is merely a convenient example. When the total number of thresholds is small, the choice of these within-class models may have a large impact on the final results and a sensitivity analysis is recommended to find how the final results vary with the choice of within-class distributions.

## Jointly MultiGaussian Random Functions

Finally, we will extend the results on the simulation of a multiGaussian random function to the co-simulation of two (or more) random functions,  $Y(\mathbf{x})$  and  $Z(\mathbf{x})$  which are strict-sense stationary and jointly multiGaussian.

By jointly multiGaussian, we mean that any  $n$ th-order joint cdf of  $Y(\mathbf{x})$  and  $Z(\mathbf{x})$

$$F(y_1, \dots, y_n, z_1, \dots, z_n; \mathbf{x}_1, \dots, \mathbf{x}_n) \\ = P\{Y(\mathbf{x}_1) \leq y_1, \dots, Y(\mathbf{x}_n) \leq y_n, Z(\mathbf{x}_1) \leq z_1, \dots, Z(\mathbf{x}_n) \leq z_n\}$$

is Gaussian.

Since they are strict-sense stationary their joint distribution is fully characterized by their means  $m_Y$  and  $m_Z$ , their covariances  $C_Y(\mathbf{r})$  and  $C_Z(\mathbf{r})$  and their stationary cross-covariances  $C_{YZ}(\mathbf{r})$  and  $C_{ZY}(\mathbf{r})$ , with

$$C_{YZ}(\mathbf{r}) = C_{ZY}(\mathbf{r}) = E\{(Y(\mathbf{x}) - m_Y)(Z(\mathbf{x} + \mathbf{r}) - m_Z)\}$$

By using the definition of conditional probability we can decompose the joint multivariate pdf in the product of conditional univariate pdfs in a manner similar to (3.2):

$$\begin{aligned}
& f(y_i, z_i; \mathbf{x}_i, i \in (N)) \\
&= f_{Y_N|(N-1),(N)}(y_N; \mathbf{x}_N | y_i, z_j; \mathbf{x}_i, i \in (N-1), \mathbf{x}_j, j \in (N)) \\
&\quad f_{Z_N|(N-1),(N-1)}(z_N; \mathbf{x}_N | y_i, z_i; \mathbf{x}_i, i \in (N-1)) \\
&\quad \cdots f_{Z_2|1,1}(z_2; \mathbf{x}_2 | y_1, z_1; \mathbf{x}_1) f_{Y_1|-1,1}(y_1; \mathbf{x}_1 | z_1; \mathbf{x}_1) f(z_1; \mathbf{x}_1)
\end{aligned} \tag{3.3}$$

where  $f_{Y_n|(n-1),(n)}$  represents the conditional pdf of the random variable  $Y(\mathbf{x}_n)$  given the  $y$  data at locations  $(n-1)$  and the  $z$  data at locations  $(n)$ ; and similarly for  $f_{Z_n|(n-1),(n-1)}$ .

For the joint multiGaussian case, all conditional probabilities appearing in the previous decomposition are Gaussian; the mean and variance of each is given by the solution of a multivariate version of the normal equations also known as simple co-kriging system. For instance, the mean and variance of the conditional probability of  $Y(\mathbf{x})$  given the sets of data  $\{y_i; \mathbf{x}_i : i \in (n_y)\}$  and  $\{z_j; \mathbf{x}_j : j \in (n_z)\}$  are

$$\begin{aligned}
E\{Y(\mathbf{x}) | Y(\mathbf{x}_i) = y_i, Z(\mathbf{x}_j) = z_j, i \in (n_y), j \in (n_z)\} \\
= m_Y + \sum_{i \in (n_y)} \lambda_i(\mathbf{x})(y_i - m_Y) + \sum_{j \in (n_z)} \nu_j(\mathbf{x})(z_j - m_Z)
\end{aligned}$$

$$\begin{aligned}
\text{Var}\{Y(\mathbf{x}) | Y(\mathbf{x}_i) = y_i, Z(\mathbf{x}_j) = z_j, i \in (n_y), j \in (n_z)\} \\
= C_Y(0) - \sum_{i \in (n_y)} \lambda_i(\mathbf{x}) C_Y(\mathbf{x} - \mathbf{x}_i) \\
- \sum_{j \in (n_z)} \nu_j(\mathbf{x}) C_{YZ}(\mathbf{x} - \mathbf{x}_j)
\end{aligned}$$

where the coefficients  $\lambda_i$  and  $\nu_j$  are given by the following set of simple co-kriging equations

$$\begin{aligned}
\sum_{i \in (n_y)} \lambda_i(\mathbf{x}) C_Y(\mathbf{x}_i - \mathbf{x}_k) + \sum_{j \in (n_z)} \nu_j(\mathbf{x}) C_{YZ}(\mathbf{x}_j - \mathbf{x}_k) &= C_Y(\mathbf{x} - \mathbf{x}_k) \quad \forall k \in (n_y) \\
\sum_{i \in (n_y)} \lambda_i(\mathbf{x}) C_{YZ}(\mathbf{x}_i - \mathbf{x}_k) + \sum_{j \in (n_z)} \nu_j(\mathbf{x}) C_Z(\mathbf{x}_j - \mathbf{x}_k) &= C_{YZ}(\mathbf{x} - \mathbf{x}_k) \quad \forall k \in (n_z)
\end{aligned}
\tag{3.4}$$

**Extension to More Than Two Random Functions Jointly MultiGaussian.** The extension to three or more RFs jointly multiGaussian is straightforward. The joint conditional pdf of all the RFs is decomposed in a manner similar to (3.3) as a product of conditional probabilities of each random variable given the other ones. All conditional probabilities are Gaussian with mean and variance derived from a set of simple co-kriging equations. To set up these equations requires that all covariances and cross-covariances between any two of the RFs be known, in addition to their expected values.

### 3.3 Implementation

This section contains the author's contribution. It discusses the major problems encountered during the implementation of the sequential simulation technique.

#### Markov Paradigm

The sequential simulation algorithm as described in section 3.1 is completely general and has no exception. Expressions for the conditional probabilities have been provided for three possible random function models. However, the number of equations that must be solved to obtain the estimates of the conditional pdfs increases with the number of previously simulated points and quickly becomes unwieldy. In the limit, at the  $N$ th step, the conditional probability of  $Z(\mathbf{x}_N)$  given the  $(N - 1)$  other points has to be estimated. If  $N$  is larger than a few hundred, to compute exactly

the conditional distribution functions is an extremely costly if not impossible task. Therefore, approximations are required.

A good approximation of the conditional probabilities in (3.2) can be obtained by retaining only those conditioning values which are most consequential.

For example, approximate

$$f_{N|(N-1)}(z_N; \mathbf{x}_N | z_i; \mathbf{x}_i : i \in (N-1))$$

by

$$f_{N|(n)}(z_N; \mathbf{x}_N | z_j; \mathbf{x}_j : j \in (n) \subset (N-1))$$

with  $n \ll N-1$ . Of all possible subsets  $\{z_j; \mathbf{x}_j : j \in (n)\}$  of size  $n$ , we should retain the one that allows a best approximation of the conditional pdf  $f_{N|(N-1)}(z_N; \mathbf{x}_N | z_i; \mathbf{x}_i : i \in (N-1))$ .

In most cases, that subset of size  $n$  is constituted by the conditioning values “closest” to  $Z(\mathbf{x}_N)$ ; “closest” being defined in terms of some correlation function. For instance, if the  $N$  random functions represent hydraulic conductivities at  $N$  locations, and the variogram  $\gamma(\mathbf{r})$  is monotonic increasing, the  $(n)$  most consequential values will generally be the closest values using the variogram value  $\gamma(\mathbf{x}_1 - \mathbf{x}_2)$  as the distance between locations  $\mathbf{x}_1$  and  $\mathbf{x}_2$ . The exception being when the conditioning data are clustered, and therefore redundant, in which case it would be better to retain one datum per cluster and fetch more data in an unclustered zone even though their distance to the point being estimated could be larger than the distance from the cluster.

Retaining the “closest” values amounts to assume that the RF features some Markovian behavior: for a one-dimensional Markov process  $A(t)$ , the conditional probability  $P\{A(t)|A(t-1), A(t-2), \dots, A(t_0)\}$  is equal to  $P\{A(t)|A(t-1)\}$ , i.e., the closest random variable “screens” the information provided by all other random variables.

In practice, an ellipsoidal search neighborhood homothetic to the variogram anisotropy ellipsoid centered at  $\mathbf{x}_N$  is defined and only the closest  $n_0$  conditioning locations in each of the eight octants with apex  $\mathbf{x}_N$  are retained. “Closeness” is defined in terms

of the variogram distance  $\gamma(\mathbf{r})$  instead of the Euclidean distance  $|\mathbf{r}|$ . An example of this procedure is illustrated in Fig 3.2 for a two-dimensional case. In this figure, four quadrants are defined by the principal axes of the search ellipse. A maximum of two points is retained per quadrant. In quadrant I, datum  $a$  is preferred to the closer (in an Euclidean sense) datum  $b$  because the variogram value for the vector joining  $x_N$  and  $a$  is smaller than the variogram value for the vector joining  $x_N$  and  $b$ ; in quadrant II, there is only one datum; in quadrant III, the two closest values are retained; and in quadrant IV, there is a cluster of data from which the two closest values are retained; note that because of the redundancy of the remaining data in quadrant IV, it is preferable to select the only datum in quadrant II than any of the closer values in quadrant IV.

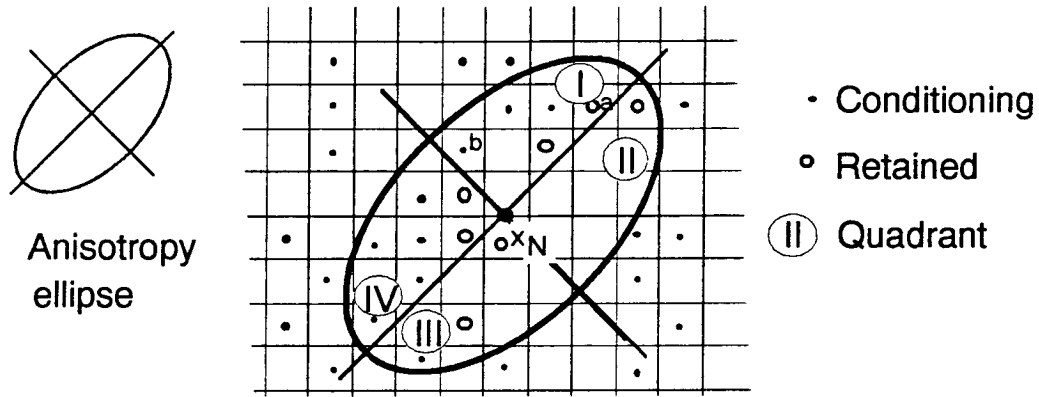


Figure 3.2: **Search neighborhood.** Example of how to select the most consequential points to approximate the conditional density of  $Z(\mathbf{x}_N)$  given a large number of points using the concepts of search neighborhood, octant search and variogram distance

The use of a search neighborhood implies that only the covariances for lags up to the dimensions of the search neighborhood can be reproduced in the final set of realizations. For this reason, we recommend that the search neighborhood should be at least as large as the correlation ranges of the variogram in every direction.



## Visiting Sequence

The sequence employed to visit the  $N$  locations used to define the realizations does not influence their statistics since in the expansion of the  $n$ th-order density function as a product of univariate conditional simulations (Eq. 3.2) there is no implicit ordering of the sequence  $\mathbf{x}_1, \mathbf{x}_2, \dots, \mathbf{x}_N$ . However, because of the simplifications required for the computation of these conditional probabilities, namely, the use of the Markov paradigm and the use of an octant search within the search neighborhood, we recommend a visiting sequence following a random path through the  $N$  nodes. Such a random path also minimizes the artifacts that may appear on a spatially sequential path.

## Order Relation Violations

In the non-parametric evaluation of the conditional probabilities in Eq. (3.2), estimates for different thresholds are obtained. These estimates may violate some of the order relations that any cdf should fulfill:  $F_{Z|n}^*(z_k; \mathbf{x}|(n)) \geq 0$ ,  $F_{Z|n}^*(z_k; \mathbf{x}|(n)) \leq 1$  or  $F_{Z|n}^*(z_k; \mathbf{x}|(n)) \leq F_{Z|n}^*(z'_k; \mathbf{x}|(n))$  for  $z_k > z'_k$ . When any of these inequalities are violated, the estimates  $F_{Z|n}^*(z_k; \mathbf{x}|(n))$  and  $F_{Z|n}^*(z'_k; \mathbf{x}|(n))$  must be corrected. (For more details on how to carry out this correction see Sullivan, 1984, p. 36–24.)

## Programming

The writing of efficient code to implement the sequential simulation algorithm required the solution of a number of problems that are discussed below.

The programs have been designed to generate a realization over a rectangular grid with a total of  $N$  nodes. In this way the coordinates of the points to be simulated can be determined by the number of nodes in each coordinate direction, the size of the unit cell, and the coordinates of the first node. The programs could be modified easily to handle an irregular grid; in such a case, the coordinates of each node must be provided explicitly.

**Random Path.** As discussed earlier, the visiting sequence for the simulation of values at the  $N$  nodes must be given by a random path. An integer index is assigned to each node and a random sequence of these indices is generated using a congruential generator of the form (Bratley et al., 1983):

$$\text{index}_i = (5 \times \text{index}_{i-1} + 1) \bmod 2^n$$

This generator produces once and only once each integer value between 1 and  $2^n$ . By selecting the smallest power of 2 that is larger than  $N$  we are assured that all indices are generated. Index values that are larger than the total number of nodes are simply discarded.

**Searching.** When simulating a value, only the data within the search neighborhood are considered and, furthermore, only the closest  $n_0$  such data per octant are used—where  $n_0$  is a value preset by the user. A procedure for the fast retrieval of the closest  $n_0$  conditioning values per octant within the search neighborhood is required.

The conditioning values could be close to the point being simulated or they could be widely scattered within the search neighborhood. At the beginning of the simulation when only few nodes have been simulated and the conditioning data set is small, the points retained for kriging can be located as far as the limits of the search neighborhood. Conversely, towards the end of the random path, the conditioning data set will have grown large—it may include almost all nodes within the search neighborhood—and the closest points retained will be located close to the node being simulated.

The procedure implemented for efficient search for the closest data is based on a lookup table containing distances from, and relative coordinates to, the centerpoint. Since the simulation grid is regular, we can build a template, independent of the point being simulated, that contains the relative coordinates to the centerpoint of all nodes within the search neighborhood ordered from closest to the centerpoint to farthest. This template should also contain the octant to which each point belongs. (Remember that “closeness” is defined using the variogram distance instead of the

Euclidean distance.) When simulating a value, the template is searched to find which values have already been simulated. The search stops when  $n_0$  values per octant are found. Thus, there is only one prior search to establish the search template, then the selection of points to be used for the simulation of any node is done by looking in a template of ordered distances.

**Covariance Lookup Table.** Once the conditioning data have been selected, the normal systems of linear equations must be built. These systems of equations contain all possible covariance values between: i) any two conditioning values, ii) any conditioning value and the value being simulated. The conditioning data are limited to those within the search neighborhood, the covariance is stationary, and the nodes are over a regular grid. Therefore, the number of possible different covariance values used to simulate any point is finite; these covariances can be computed a priori and stored in central memory. In this way, building the kriging systems reduces to looking up the covariance values in a table.

**Note 1.** In the non-parametric approach to the estimation of conditional cdfs, the number of covariance tables will equal the number  $K$  of thresholds used to discretize the range of variability of  $Z(\mathbf{x})$  since the indicator covariances may be different from one another. Similarly, in the joint simulation of several variables, tables for the covariances of each variable and for the cross-covariances between every pair of variables are needed.

**Note 2.** The covariance look-up table as well as the search template assume that the initial conditioning data have been relocated to the nearest grid nodes, so that both conditioning data and simulated nodes fall in a regular grid.

**Two-steps Simulation.** The covariance tables may contain an extremely large number of entries if the search neighborhood contains a large number of points. This will be the case if the node spacing is small with respect to the ranges of the variogram. To reduce the central memory requirements in these cases a two-steps approach is used.

In the two-steps approach the random path is divided into two paths. The first

path visits all nodes located over a coarse grid, the spacing of which is a multiple integer of the spacing in the final fine grid. The second path visits the remaining nodes located on the fine grid. During the simulation of the nodes on the first path, the search neighborhood will be large in size, yet the number of points on the coarse grid contained within the search neighborhood will be small. During the simulation of the nodes on the second path, the size of the search neighborhood is reduced to twice the spacing of the nodes on the coarse grid. In this way, both search neighborhoods will contain a small number of points and the size of the covariance lookup tables will be small. The lookup tables will be different for each path. In the first path, the lookup tables will contain covariance values for large distances. In the second path, the lookup tables will contain covariance values for small distances. The objective of the two-steps simulation is to reproduce the covariances for both large and short distances without having to resort to the use of a large neighborhood on a fine grid. The simulation over the coarse grid using a large search neighborhood will allow the reproduction of the large scale correlation; whereas the simulation over the small grid using a smaller search neighborhood will reproduce the small scale correlation.

**Simple Kriging or Ordinary Kriging?** Theory indicates that simple kriging equations be used for the evaluation of the conditional density functions in section 3.2, whereas experience indicates that ordinary kriging is more appropriate. Indeed, ordinary kriging provides better robustness with regard to the assumption of stationarity. The use of a search neighborhood along with ordinary kriging—amounts to an implicit re-estimation of the mean value of the random function at each location using the conditioning data within the search neighborhood. Thus, the assumption of stationarity of the random function is relaxed allowing its mean to vary, smoothly, from one location to another. It is said that “ordinary kriging corrects for local departures from stationarity” (Journel and Rossi, 1989).

Thus, sometimes we may wish to use ordinary kriging to estimate the conditional density functions particularly if the number of conditioning data is large and we observe spatial trends in the data values that may be interpreted as local departures from the stationarity decision. In such cases, the ordinary kriging estimation of the

conditional density functions is not anymore theoretically correct, but from a practical point of view, it may yield better results than using the simple kriging equations.

The ordinary kriging equations for the three cases discussed in section 3.2 follow. The first case corresponds to multiGaussian random functions.

$$\begin{aligned} E\{Z(\mathbf{x})|Z(\mathbf{x}_i) = z_i : i \in (n)\} &\approx \sum_{i \in (n)} \lambda_i(\mathbf{x}) z_i \\ \text{Var}\{Z(\mathbf{x})|Z(\mathbf{x}_i) = z_i : i \in (n)\} &\approx C(0) - \sum_{i \in (n)} \lambda_i(\mathbf{x}) C(\mathbf{x} - \mathbf{x}_i) - \mu(\mathbf{x}) \end{aligned}$$

where the coefficients of  $\lambda_i(\mathbf{x})$  and  $\mu(\mathbf{x})$  are given by the following set of ordinary kriging equations

$$\begin{aligned} \sum_{i \in (n)} \lambda_i(\mathbf{x}) C(\mathbf{x}_i - \mathbf{x}_j) + \mu(\mathbf{x}) &= C(\mathbf{x} - \mathbf{x}_j), \quad \forall j \in (n) \\ \sum_{i \in (n)} \lambda_i(\mathbf{x}) &= 1 \end{aligned}$$

The second case corresponds to random functions with a second-order density not necessarily Gaussian. The use of ordinary kriging to estimate the conditional probabilities is equivalent to assuming that the expected value of the indicator functions, i.e., the marginal distribution function of  $Z(\mathbf{x})$ , varies smoothly with  $\mathbf{x}$  while the indicator covariance functions remain stationary. The estimate of the conditional probabilities for the set of thresholds  $\{z_k, k = 1, \dots, K\}$  is given by

$$F_{Z|(n)}^*(z_k; \mathbf{x} | z_i, \mathbf{x}_i : i \in (n)) \approx \sum_{i \in (n)} \lambda_i(z_k; \mathbf{x}) i(z_k; \mathbf{x}_i), \quad \forall k = 1, \dots, K$$

where the weights are obtained by solving the indicator ordinary kriging systems

$$\begin{aligned} \sum_{i \in (n)} \lambda_i(z_k; \mathbf{x}) C_I(z_k; \mathbf{x}_i - \mathbf{x}_j) + \mu(z_k; \mathbf{x}) &= C_I(z_k; \mathbf{x} - \mathbf{x}_j) \quad \forall j \in (n) \\ \sum_{i \in (n)} \lambda_i(z_k; \mathbf{x}) &= 1 \\ &k = 1, \dots, K \end{aligned}$$

Finally, the third case corresponds to jointly multiGaussian random functions. Its extension allows local departure from stationarity of the means of both RFs  $Y(\mathbf{x})$  and  $Z(\mathbf{x})$

$$\begin{aligned}
& E\{Y(\mathbf{x})|Y(\mathbf{x}_i) = y_i, Z(\mathbf{x}_j) = z_j, i \in (n_y), j \in (n_z)\} \\
& \approx \sum_{i \in (n_y)} \lambda_i(\mathbf{x}) y_i + \sum_{j \in (n_z)} \nu_j(\mathbf{x}) z_j \\
& \text{Var}\{Y(\mathbf{x})|Y(\mathbf{x}_i) = y_i, Z(\mathbf{x}_j) = z_j, i \in (n_y), j \in (n_z)\} \\
& \approx C_Y(0) - \sum_{i \in (n_y)} \lambda_i(\mathbf{x}) C_Y(\mathbf{x} - \mathbf{x}_i) - \sum_{j \in (n_z)} \nu_j(\mathbf{x}) C_{YZ}(\mathbf{x} - \mathbf{x}_j) - \mu_1(\mathbf{x})
\end{aligned}$$

where the parameters  $\lambda_i(\mathbf{x})$ ,  $\nu_j(\mathbf{x})$  and  $\mu_1(\mathbf{x})$  are given by the following set of ordinary co-kriging equations

$$\begin{aligned}
\sum_{i \in (n_y)} \lambda_i(\mathbf{x}) C_Y(\mathbf{x}_i - \mathbf{x}_k) + \sum_{j \in (n_z)} \nu_j(\mathbf{x}) C_{YZ}(\mathbf{x}_j - \mathbf{x}_k) + \mu_1(\mathbf{x}) &= C_Y(\mathbf{x} - \mathbf{x}_k) \quad \forall k \in (n_y) \\
\sum_{i \in (n_y)} \lambda_i(\mathbf{x}) C_{YZ}(\mathbf{x}_i - \mathbf{x}_k) + \sum_{j \in (n_z)} \nu_j(\mathbf{x}) C_Z(\mathbf{x}_j - \mathbf{x}_k) + \mu_2(\mathbf{x}) &= C_{YZ}(\mathbf{x} - \mathbf{x}_k) \quad \forall k \in (n_z) \\
\sum_{i \in (n_y)} \lambda_i(\mathbf{x}) &= 1 \\
\sum_{j \in (n_z)} \nu_j(\mathbf{x}) &= 0
\end{aligned}$$

The use of the ordinary kriging equations introduces the problem of what to do if no data points are found within the search neighborhood. In such a case, a reasonable approach is to revert to the simple kriging equations and use a default value, preset by the user, for the expected values of  $Z(\mathbf{x})$ ,  $I(z_k, \mathbf{x})$  or  $Y(\mathbf{x})$ .

Building on these ideas, the sequential simulation programs used in this dissertation allow the user to specify a minimum number of conditioning points within the search neighborhood below which the program switches to simple kriging. If this number is zero, ordinary kriging always will be used except when no points are found within the search neighborhood. If this number is very large, simple kriging always

will be used since the search neighborhood will never contain as many points as specified. From our experience, we recommend to setting this minimum number to a value larger than 1 to avoid artifacts that may appear if the number of conditioning data points is small or the search neighborhood is very large.

### 3.4 Advantages of Sequential Simulation

Sequential simulation has several advantages over other simulation techniques of which the two most important are: (1) it is completely general, and (2) it is faster than any indirect method for the generation of Gaussian conditional simulations.

The technique of sequential simulation is not limited to the simulation of Gaussian random fields. It can be used for the generation of any random function provided that the conditional probabilities in (3.2) can be estimated. Ways to compute those conditional probabilities have been provided, and, to the best of our knowledge, sequential simulation is presently the only technique that can generate realizations from a random function with a generic bivariate distribution.

Sequential simulation is faster than any indirect technique for the generation of conditional realizations of Gaussian random fields. The cost involved in the generation of a conditional simulation using sequential simulation is that required for the estimation of the conditional pdf at each node being simulated. For the Gaussian case, this reduces to the solution of a simple kriging system of linear equations; the number of equations is limited by the maximum number of points retained within the search neighborhood. On the other hand, the cost involved in the generation of a conditional simulation using an indirect method can be decomposed in the cost required for the generation of an unconditional realization plus the cost required in transforming the unconditional realization into a conditional one. The cost involved in the first step depends on the technique used; but, the conditioning step alone requires the solution of a simple kriging system of linear equations for each node being simulated (see section 2.1). The number of equations cannot be larger than the number of conditioning data or, if this number is too large, than a maximum

number preset by the user. Therefore, unless the number of conditioning data is very small, the cost involved simply in the conditioning step of any indirect method will be comparable to the cost required for the entire conditional sequential simulation.

### 3.5 Programs

Three sequential simulation codes have been written corresponding to the three possible random function models described in section 3.2. The skeleton of these three programs is the same. Differences are related to the specifics of computing the conditional density functions. These three programs called GSIM3D, ISIM3D, and GCOSIM3D are described in Appendix A.



## Chapter 4

# Block Hydraulic Conductivity

The simulation algorithms presented in the previous chapter allows for the fast generation of conditional simulations with possibly hundreds of thousands of nodes. Realizations can be generated at the scale of the measurements allowing reproduction of the spatial variability observed in the field. However, such detailed representations cannot be used because the available numerical codes for flow and transport cannot handle more than a few thousands nodes due to time and/or memory limitations.

This chapter proposes an answer to the previous problem. The detailed realizations still can be used in a Monte-Carlo analysis of flow and transport if the small scale conductivities can be averaged into a larger scale that can be handled efficiently by currently available numerical codes.

Two methods for computing block hydraulic conductivities will be discussed. The first, analytical method is limited to two-dimensions with small, isotropic variability of the logarithm of hydraulic conductivity. The development of this method closely follows the paper by Rubin and Gómez-Hernández (1990). The second is numerical and it is not subject to any limit statistics; although developed in two dimensions it can be straightforwardly extended to three.

The starting point is a hydraulic conductivity field, generated at the data scale by one of the simulation algorithms described in the previous chapter. Such realizations

are assumed completely known at the scale of the simulation grid. The objective is to find a procedure to derive from it block hydraulic conductivities. This procedure could be as simple as taking the geometric mean of the point values within each block or as complex as a function of the values within and around the block, of their variability, of spatial correlation, of the block size and of the flow patterns resulting from different boundary conditions.

## 4.1 Statement of the Problem

Given a block of volume  $V$  exhaustively sampled for hydraulic conductivity, we define block hydraulic conductivity as a tensor  $\mathbf{K}_V$  that satisfies relation (2.2). This relation, reproduced below, can be interpreted as Darcy's law at the block level,

$$\overline{\mathbf{q}} = -\mathbf{K}_V \overline{\nabla h}, \quad \text{for given boundary conditions} \quad (4.1)$$

where the overbar is used to denote a spatial average over the block, that is,

$$\begin{aligned} \overline{\mathbf{q}} &= \frac{1}{V} \int_V \mathbf{q} \, d\mathbf{x} \\ \overline{\nabla h} &= \frac{1}{V} \int_V \nabla h \, d\mathbf{x} \end{aligned}$$

and where  $\mathbf{q}$  and  $\nabla h$  are related through Darcy's law at the smallest scale:

$$\mathbf{q} = -\mathbf{K} \nabla h. \quad (4.2)$$

where  $\mathbf{K}$  is the point hydraulic conductivity tensor,  $\mathbf{q}$  is the specific discharge and  $h$  is the hydraulic head equal to  $z + p/\rho g$  ( $z$  being elevation with respect some datum,  $\rho$  the fluid density and  $p$  the pressure and  $g$  is the acceleration of gravity).

Note that the values of  $\mathbf{q}$  and  $\nabla h$  can only be obtained after boundary conditions have been specified around the block; therefore, the definition of  $\mathbf{K}_V$  also depends on these boundary conditions.

This definition has two properties that justify its choice. First, if  $\mathbf{K}_V$  is seen as a realization from an ergodic random function allowing an exchange of spatial integrals

over one realization with expected values through the ensemble of realizations, the limit of relation (4.1) as  $V$  tends towards infinity coincides with the definition of effective conductivity,  $\mathbf{K}_{\text{eff}}$ , as given in (2.3). Second, when the boundary conditions used are those in Fig. 2.3, the resulting  $\mathbf{K}_V$  identifies the traditional value obtained using Eq. (2.12) (see p. 25 and following).

In the analytical approach we will consider that the point hydraulic conductivity is isotropic to flow; therefore, it can be represented by the scalar function  $K(\mathbf{x})$ . This assumption is not required for the numerical approach. Even though all examples use isotropic point conductivities in two dimensions, the numerical approach proposed can handle anisotropic hydraulic conductivities.

The following conventions are used throughout this chapter. Upper case boldface letters denote tensorial quantities, such as  $\mathbf{K}_V$ ; lower case boldface letters denote vectors, such as  $\mathbf{q}$ , and plain letters denote scalars, such as  $h$ . Unless necessary, no explicit reference will be made to the space dimensionality (whether two or three). We refer to the “volume”  $V$ ; however,  $V$  can represent an area in two dimensions, or a volume in three. Furthermore, if explicit reference to the components of a coordinate vector  $\mathbf{x}$  is needed we will use Cartesian coordinates  $(x, y)$  or  $(x, y, z)$ . There should be no confusion between the vector  $\mathbf{x}$  and its first component  $x$ . Similarly,  $\mathbf{K}_V$  is a two by two symmetric, positive-definite, tensor in two-dimensions, and three by three in three dimensions.

## 4.2 Analytical approach

### Necessary Assumptions

The following assumptions are made:

1. Point hydraulic conductivity is isotropic to flow; therefore, it can be described by a scalar function  $K(\mathbf{x})$ .
2. The spatial variability of  $K(\mathbf{x})$  is isotropic: that is, there is no preferential direction of continuity.

3. The spatial variability of  $K(\mathbf{x})$  is small. More precisely, we require that the fluctuations of the log-conductivity  $Y(\mathbf{x}) = \ln K(\mathbf{x})$  about its spatial average be small, so that fluctuations raised to a power larger than two are negligible.
4. The block is embedded in an infinite domain with boundary conditions given by a constant flow at infinity.
5. The flow regime is at steady-state.

In the most common case, as a result of assumptions 1 and 2, the block conductivity is also isotropic to flow; therefore, it can be represented by a scalar  $K_V$ . Thus, we can assume that average flow and average gradient are co-linear.

From these assumptions, the flow pattern can be described by a set of quasi-parallel flow lines. The flow vector  $\mathbf{q}$  at any given location can be decomposed as a constant vector equal to the arithmetic average over the entire aquifer plus a fluctuation vector, the components of which are small. Similarly, the gradient vector  $\nabla h$  is decomposed as a constant vector equal to its arithmetic average over the entire aquifer plus a small fluctuation.

## Development

At any location  $\mathbf{x}$  we can write,

$$\begin{aligned} Y(\mathbf{x}) &= \ln K(\mathbf{x}) \\ Y(\mathbf{x}) &= Y_a + Y'(\mathbf{x}) \\ K(\mathbf{x}) &= K_g \exp(Y'(\mathbf{x})); \quad K_g = \exp(Y_a) \end{aligned}$$

$$\begin{aligned} \mathbf{j}(\mathbf{x}) &= \nabla h(\mathbf{x}) \\ \mathbf{j}(\mathbf{x}) &= \mathbf{j}_a + \mathbf{j}'(\mathbf{x}) \end{aligned} \tag{4.3}$$

$$\mathbf{q}(\mathbf{x}) = \mathbf{q}_a + \mathbf{q}'(\mathbf{x}) \tag{4.4}$$

where the subindex  $a$  indicates the arithmetic average computed over the **entire** aquifer, and  $g$  the geometric average; the primed quantities are the fluctuations about the arithmetic means. As stated in the assumptions, fluctuations raised to a power larger than 2 can be neglected.

If the  $x$ -axis is aligned with the average gradient vector ( $\mathbf{j}_a$ ) (also the direction of the average flow vector), the only non-zero components of  $\mathbf{j}_a$  and  $\mathbf{q}_a$  will be their  $x$ -components. Taking the arithmetic average of (4.3) and (4.4), substituting in (4.1) and rewriting in terms of the vector components in two dimensions results in

$$\begin{aligned} q_a + \overline{q'_x} &= -K_V (j_a + \overline{j'_x}) \\ \overline{q'_y} &= -K_V \overline{j'_y} \end{aligned}$$

The second equation is discarded because it only involves spatial averages of small perturbations (the limits of which, as the block tends towards infinity, are zero). From the first linear equation we obtain the value for  $K_V$

$$K_V = - \frac{q_a + \overline{q'_x}}{j_a + \overline{j'_x}} \quad (4.5)$$

The value in the numerator ( $q_a + \overline{q'_x}$ ) can be obtained from Darcy's law (4.2): the  $x$ -component of  $\mathbf{q}$  is

$$q_a + q'_x(\mathbf{x}) = -K(\mathbf{x})(j_a + j'_x(\mathbf{x})).$$

Averaging over the block and dropping the explicit dependence of the various quantities on  $\mathbf{x}$  yields

$$q_a + \overline{q'_x} = -\overline{K(j_a + j'_x)}.$$

Substituting in (4.5) leads to

$$K_V = \frac{\overline{K(j_a + j'_x)}}{j_a + \overline{j'_x}}.$$

Substituting  $K$  by its expression in (4.3) gives

$$K_V = K_g \frac{\overline{\exp(Y')(j_a + j'_x)}}{j_a + \overline{j'_x}}.$$

Expanding  $\exp(Y')$  and  $1/(j_a + \overline{j'_x})$  in Taylor series and retaining only the terms up to second order we arrive at

$$K_V = K_g \left[ \overline{\left(1 + Y' + \frac{Y'^2}{2} + \dots\right)(j_a + j'_x)} \right] \frac{1}{j_a} \left(1 - \frac{\overline{j'_x}}{j_a} + \frac{\overline{j'^2_x}}{j_a} + \dots\right).$$

Further expansion ignoring terms of order larger than two leads to

$$\begin{aligned} K_V &= K_g \left(1 + \overline{Y'} + \frac{\overline{Y'^2}}{2} + \frac{\overline{j'_x}}{j_a} + \frac{\overline{Y'j'_x}}{j_a}\right) \cdot \left(1 - \frac{\overline{j'_x}}{j_a} + \frac{\overline{j'^2_x}}{j_a}\right) \\ &= K_g \left[1 + \overline{Y'} + \frac{\overline{Y'^2}}{2} + \frac{1}{j_a} (\overline{Y'j'_x} - \overline{Y'} \overline{j'_x})\right] \end{aligned} \quad (4.6)$$

Equation (4.6) is a closed-form approximation for the value of  $K_V$ . From this expression we observe that the block value is a function of the geometric mean of the point values over the entire aquifer, of the variation of the point values within the block ( $\overline{Y'}$  and  $\overline{Y'^2}$ ), and of the flow pattern within the block through the term  $\overline{j'_x}$ . The dependence on  $\overline{j'_x}$  implies dependence on the boundary conditions existing at the sides of the block.

It is interesting to analyze Eq. (4.6) for the limiting case of  $V$  tending towards infinity. In this case, and under ergodic assumptions, the block conductivity should be equal to the effective conductivities discussed in the literature review (see chapter 2). To exchange spatial integrals over the entire aquifer with expected values through the ensemble, we will assume that the underlying conductivity random function is mean- and covariance-ergodic, and that it is also cross-covariance ergodic with the random function model  $j_x$ . Then, the limiting value for  $K_V$  is

$$\lim_{V \rightarrow \infty} K_V = K_g \left(1 + \frac{\sigma_Y^2}{2} + \frac{C_{Yj_x}(0)}{j_a}\right) \quad (4.7)$$

where  $\sigma_Y^2$  is the stationary variance of the RF  $Y(\mathbf{x})$  and  $C_{Yj}$  is the stationary cross-covariance between  $Y$  and  $j_x$ .

The value of the term  $C_{Yj_x}(0)/j_a$  in (4.7) has been evaluated by Gutjahr *et al.* (1978) for one, two and three dimensions using a small fluctuation approach. The result is independent of the form of the covariance of the RF  $Y(\mathbf{x})$  (as long as the assumptions made at the beginning of the section are met). It is equal to  $-\sigma_Y^2/N$ , where  $N$  is the number of dimensions of the space. Substituting this value in (4.7) the limiting values of  $K_V$  are,

$$\lim_{V \rightarrow \infty} K_V = \begin{cases} K_g(1 - \sigma_Y^2/2) & \text{in 1-D} \\ K_g & \text{in 2-D} \\ K_g(1 + \sigma_Y^2/6) & \text{in 3-D} \end{cases}$$

which identify the effective conductivities reported in the literature for the small perturbation approach.

Expression (4.6) has limited practical use for the derivation of  $K_V$  because it requires prior solution of the flow problem within the block in order to evaluate the terms  $\overline{Y'j'_x}$  and  $\overline{j'_x}$ . With such solution, Eq. (4.1), which is completely general and does not require any limiting assumptions, can be used directly. However, Eq. (4.6) is important for the understanding of the factors that determine  $K_V$  and, as discussed in chapter 5, it plays an important role for the stochastic modeling of block conductivities.

### 4.3 Numerical Approach

The numerical approach presented in this section has been designed from a practical point of view. The finite difference method for the solution of the partial differential equation of groundwater flow is selected, and a specific scale-up procedure is proposed.

All figures, examples and formulations will be for a two-dimensional aquifer with square blocks. The extension to three dimensions and/or rectangular blocks is straightforward.

### Starting Point

Following Haldorsen's hierarchy of scales (Haldorsen, 1986), two scales of definition for the hydraulic conductivities are considered: the macroscale, which is the smallest scale at which data (core and well logs) are available, and the megascale, which is the scale of the blocks used in the numerical flow model. The term cell will be used to refer to the discretization unit at the macroscale, and the term block will be reserved for the discretization unit at the megascale. Each cell represents the volume of one possible measurement. Hydraulic conductivity is considered constant within each such cell, which actually amounts to a first averaging. The inter-cell flows will be referred to as macroflows, and the hydraulic heads at the center of each cell as macroheads (see Fig. 4.1). Similarly, the interblock flows will be referred to as megafloes and the block heads as megaheads (see Fig. 4.2). The subscript  $V$  will be used with the megascale variables.

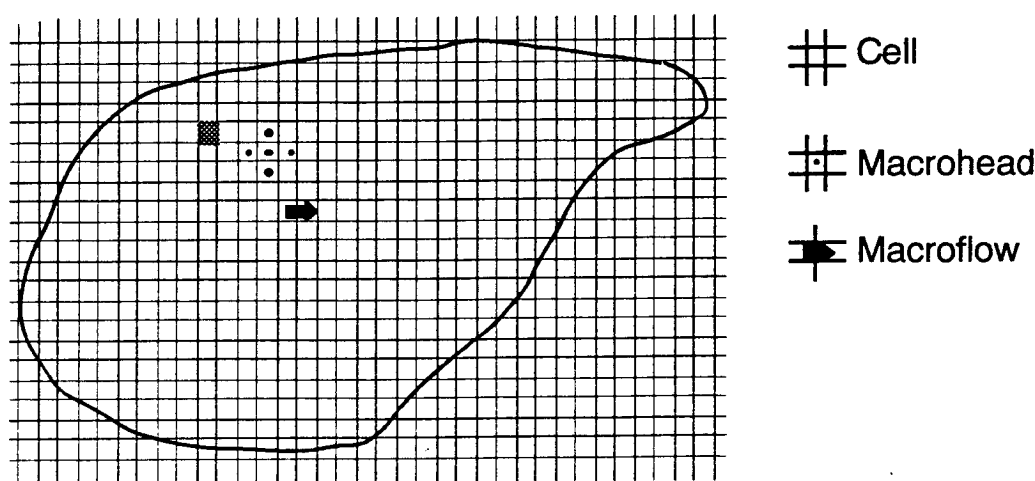


Figure 4.1: **Macroscale discretization.** The cells are at the scale of the measurements. Hydraulic conductivity can be considered constant within each cell

Since measurements of hydraulic conductivity at the megascale are not available (or at least they are too expensive), the objective of this chapter is to find the megascale hydraulic conductivity values that should be used in the numerical flow simulator, so that the following two conditions are met. First, the megahead  $h_V(I, J)$  associated



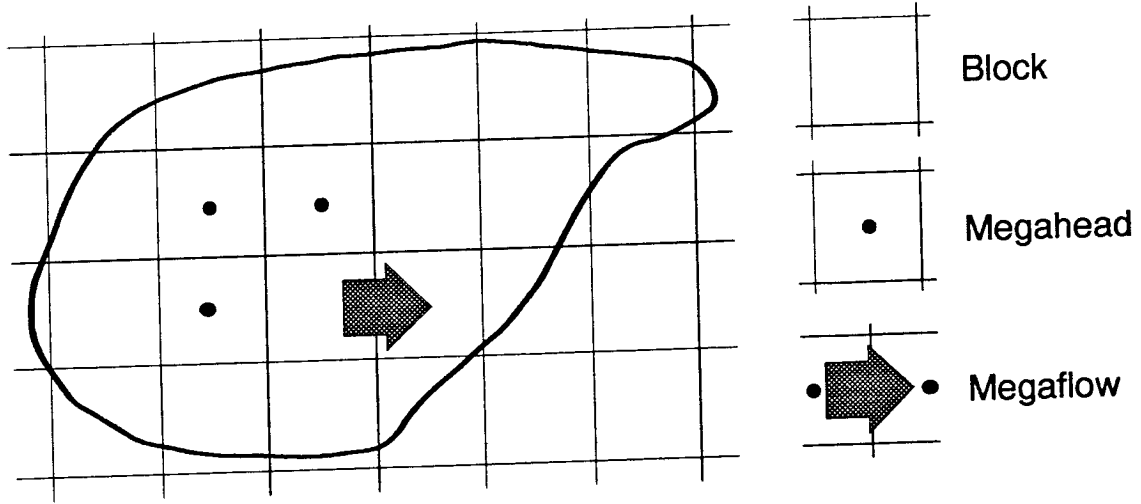


Figure 4.2: **Megascale discretization.** The megascale blocks overlay the macroscale cells

with block  $(I, J)$  should equal the arithmetic average of the macroheads within the block.

$$h_V(I, J) = \frac{1}{n_V} \sum_{(i,j) \in V} h(i, j) \quad (4.8)$$

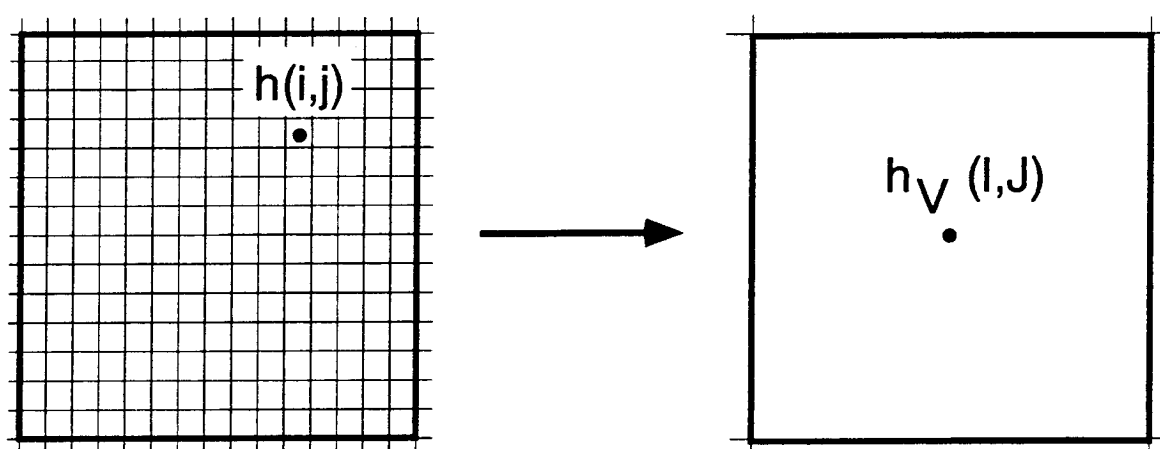
where  $n_V$  is the number of cells in the block, the lower case indices  $(i, j)$  relate to cells, while the upper case indices  $(I, J)$  relate to blocks. Secondly, the megaflow  $q_V(I, J)$  crossing the interface between blocks  $(I, J)$  and  $(I + 1, J)$  should be equal to the average of the macroflows crossing the cell interfaces that are aligned with the block interface (Fig. 4.4)<sup>1</sup>.

$$q_V(I + 1/2, J) = \frac{1}{n_s} \sum_{(i+1/2,j) \in \text{interface}} q(i + 1/2, j) \quad (4.9)$$

where  $n_s$  is the number of cell interfaces, and  $q(i + 1/2, j)$  is the flow through the block interface.

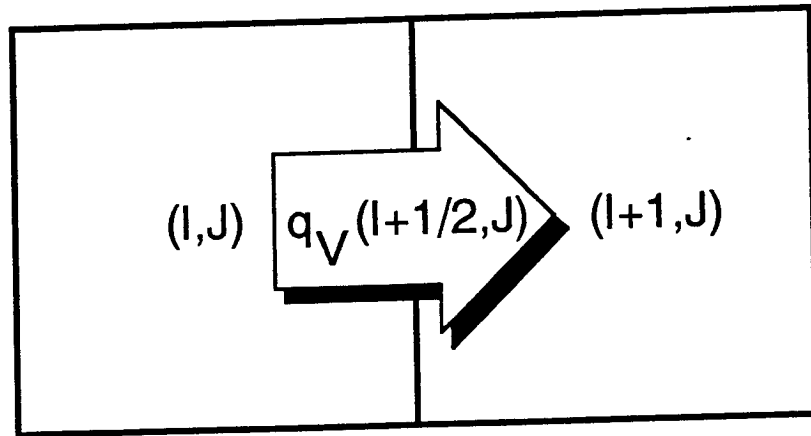
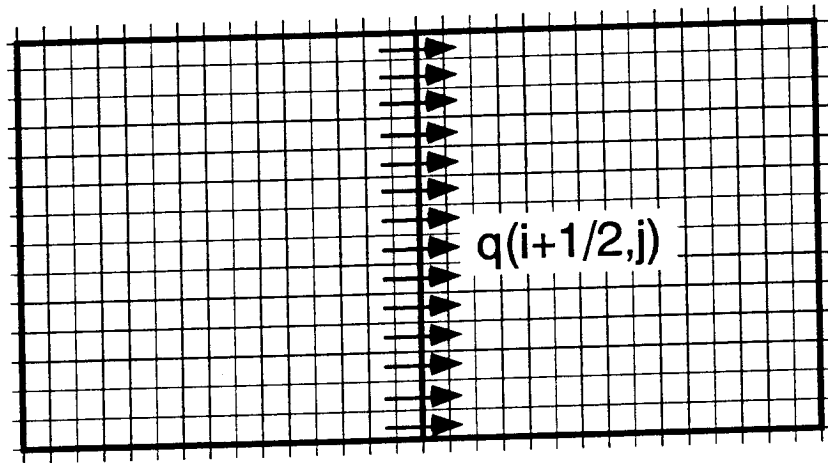
Were the flow equation solved for the entire aquifer with the detailed discretization,

<sup>1</sup>Recall that the flows used in Darcy's equation are in fact specific discharges defined as total flow divided by cross-section



$$h_V(l,J) = \frac{1}{n_V} \sum_{(i,j) \in V} h(i,j)$$

Figure 4.3: **Megahead**. Defined as the average of the macroheads within the block



$$q_v(l+1/2,J) = \frac{1}{n_L} \sum_{(i+1/2,j) \in \text{interface}} q(i+1/2,j)$$

Figure 4.4: **Megaflow**. Defined as the average of the macroflows

then relations (4.8) and (4.9) could be used to obtain the set of megaheads and megaflows that would provide a correct solution to the flow problem at the megascale. Once the megaheads and megaflows are obtained, an inverse problem can be stated as: find the megascale parameter values required by a finite difference formulation to reproduce these megaflows and megaheads.

**Finite Difference Parameters.** At this point in our presentation it is important to discuss which parameter values are required for a finite difference model of groundwater flow.

One way to establish the finite difference formulation is to apply mass conservation to a specific block  $(I, J)$  such as that of Fig. 4.5. Under steady state conditions and assuming that there are no external sinks or sources, the sum of the flows entering through the four sides of the block should equal zero. The flow entering through each side can be obtained using the multidimensional expression of Darcy's law.

$$\begin{Bmatrix} q_x \\ q_y \end{Bmatrix} = - \begin{Bmatrix} K_{xx} & K_{xy} \\ K_{xy} & K_{yy} \end{Bmatrix} \begin{Bmatrix} \partial h / \partial x \\ \partial h / \partial y \end{Bmatrix} \quad (4.10)$$

In particular, the megaflow  $q_{V,x}(I + 1/2, J)$  crossing the interface between blocks  $(I, J)$  and block  $(I + 1, J)$  would be given by

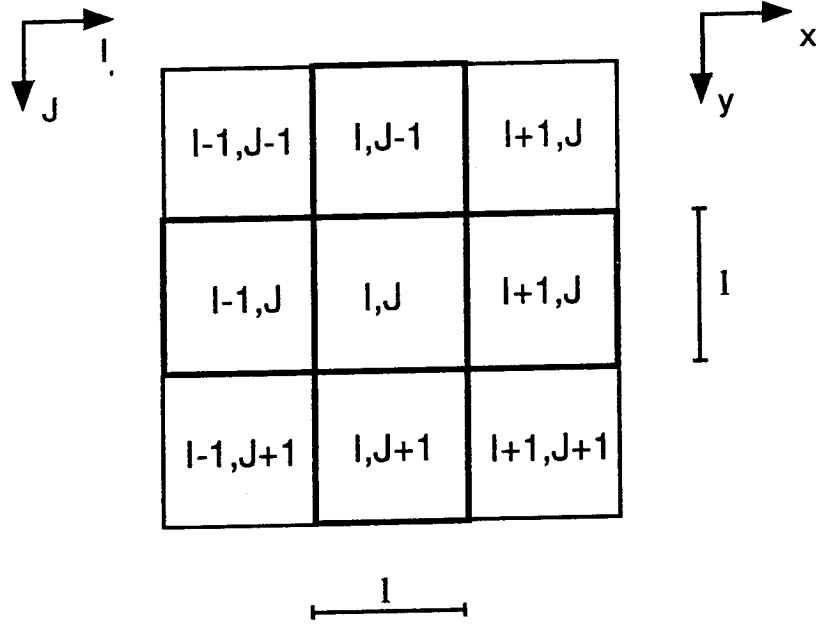
$$q_{V,x}(I + 1/2, J) = - K_{V,xx} \frac{\partial h_V}{\partial x} \Big|_{(I+1/2,J)} - K_{V,xy} \frac{\partial h_V}{\partial y} \Big|_{(I+1/2,J)} \quad (4.11)$$

The finite-difference equation associated to block  $(I, J)$  is

$$q_{V,x}(I + 1/2, J) + q_{V,x}(I - 1/2, J) + q_{V,y}(I, J + 1/2) + q_{V,y}(I, J - 1/2) = 0, \quad (4.12)$$

where the flow crossing the other three block interfaces are given by a similar expression. The megahead gradients at the block interfaces, are estimated by central differences from the megaheads at the nine blocks surrounding  $(I, J)$ . That is,

$$\frac{\partial h_V}{\partial x} \Big|_{(I+1/2,J)} \approx \frac{h_V(I + 1, J) - h_V(I, J)}{l}$$

Figure 4.5: **Finite differences discretization.** Nine-point scheme

$$\left. \frac{\partial h_V}{\partial x} \right|_{(I+1/2, J)} \approx \frac{1}{2} \left( \frac{h_V(I, J+1) - h_V(I, J-1)}{2l} + \frac{h_V(I+1, J+1) - h_V(I+1, J-1)}{2l} \right)$$

Substitution of the estimates of the megahead gradients in (4.12) leads to a linear equation relating the megaheads at the nine blocks surrounding  $(I, J)$ . As shown in Appendix B this equation is, for a square block,

$$\begin{aligned} & K_{V,xx}(I+1/2, J)(h_{I+1,J} - h_{I,J}) \\ & + K_{V,xy}(I+1/2, J) \frac{1}{4} (h_{I+1,J+1} - h_{I-1,J+1} + h_{I+1,J} - h_{I-1,J}) \\ & + K_{V,xx}(I-1/2, J)(-h_{I,J} + h_{I-1,J}) \\ & + K_{V,xy}(I-1/2, J) \frac{1}{4} (-h_{I+1,J} + h_{I-1,J} - h_{I+1,J-1} + h_{I-1,J-1}) \\ & + K_{V,yy}(I, J+1/2)(h_{I,J+1} - h_{I,J}) \\ & + K_{V,xy}(I, J+1/2) \frac{1}{4} (h_{I+1,J} - h_{I-1,J} + h_{I+1,J+1} - h_{I-1,J+1}) \end{aligned}$$

$$\begin{aligned}
& +K_{V,yy}(I, J - 1/2)(-h_{I,J} + h_{I,J-1}) \\
& +K_{V,xy}(I, J - 1/2)\frac{1}{4}(-h_{I+1,J} + h_{I-1,J} - h_{I+1,J-1} + h_{I-1,J-1}) = 0
\end{aligned}$$

Writing this equation for all blocks yields a system of linear equations with the megaheads as unknowns. The coefficients in this system of linear equations are functions of the estimated block hydraulic conductivities at the block interfaces. More precisely, for any given block  $(I, J)$  we need estimates of  $K_{V,xx}$ ,  $K_{V,xy}$  at  $(I + 1/2, J)$  and  $(I - 1/2, J)$ , and of  $K_{V,yy}$ ,  $K_{V,xy}$  at  $(I, J + 1/2)$  and  $(I, J - 1/2)$ .

The common practice in finite-difference modeling is to assume that the principal directions of the hydraulic conductivity tensor is the same for all blocks, allowing an alignment of the block sides and principal directions. This limits the interface block conductivities to their principal components, that is, only  $K_{V,xx}$  and  $K_{V,yy}$  are considered. Their values are typically obtained by a harmonic average of the corresponding components of the neighboring block conductivity tensors, for example,  $K_{V,xx}(I + 1/2, J)$  is equal to the harmonic mean of  $K_{V,xx}(I, J)$  and  $K_{V,xx}(I + 1, J)$ . This approach has two shortcomings: first, it cannot handle conductivity tensors with principal components not parallel to the block sides (it is not clear how the off-diagonal terms of the block conductivity tensors should be averaged); and second, the harmonic mean of adjacent heterogeneous block values does not necessarily yield the interface conductivities that reproduce flows observed at the macroscale.

For these two reasons, we will attempt a direct estimation of the interface conductivity values; since these are the parameter values required by the finite-difference model. The approach proposed in this dissertation is then compared to the results obtained by two other approaches. These other approaches do not determine directly the interface conductivities, instead, they determine block conductivities which are later averaged to give the interface conductivities. To avoid artifacts that may be introduced by this averaging, the interface conductivities will be also directly computed by assimilating them to the conductivities of the block that stretches between adjacent block centerpoints (Fig. 4.6). This block will be referred to, hereafter, as the interblock.

Returning to the inverse problem stated earlier, the estimation of the two conductivity values associated with each interface is undetermined unless some other

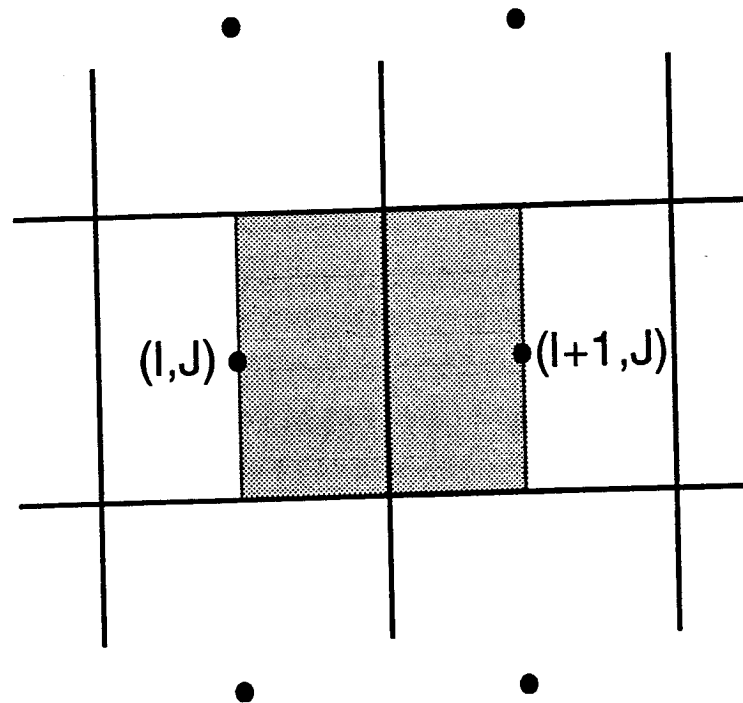


Figure 4.6: **Interblock.** Defined as the area of the aquifer attached to the block interface.

constraint is introduced. Indeed, after having solved for flow at the macroscale over the entire aquifer and calculated the megaheads and megafloWS, Eq. (4.11) can be established for each interface yielding one single linear equation with two parameters to be determined. For example, at the interface  $(I + 1/2, J)$ , we can write (see Fig. 4.5),

$$\begin{aligned}
 q_V(I + 1/2, J) = & -K_{V,xx}(I + 1/2, J) \frac{h_V(I + 1, J) - h_V(I, J)}{l} \\
 & - K_{V,xy}(I + 1/2, J) \frac{1}{2} \left[ \frac{h_V(I, J + 1) - h_V(I, J - 1)}{2l} \right. \\
 & \left. + \frac{h_V(I + 1, J + 1) - h_V(I + 1, J - 1)}{2l} \right] \quad (4.13)
 \end{aligned}$$

where  $l$  is the block side length, the gradient  $\partial h_V / \partial x$  at  $(I + 1/2, J)$  has been obtained by central differences using the megaheads at  $(I, J)$  and  $(I + 1, J)$  and the gradient  $\partial h_V / \partial y$  at  $(I + 1/2, J)$  has been evaluated by averaging the central difference approximations of the gradients at  $(I, J)$  and  $(I + 1, J)$ . This equation is not enough to determine both  $K_{V,xx}$  and  $K_{V,xy}$ <sup>2</sup>

At least, one more relation involving the two interface parameters is required. White (White, 1987; White and Horne, 1987) suggests that solutions to groundwater flow **over the entire aquifer** should be obtained for a set of four different boundary conditions, none of which needs to correspond exactly to the field boundary conditions. The four boundary conditions proposed by White are a combination of no flow and prescribed head that forces overall flow patterns at 0, 45, 90 and 135° with respect to the block sides. Each solution produces a single equation with two unknowns for each interface; the set of all four solutions thus result in an overdetermined system of linear equations that is solved by standard least squares. In the case proposed by White there will be four linear equations for each pair of interface conductivities. The use of least squares to obtain the two interface block conductivities provides an approximation of the megafloWS for different flow patterns.

---

<sup>2</sup>Note that (4.13) can be interpreted as an *ad-hoc* version of (4.1) for the case in which a finite-difference formulation is used. The average of the floWS across the interface substitutes for the average of the floWS over the block, and the gradient of the average heads (megaheads) substitutes for the average of the gradients in (4.1).



However, simulating flow at the macroscale over the entire aquifer as proposed by White is only feasible for discretizations with a few hundred nodes. Such a detailed flow simulations may only be justified if the resulting block conductivities are going to be used in a more complex, consequently more demanding, numerical code, such as for multiphase flow simulation.

The most common approach to numerically compute block conductivities, hereafter referred to as the traditional approach, was described in the literature review starting on page 36. That approach provides block conductivities that are later averaged (through harmonic average) to give the interface conductivities. For comparison purposes, and to eliminate artifacts that may result from such an averaging of already scaled-up values, we identify the interface conductivity between nodes  $(I, J)$  and  $(I + 1, J)$  to the block conductivity of the block straddling the interface between block centerpoints (Fig. 4.6).

In the traditional method, the cells within the block are isolated, then groundwater flow is solved within the block for the specific boundary conditions shown in Fig. 2.3; then, a value for  $K_{V,xx}$  is obtained using (2.12). The procedure is repeated after a  $90^\circ$  rotation of the boundary conditions in Fig. 2.3 and a value for  $K_{V,yy}$  is similarly obtained.

The traditional approach, has two problems. First, it cannot account for the principal directions of  $\mathbf{K}_V$  not aligned with the block sides. Second, the previous specific boundary conditions may not be relevant.

This traditional approach has been favored by many researchers (Warren and Price, 1961; Bouwer, 1969; Journel et al., 1986; Desbarats, 1987a; Desbarats, 1987b; Desbarats, 1988; Deutsch, 1987; Deutsch, 1989; Begg et al., 1989; Bachu and Cuthiell, 1990) mostly on the basis that it retrieves the correct analytical results for effective conductivities of infinite aquifers formed by perfectly stratified layers; more precisely, the arithmetic mean for flow parallel to layering and the harmonic mean in the orthogonal direction. However, what may be regarded as a proof that the traditional approach retrieves the “exact” block conductivities is nothing but a consequence of the very specific boundary conditions used.

Consider the two aquifers in Fig. 4.7. Both aquifers are much larger than the

block outlined in the center. On the left, the block is embedded in a uniform aquifer with constant isotropic conductivities everywhere (except for the block itself). On the right, the block is part of five layers in a perfectly stratified aquifer. If these blocks are isolated to obtain their block conductivities, they cannot be distinguished one from another. However, if block conductivity is defined such that it perturbs the least the flow patterns within the aquifer, then the same block conductivity cannot be used in both cases.

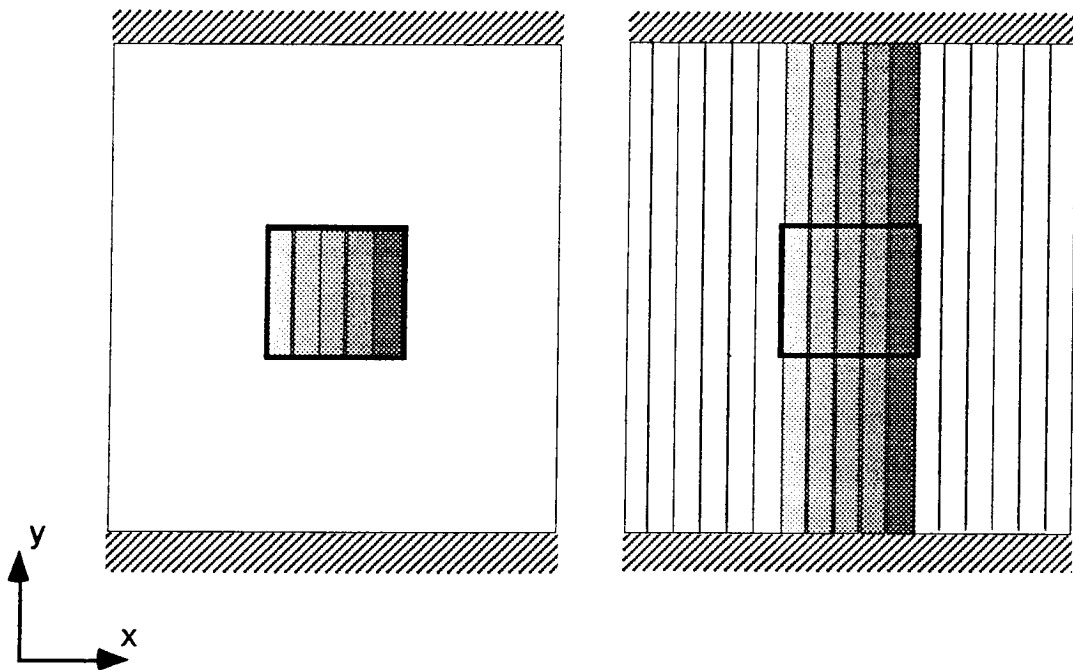


Figure 4.7: **One block from two aquifers.** The blocks outlined in the center of both aquifers cannot be distinguished one from another in the basis of the conductivities within the block. However, when the aquifers are subject to flow in the  $x$ -direction, the boundary conditions around the center blocks are very different.

Consider the flow solution for both aquifers using prescribed heads on the boundaries parallel to the  $y$ -axis. These prescribed heads are uniform along each boundary but different from each other. The blocks at the center will have very different flow patterns, depending on which aquifer is considered. The boundary conditions as given in Fig. 4.8 are only an approximation of those prevailing around the blocks in

Fig. 4.7; however, the only objective of this discussion is to show that a given block subject to different boundary conditions should have different block hydraulic conductivities. Consider that the hydraulic conductivities of the five layers within the block have values of 1, 10, 100, 1000 and 10000. Flow is solved for the two blocks in Fig. 4.8, and block conductivity is defined as the ratio of the average flow to the average gradient in the  $x$ -direction within the block; this results in a value of 350 for the block on the left and of 3.6 for the block on the right of Fig. 4.8. A difference of two orders of magnitude! Such a discrepancy is explained by the fact that for the left case, flow gets into the block through the upper and lower faces resulting in a larger average flow than for the right case with no flow boundaries. The point being made is that reproduction of the effective parameters corresponding to perfectly stratified aquifers cannot be used as the only validation tool for the traditional or any other approach when determining block conductivities for blocks of finite size. A better validation technique consists of checking whether the flow pattern within the entire aquifer obtained with the block values reproduce the reference flow pattern obtained by simulation at the smallest scale.

In conclusion, computation of block conductivities should account for the conductivities surrounding the block. In other words, the boundary conditions chosen to compute block conductivities are of paramount importance and should be carefully chosen depending on the expected distribution of conductivities around that block. For blocks larger than the correlation scale, the effect of such boundary conditions on the flow pattern within the block quickly vanishes beyond a short distance of the block boundaries (Rubin and Dagan, 1988; Dagan and Rubin, 1988; Rubin and Dagan, 1989). In which case, the flow pattern within the block is mostly determined by the conductivities within the block and not so much by the conductivities outside; the traditional method does provide good results.

In this dissertation an approach lying between White's approach and the traditional one is proposed. As in White's approach the block conductivity is calculated from the solutions of flow for several alternative boundary conditions. However, these boundary conditions are applied not on the field boundaries but on the boundaries of a "skin" surrounding that block, see Fig. 4.9. The use of a "skin" allows accounting

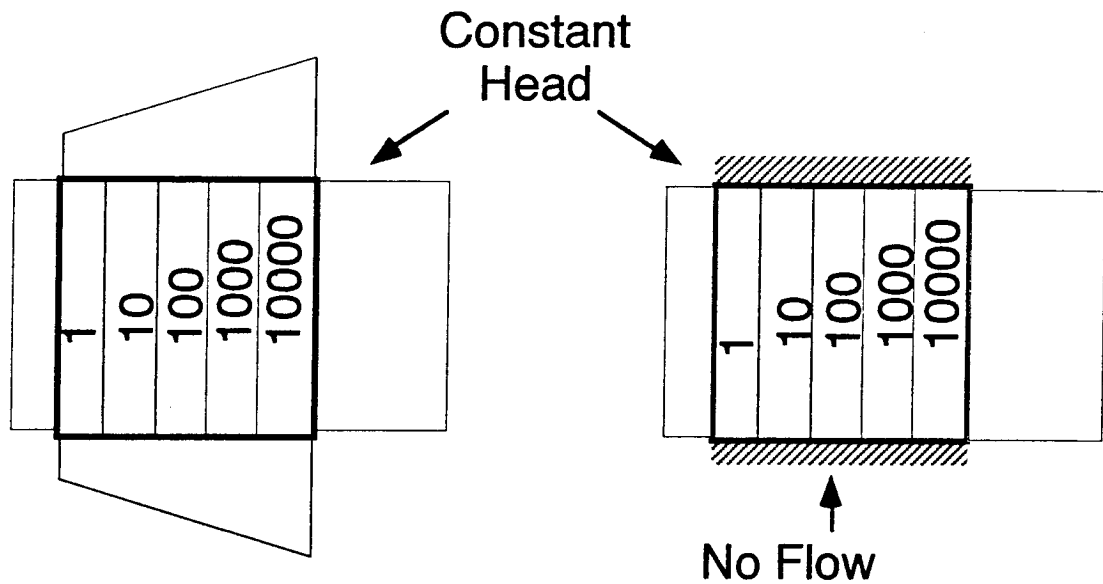


Figure 4.8: **Approximate boundary conditions.** for the blocks in Fig. 4.7

for some of the influence of the neighboring cells, without having to solve flow over the entire aquifer as requested by White's approach. Note that if the "skin" is extended to be the entire aquifer, our approach identifies that of White.

We focus on the computation of estimates of the conductivities at the interface, instead of block conductivities. Therefore, the objective is to obtain the coefficients relating megaflows to megaheads in Eq. (4.13). The procedure proposed in this dissertation follows:

- (a) Define an area surrounding the interface for which estimates of the coefficients in (4.13) are to be calculated. Ideally, this area should be the entire aquifer but, in practice, it is limited to a smaller area. In this dissertation the area chosen is the interblock straddling between block centers plus a "skin" arbitrarily set to half the block size in each direction, see Fig. 4.9.
- (b) Solve for flow at the macroscale within the previous area for a series of boundary conditions that may include combinations of prescribed head and/or imposed flux.

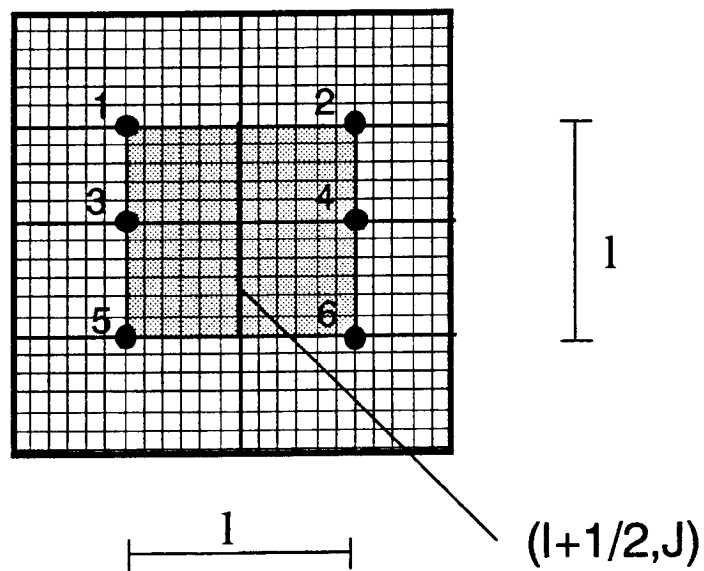


Figure 4.9: **Computing the interface conductivity.** The interface coefficients will be retrieved after solving for heads within an area formed by the block determined by points 1, 2, 5 and 6 plus a “skin” surrounding it of width equal to half the block size in each direction

(c) For each boundary condition evaluate the megafLOW across the block interface (Eq. 4.9) and the megaheads at the locations numbered 1 through 6 (Eq. 4.8) in Fig. 4.9.

(d) Approximate the megahead gradients as follows

$$\begin{aligned}\frac{\partial h_V(I + 1/2, J)}{\partial x} &\approx \frac{h_V(4) - h_V(3)}{l} \\ \frac{\partial h_V(I + 1/2, J)}{\partial y} &\approx \frac{h_V(5) - h_V(1) + h_V(6) - h_V(2)}{2l}\end{aligned}$$

(d) Finally, develop relation (4.11) for each boundary condition leaving the block conductivities as unknowns, and solve the resulting overdetermined system of linear equations by a standard least squares procedure (see Appendix C).

The critical point in this approach is the selection of the set of alternative boundary conditions. These should be chosen so that they produce flow patterns approximating the expected major flow direction around the block involved. The exact flow direction within that block cannot be known unless flow is solved for the entire aquifer; however, an approximation, with a direction tolerance of  $\pm 45^\circ$ , should be accessible.

## Demonstration Using Synthetic Aquifers

The proposed approach will be demonstrated using four synthetic aquifers. The hydraulic conductivity of the first aquifer has a multilognormal distribution with isotropic covariance. The second aquifer has a bimodal distribution representing, for example, sand and shale, with an anisotropic indicator covariance. Finally, the third and fourth aquifers have multilognormal distributions for  $K$  with anisotropic covariance and major anisotropy axes oriented, respectively, at  $45^\circ$  and  $135^\circ$  with regard to the  $x$ -axis. For each of the four aquifers the following procedure was followed:

1. Generate the synthetic aquifer at the macroscale using one of the algorithms developed in chapter 3, by drawing a realization from a random function with specified statistical properties. Hydraulic conductivities are generated over a 200 by 200 square grid

2. Solve for heads at the  $200 \times 200$  resolution with prescribed head boundaries that impose an overall diagonal flow pattern (Fig. 4.10). This solution will be used as the reference macroscale solution.
3. Scale-up the aquifer to a 20 by 20 square grid, and obtain each of the interface conductivities. Each block thus contains 10 by 10 cells. For each interface (or for the associated interblock in Fig 4.6) three interface conductivities are computed: first, the geometric mean of the conductivities within the interblock; second, using the traditional approach on the interblock; and third, using the proposed approach that provides estimates of the two interface conductivities required by the finite difference formulation. In the proposed method the interblock conductivities are computed by least-squares after numerically solving for heads within the area indicated in Fig. 4.9 for four sets of boundary conditions. The four sets of boundary conditions correspond to prescribed head boundaries values given by tilting planes with gradients parallel to the block sides and to the block diagonals as shown in Fig. 4.11.
4. Solve the flow problem at the megascale for the three sets of scaled-up interface conductivities using the same field boundary conditions as in the reference macroscale solution. The megafloes obtained from these solutions are referred to as the scaled-up values.
5. From the reference solution at the macroscale, compute the megafloes using equation (4.9). These megafloes are referred to as the reference values.
6. Compare the reference megafloes obtained in step 5 with the three sets of scaled-up megafloes obtained in step 4. Two comparisons are made with the objective of determining how well the different scale-up techniques perform. Locally, a one-to-one comparison is made between the reference values and the scaled-up ones. Globally, the comparison relates to the total flows through cross-sections aligned with the block edges (see Fig 4.12)

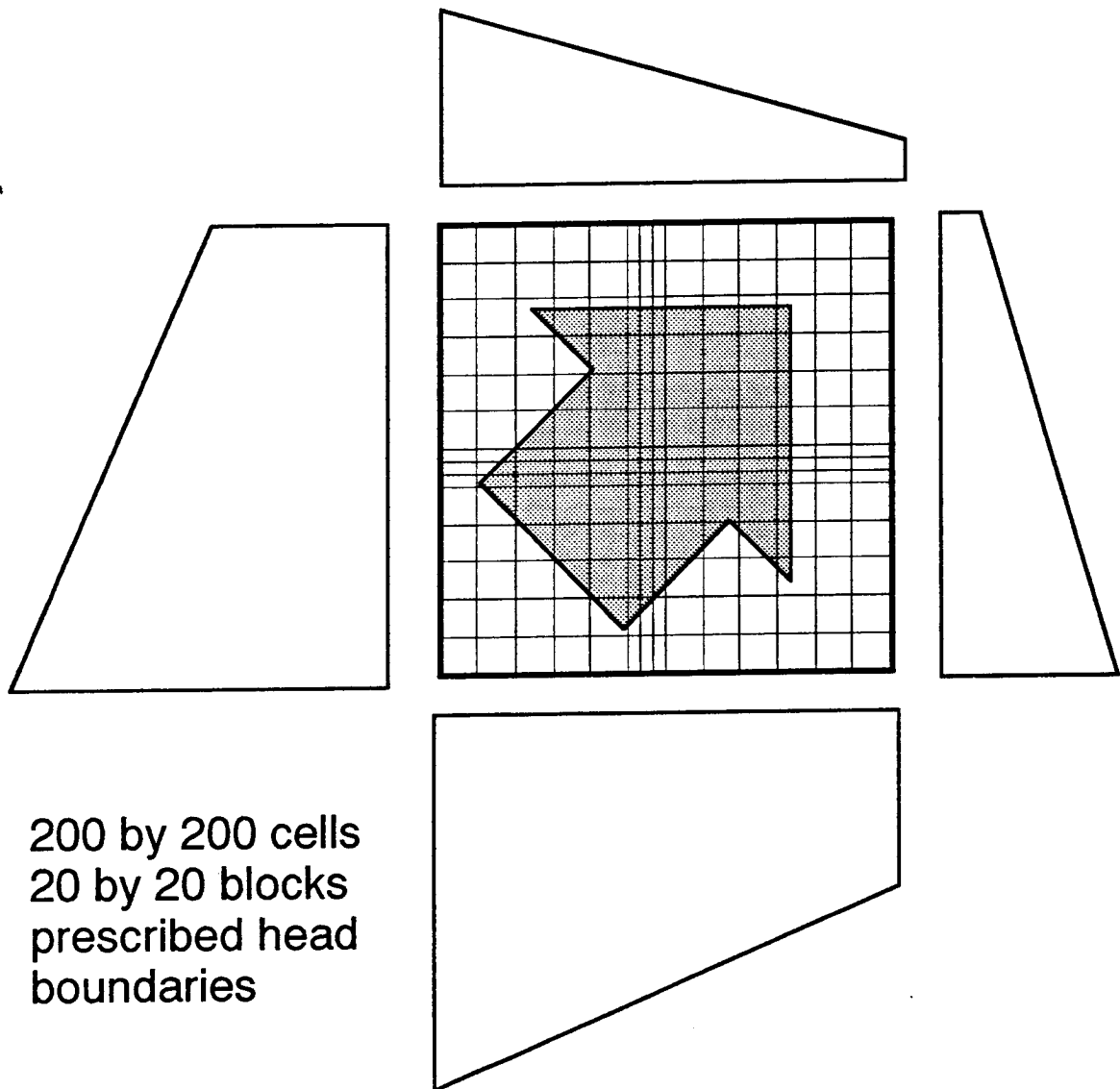


Figure 4.10: **Field boundary conditions.** To check the scale-up technique, flow is solved for numerically within the aquifer for prescribed head boundary conditions imposing an overall diagonal flow pattern.



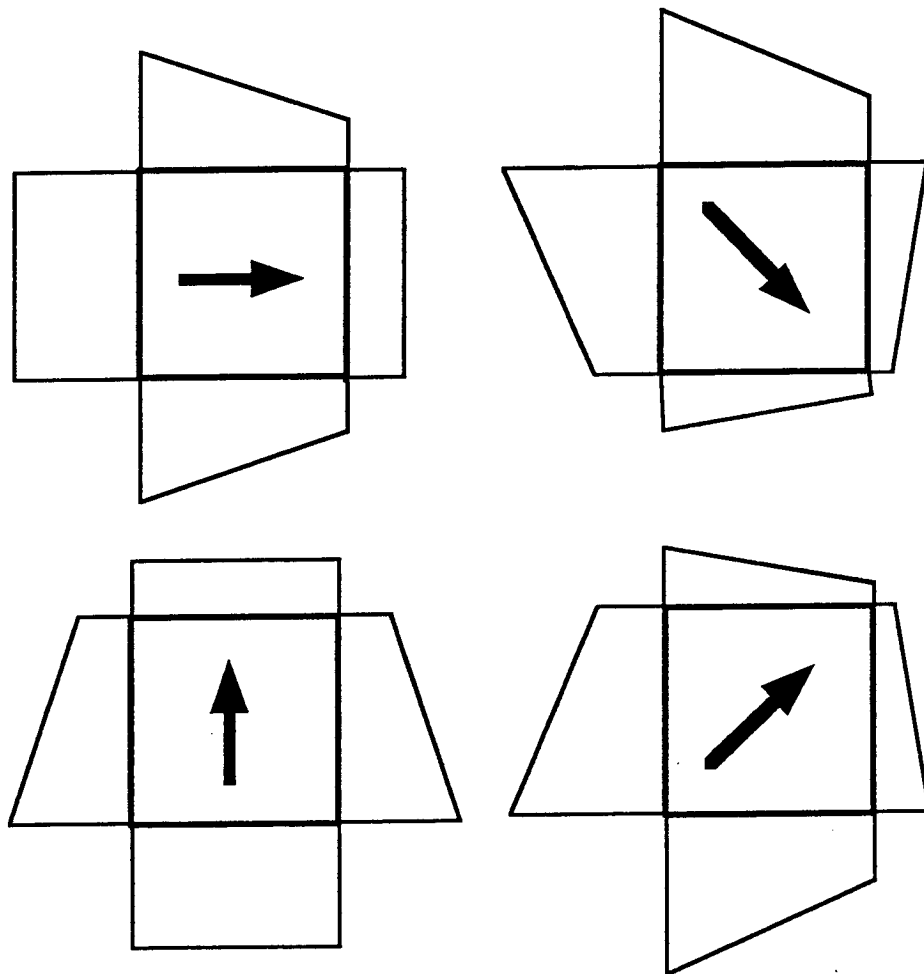


Figure 4.11: **Boundary conditions used in the proposed method.** The hydraulic conductivity coefficients required by the formulation of finite differences are estimated by least-square estimation, after solving for heads within the skin surrounding the interface as shown in Fig. 4.9

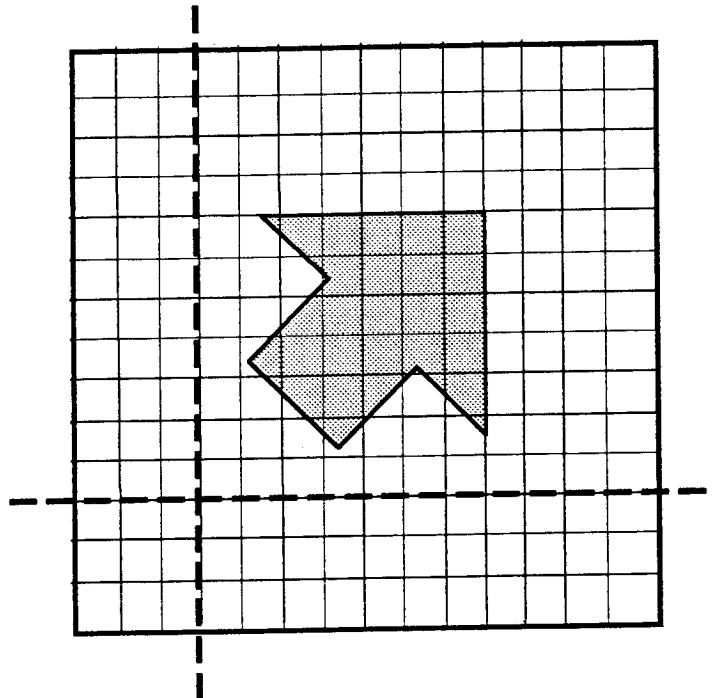


Figure 4.12: **Cross-sections for the global comparison.** The flow crossing all possible horizontal and vertical cross-sections will be used to assess how the scaling-up methods perform. The arrow indicates the overall flow gradient

### Statistically Isotropic Hydraulic Conductivities

A realization of log-hydraulic conductivities is drawn from a stationary and ergodic multiGaussian random function model. The random function has zero mean and unit variance and its variogram is exponential with practical range  $a$  equal to  $3/20$  of the aquifer length  $L$ :

$$\gamma(\mathbf{r}) = 1 - \exp\left(-\frac{3|\mathbf{r}|}{a}\right) \quad (4.14)$$

The realization extends over a square area discretized in 200 by 200 square cells; thus the cell size is  $1/30$  the practical range  $a$ . Hydraulic conductivities are obtained for each cell by straight exponentiation (no linear transform) of the Gaussian values. These hydraulic conductivities are considered isotropic to flow and constant within each cell.

The multilognormal realization was generated using the program GSIM3D described in Appendix A. It is displayed in Fig. 4.13. The statistics given in this figure confirm that the cell log-hydraulic conductivities are Gaussian and that the exponential variogram model (4.14) is reasonably well reproduced.

These conductivities are scaled-up into 20 by 20 square blocks. Each block of side  $l = (1/3)a$  contains 10 by 10 cells. The objective of the exercise is to check how well the flow patterns featured by the reference simulation at the macroscale are reproduced after scaling-up.

Flow was solved over the reference 200 by 200 cell aquifer using prescribed head boundaries displayed in Fig 4.10 and given by the equation:

$$h(i, j) = (i + j) dx \quad \forall(i, j) \text{ along the aquifer boundary} \quad (4.15)$$

where  $dx$  is the cell size and  $i, j$  are the integer indices used to specify each cell. These boundary conditions create an overall gradient at a  $45^\circ$  angle with respect to the aquifer boundaries (see Fig. 4.10). The numerical solution of the groundwater flow equation was carried out using a finite-differences formulation. A specific program, custom-made for the cases studied in this dissertation, was written using the strongly

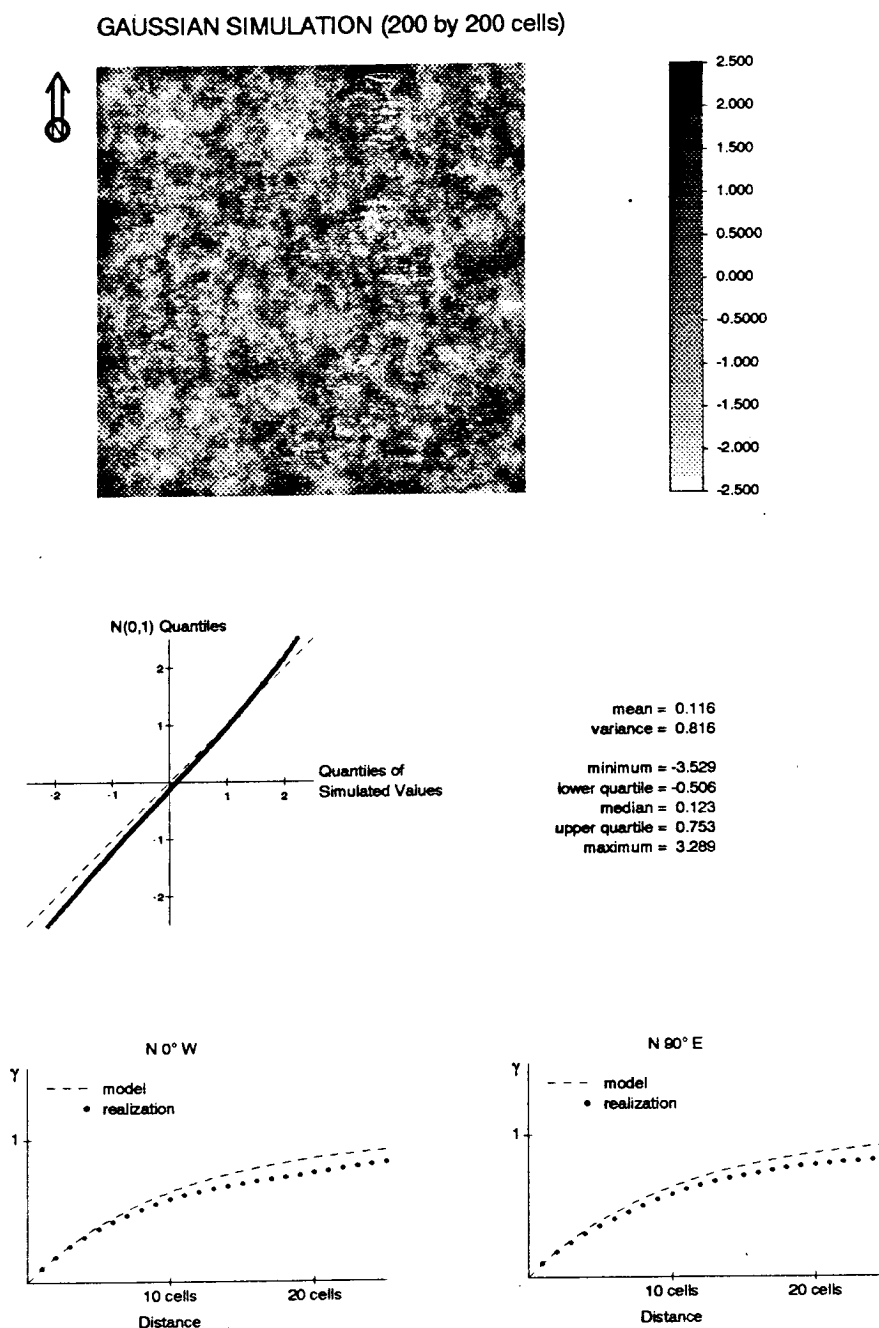


Figure 4.13: **A realization of log-hydraulic conductivities (isotropic covariance).** Top: Grey-scale map of log-hydraulic conductivities. Center: Q-Q plot of generated values versus normal quantiles, and statistics of the realization. Bottom: Model variogram and experimental variogram as inferred from the realization for two orthogonal directions

implicit procedure (SIP) as the iterative linear system solver. The SIP subroutine was taken from MODFLOW (McDonald and Harbaugh, 1984).

The traditional method, the geometric mean and the proposed method for scaling-up were each used to obtain interface hydraulic conductivities. A program especially designed to solve the finite-difference approximation of the groundwater flow equation without assuming that the principal directions of hydraulic conductivity are aligned to the cartesian axes was written. The details of its code are given in Appendix B.

Two comparisons were made. The first one looks at flows at a local scale. The scaled-up megaflows, that is, those obtained after solving the flow equations using the scaled-up conductivity values, are compared to the reference values, that is, those obtained from the solution at the macroscale. Ideally, the scaled-up megaflows should be equal to the reference values. Since, this will never be exactly the case, two performance indices are used to assess the magnitude of the errors. One is the relative bias ( $RB$ ) defined as the percent ratio of the average difference to the average reference megaflow, and the other is the relative sum of squared differences ( $RSSE$ ) equal to the percent ratio of the average of the squared differences to the reference megaflow variance:

$$RB = 100 \times \frac{\sum \hat{q}_v - q_v}{\sum q_v}$$

$$RSSE = 100 \times \frac{\sum (\hat{q}_v - q_v)^2}{\sum (q_v - E\{q_v\})^2},$$

where  $\hat{q}_v$  is the scaled-up megaflow and  $q_v$  is the reference value;  $E\{\cdot\}$  refers to arithmetic average and the summations extend to all block interfaces.

The second comparison is made at the global scale; it consists of checking how overall flows are reproduced. The total flows across each horizontal and vertical cross-section are computed. The values obtained after scaling-up are compared to the values obtained from the macroscale reference simulation.

Figures 4.14 and 4.15 show the comparison of megaflows at the local and global scales, respectively. The line that corresponds to the exact reproduction of the reference values is shown. All three scale-up methods are seen to perform equally well.

The isotropic covariance and relatively small variability of  $\ln K$  makes the geometric mean of the points within the interblock as good an estimate as the values retrieved by the other more elaborate procedures involving numerical simulation of flow within the individual interblocks.

### Bimodal Aquifer Hydraulic Conductivities

The second case studied is a sand/shale aquifer. The conductivity values from the previous case are used as the sand conductivities. Overlaying this realization, a realization from a binary random function was generated using the program ISIM3D described in Appendix A. The binary random function is defined as

$$I(\mathbf{x}) = \begin{cases} 1 & \text{if } x \text{ in shale} \\ 0 & \text{if } x \text{ in sand} \end{cases}$$

with a mean value  $p = 0.15$ , (15% of the aquifer is shale); variance  $p(1 - p) = 0.0225$ , and an exponential variogram with practical range in the  $x$ -direction  $a_x = 0.04L = 0.8l$  and negligible range in the  $y$ -direction<sup>3</sup>,

$$\gamma_I(\mathbf{r}) = \begin{cases} 0.0225 (1 - \exp(-3|r_x|/a_x)) & \text{if } r_y = 0 \\ 0 & \text{if } r_y \neq 0 \end{cases}$$

This variogram model corresponds to a distribution of shale with average length smaller than the block side  $l$ .

The realization of the binary random function is shown at the top of Fig 4.16. This realization was superimposed on the realization of Fig 4.13 to obtain the final aquifer hydraulic conductivity distribution. On the bottom, the reproduction of the indicator variogram model is shown to be excellent.

All shales are assigned a constant log-conductivity of  $-9$ , which results in an overall mean log-conductivity of the sand/shale aquifer of  $-1.35$ ; the overall log-conductivity variance is  $17.6$ .

Figures 4.17 and 4.18 show, respectively, the comparison of local and global scale-up megafloes to the reference flows. The field boundary conditions are the same as in

<sup>3</sup>The shales are assigned the width of one cell.

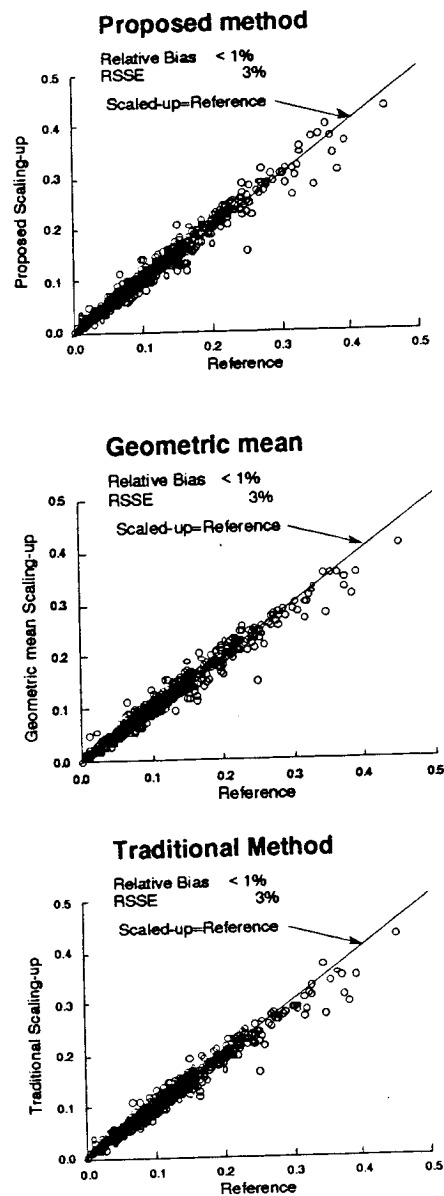


Figure 4.14: **Isotropic lognormal aquifer: Local flow comparison.** Scaled-up megaflows are displayed versus the reference megaflows as obtained by integrating the reference macroflows

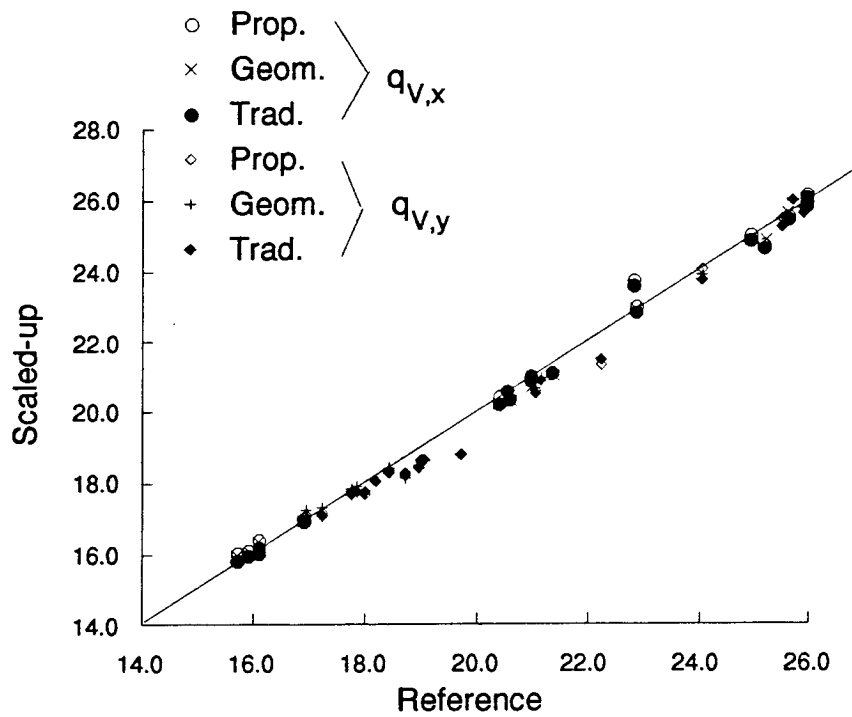


Figure 4.15: **Isotropic lognormal aquifer: Total flow comparison.** Total flows crossing the entire width (or length) of the aquifer have been obtained from the megascale simulations for the three upscaling techniques. They are displayed versus the reference megafloes as obtained by integrating the flows from the reference macroscale simulation



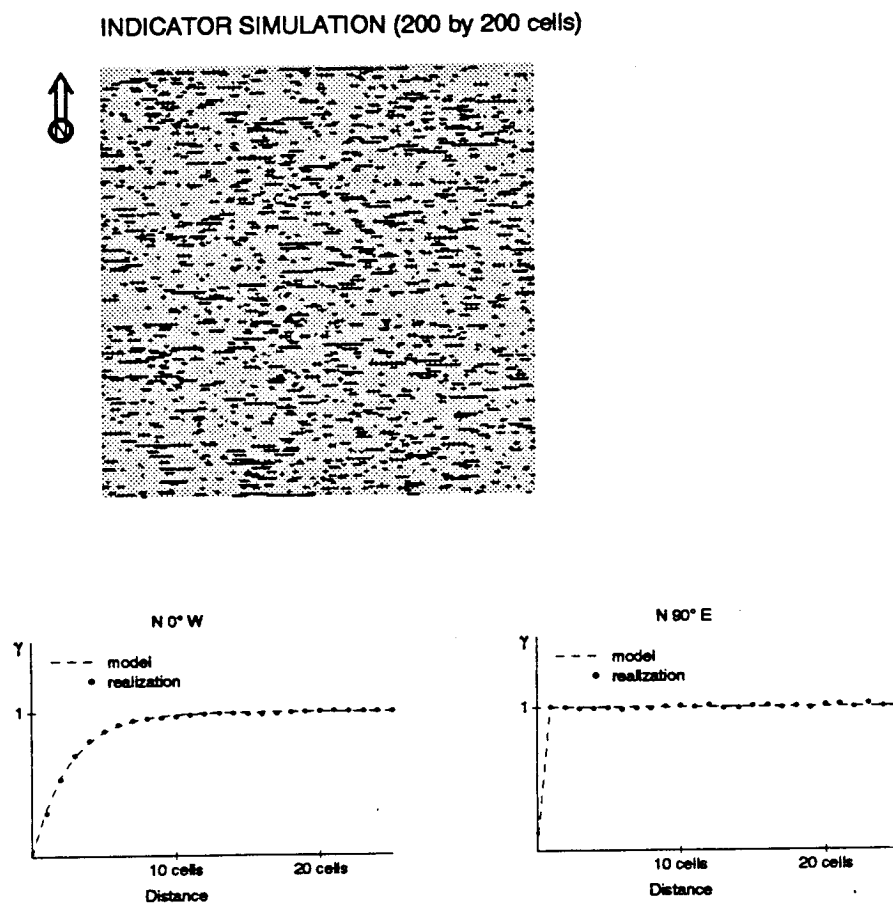


Figure 4.16: Sand/shale aquifer. Top: Grey-scale map of log-hydraulic conductivities (shales in black). Bottom: Model indicator variogram and experimental variogram as inferred from the realization for two orthogonal directions

the previous case (4.15). The geometric mean does not perform well, the reason being that a small proportion of very low conductivities suffices to drive such geometric mean very close to the low shale conductivity. The proposed method performs better than the traditional one, with a negligible relative bias and a smaller RSSE.

From Fig. 4.18 we note that the total flows orthogonal to the shale orientations are systematically underestimated when using the traditional approach. Notice also in Fig. 4.17 the set of non-zero reference megaflores estimated as zero through the traditional method. The reason for these two biases stems from the inappropriate boundary conditions used in the traditional scaling-up method.

As mentioned earlier, the indicator covariance used to generate the geometry of the shales produce shales with an average length of about 0.8 times the block size  $l$ . Thus, a certain number of those shales is larger than the block, i.e., some of the shales stretch the entire width of an interblock. When flow is simulated within one interblock completely intercepted by a shale using the the boundary conditions of the traditional method (see Fig. 4.19), the resulting block value is close to the harmonic mean of sand and shale weighted by their volume proportions. With 15% shale, averaging  $E\{\ln K\} = -9$  and 85% sand of  $E\{\ln K\} = 0$ , the natural logarithm of the harmonic average of  $K$  is approximately equal to  $-7$ , which for flow simulation purposes is impermeable relative to the sand. As a result, a fraction of the interface conductivities in the N-S direction are estimated as zero by the traditional approach. This problem associated with the traditional method was already noticed by Begg *et al.* (1989) who gives the example of an hypothetical oil reservoir for which all block conductivities would be estimated as zero, yet the overall flow crossing the reservoir is not zero, see Fig 4.20.

### Statistically Anisotropic Aquifer Hydraulic Conductivities

In this third example, a realization of log-conductivities has been drawn from a stationary and ergodic multiGaussian random function with zero mean, unit variance and anisotropic exponential variogram with principal directions of anisotropy at  $45^\circ$  from the cartesian axes. The direction of greatest continuity ( $x'$ ) is  $45^\circ$  from the

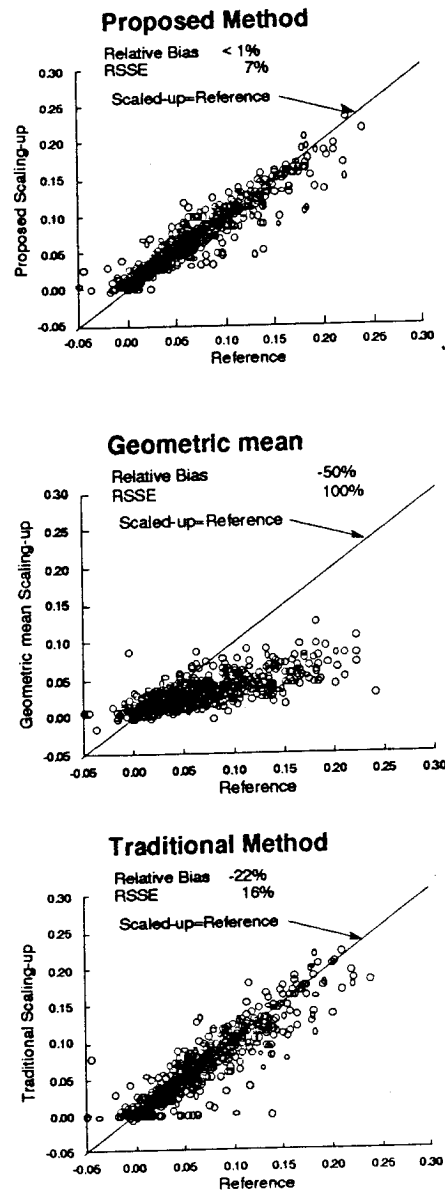


Figure 4.17: **Sand/shale aquifer: Local flow comparison.** Scaled-up megaflows are displayed versus the reference megaflows as obtained by integrating the reference macroflows

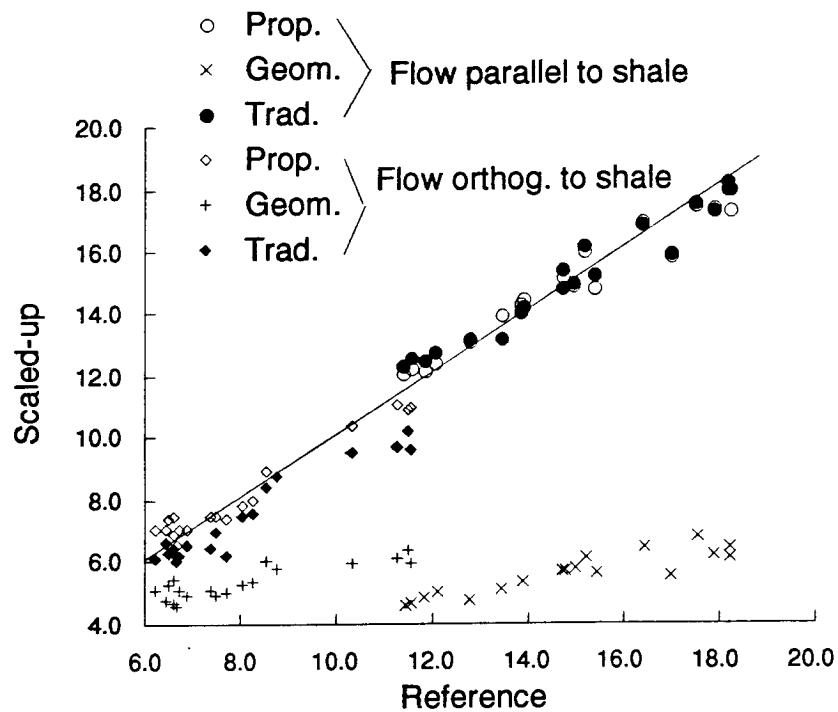


Figure 4.18: **Sand/shale aquifer: Total flow comparison.** Total flows crossing the entire width (or length) of the aquifer have been obtained from the megascale simulations for the three upscaling techniques. They are displayed versus the reference megafloes as obtained by integrating the flows from the reference macroscale simulation

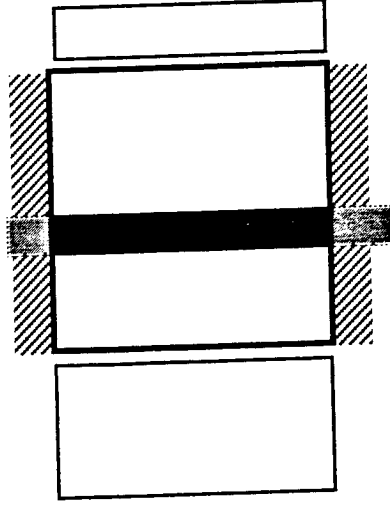


Figure 4.19: **Measuring the impact that one shale may have in determining the block conductivity.** In the traditional approach, a shale that intercepts a block from side to side will reduce the block conductivity next to that of the shale

$x$ -axis, with the practical range  $a_{x'} = 0.075L = 1.5l$ . The direction of least continuity ( $y'$ ) is  $45^\circ$  from the  $y$ -axis with practical range  $a_{y'} = 0.015L = 0.3l$ . Thus, the anisotropy ratio is,  $1.5/.3=5$ . The variogram is

$$\gamma(\mathbf{r}) = 1 - \exp \left( -\sqrt{\left(\frac{3r_{x'}}{1.5l}\right)^2 + \left(\frac{3r_{y'}}{0.3l}\right)^2} \right)$$

with

$$\begin{Bmatrix} x' \\ y' \end{Bmatrix} = \begin{Bmatrix} 1/\sqrt{2} & 1/\sqrt{2} \\ -1/\sqrt{2} & 1/\sqrt{2} \end{Bmatrix} \begin{Bmatrix} x \\ y \end{Bmatrix}$$

The realization of hydraulic log-conductivities was generated using GSIM3D and is shown in Fig 4.21. The mean, variance and variogram are all well reproduced by the realization.

In the two previous case-studies the axes of anisotropy ( $x', y'$ ) were aligned with the cartesian axes ( $x, y$ ); as a result, the estimates of  $K_{V,xy}$  obtained using the proposed method were negligible. In this third example the estimates of  $K_{V,xy}$  are of the same order of magnitude as the estimates of  $K_{V,xx}$  or  $K_{V,yy}$ .

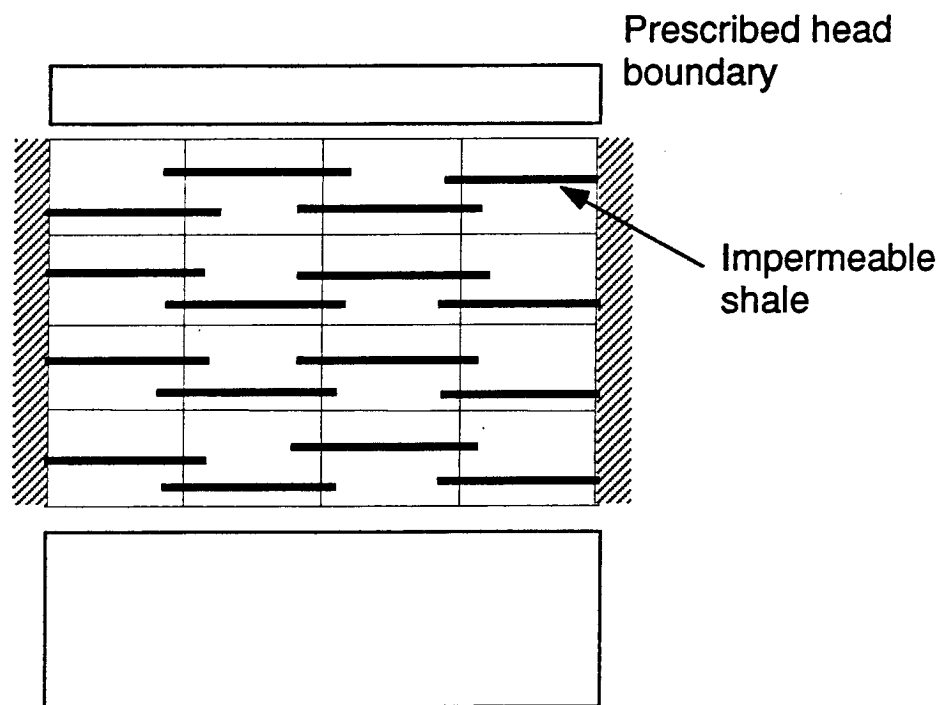


Figure 4.20: **An aquifer in which the traditional approach cannot be used.** This aquifer is clearly artificial but it serves to present a case in which the traditional method fails. Assuming that the shales are impermeable, the traditional method assigns zero vertical conductivity to all blocks in the aquifer; however, it is evident that the total flow crossing vertically the aquifer is non-zero.

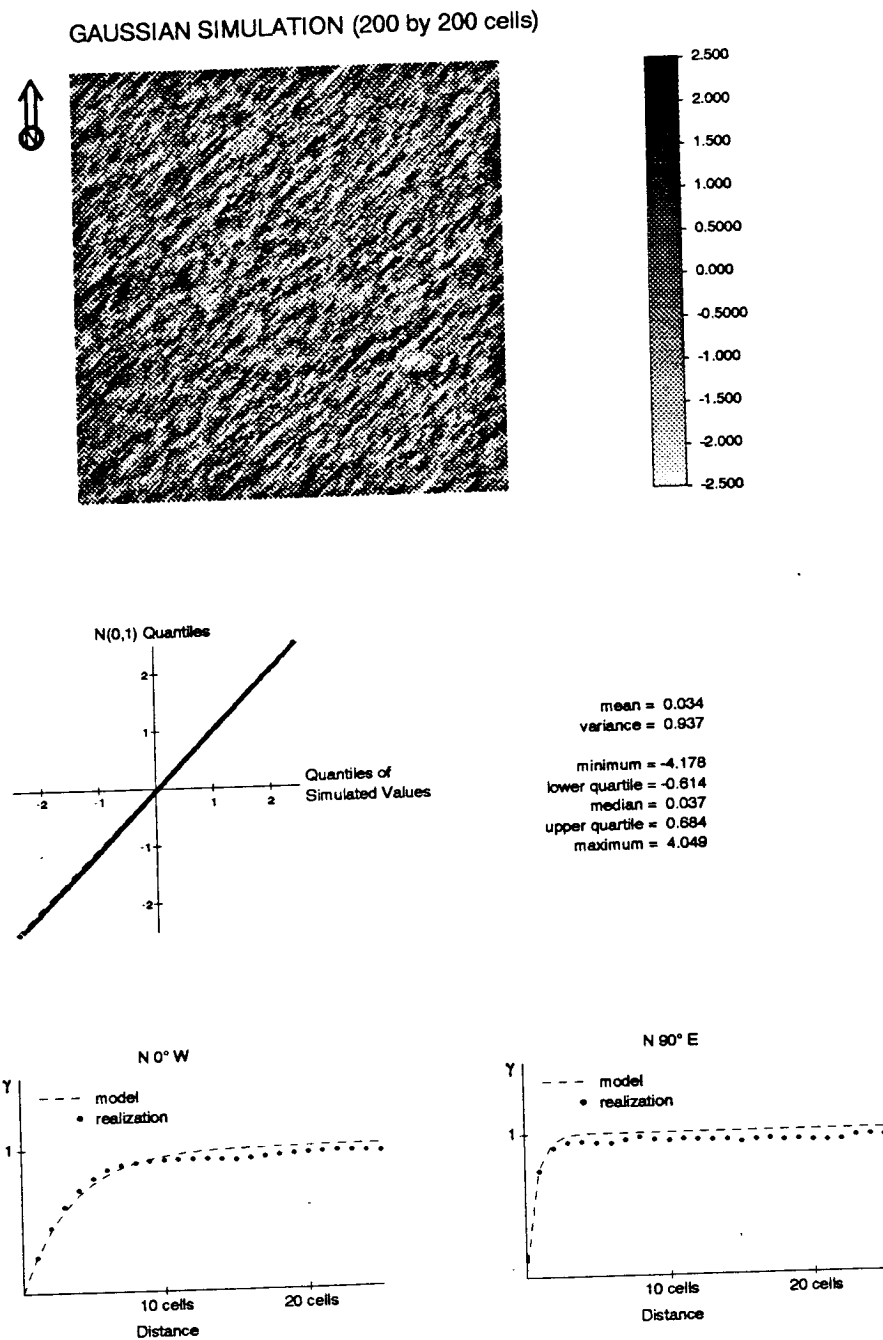


Figure 4.21: **Anisotropic lognormal aquifer.** Top: Grey-scale map of log-hydraulic conductivities. Center: Q-Q plot of generated values versus normal quantiles, and statistics of the realization. Bottom: Model variogram and experimental variogram as inferred from the realization for two orthogonal directions

Figures 4.22 and 4.23 show the bias introduced in the reproduction of the megaflows by neglecting the coefficients  $K_{V,xy}$ . The performance of the proposed method is remarkably good; whereas the geometric mean and the traditional scale-up technique both present a severe bias.

### Statistically Anisotropic Aquifer (2nd ex.)

The only difference with the previous case lies in the variogram of the Gaussian random function. The major axis ( $x'$ ) of anisotropy is now  $135^\circ$  from the  $x$ -axis. The practical ranges are now  $a_{x'} = 0.15L = 3l$  and  $a_{y'} = 0.03L = 0.6l$ , leaving the anisotropy ratio unchanged.

$$\gamma(\mathbf{r}) = 1 - \exp \left( -\sqrt{\left(\frac{3r_{x'}}{a_{x'}}\right)^2 + \left(\frac{3r_{y'}}{a_{y'}}\right)^2} \right)$$

with

$$\begin{Bmatrix} x' \\ y' \end{Bmatrix} = \begin{Bmatrix} -1/\sqrt{2} & 1/\sqrt{2} \\ -1/\sqrt{2} & -1/\sqrt{2} \end{Bmatrix} \begin{Bmatrix} x \\ y \end{Bmatrix}$$

The realization and its statistics are shown in Fig. 4.24. The results of the local and global flow comparisons are displayed in Fig. 4.25 and 4.26 respectively. The same comments as in the previous example apply except that the bias is reversed, now both the geometric mean and the traditional approach overestimate the reference values.

### Discussion

The four case-studies presented indicate that the proposed method will perform well for a variety of hydraulic conductivity spatial distributions. They also show that the geometric mean has limited use and is restricted to statistically isotropic hydraulic conductivities with small variability. The two weaknesses of the traditional method mentioned at the beginning of this section have been demonstrated. First, it should



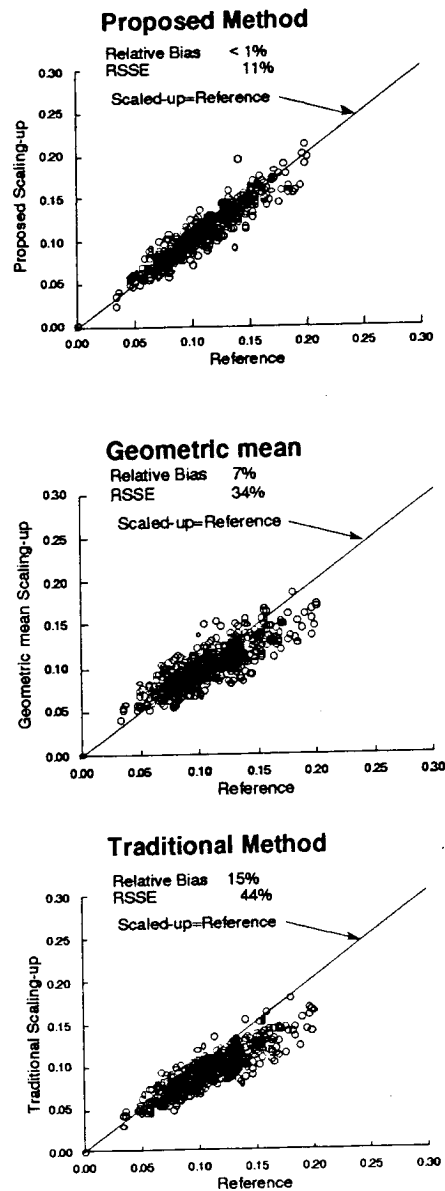


Figure 4.22: **Anisotropic lognormal aquifer: Local flow comparison.** Scaled-up megaflows are displayed versus the reference megaflows as obtained by integrating the reference macroflows

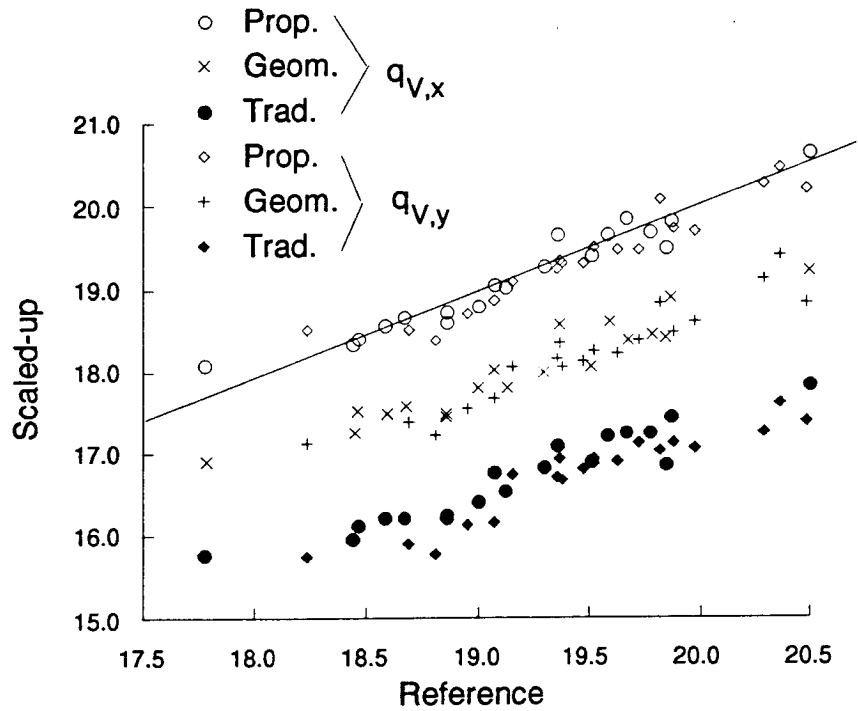


Figure 4.23: **Anisotropic lognormal aquifer: Total flow comparison.** Total flows crossing the entire width (or length) of the aquifer have been obtained from the megascale simulations for the three upscaling techniques. They are displayed versus the reference megafloes as obtained by integrating the flows from the reference macroscale simulation

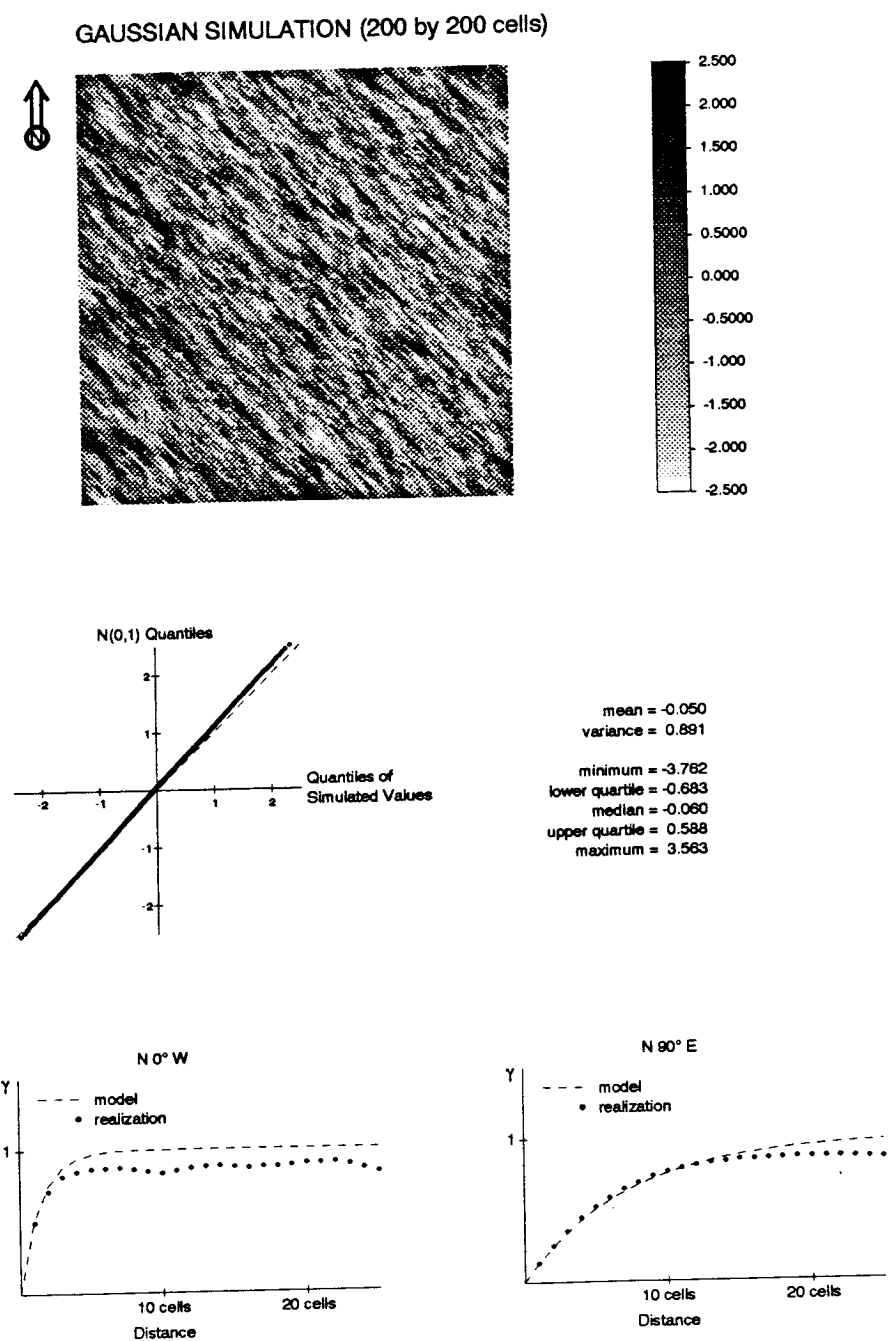


Figure 4.24: **Anisotropic lognormal aquifer (2nd ex.).** Top: Grey-scale map of log-hydraulic conductivities. Center: Q-Q plot of generated values versus normal quantiles, and statistics of the realization. Bottom: Model variogram and experimental variogram as inferred from the realization for two orthogonal directions

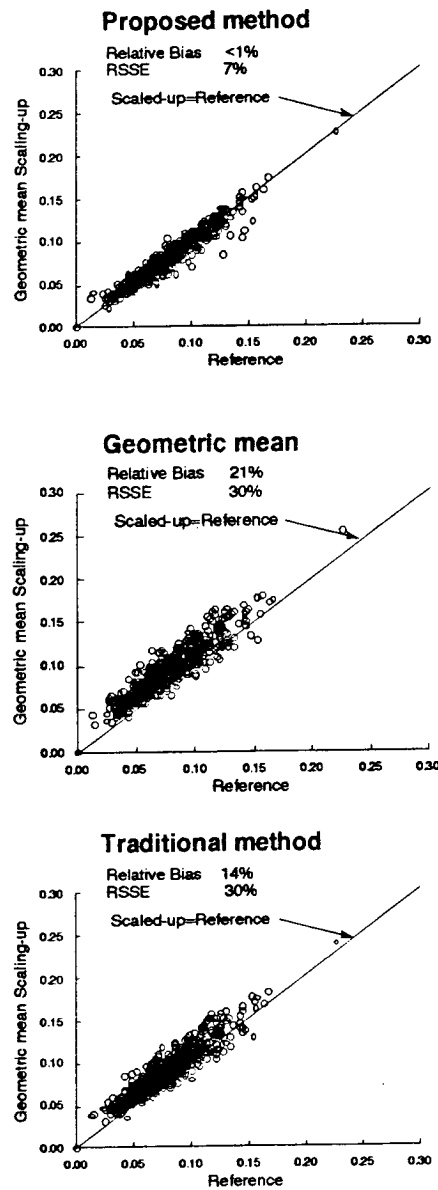


Figure 4.25: Anisotropic lognormal aquifer (2nd ex.): Local flow comparison. Scaled-up megaflows are displayed versus the reference megaflows as obtained by integrating the reference macroflows

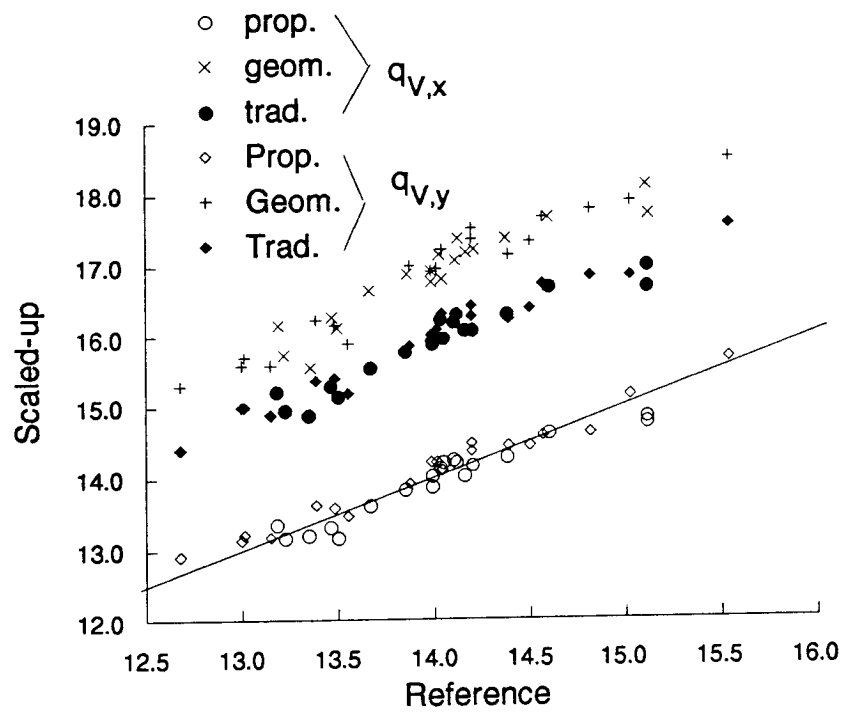


Figure 4.26: **Anisotropic covariance (2nd ex.): Total flow comparison.** Total flows crossing the entire width (or length) of the aquifer have been obtained from the megascale simulations for the three upscaling techniques. They are displayed versus the reference megaflores as obtained by integrating the flows from the reference macroscale simulation

not be used if one expects that the head gradient parallel to the block interfaces contributes to the flow through these interfaces. Second, it should be used only when the boundary conditions used to retrieve the block conductivity are close to the boundary conditions that the block actually has when embedded in the aquifer.

The ability of the proposed method to obtain estimates of  $K_{V,xy}$  at the block interfaces has been demonstrated in the two last examples, in which failing to estimate these coefficients results in systematic bias.

The delicate point in the proposed method is the selection of the various alternative boundary conditions for computing the interface conductivities. In all four examples presented, the proposed method used prescribed head boundaries applied to the “skin” boundaries; these boundaries are given by different tilted planes so that the overall flow across the interblock is forced in different directions (Fig 4.11). The choice of no-flow boundaries—favored by the traditional approach—would be justified only for extreme statistical anisotropy of the hydraulic conductivity such as shown by the aquifer on the right of Fig. 4.7.

## Chapter 5

# Direct Generation of Block Conductivities

The motivation for this dissertation is the Monte-Carlo analysis of aquifer response variables with for final objective the probabilistic assessment of aquifer performance. Such analysis requires first, the generation of multiple, equally likely, realizations of the flow parameters conditioned to the data, and second, simulating flow within the aquifer for each realization. In chapter 3 new algorithms for the generation of hydraulic conductivity realizations at the scale of the measurements were presented. These realizations may comprise millions of nodes; however, flow cannot be simulated in such a fine detail. Chapter 4 proposed a new approach for the averaging of conductivity values, so that the final flow model has a tractable number of block values. With these elements a Monte-Carlo analysis of aquifer performance can now be carried out according to the flow chart in Fig. 5.1.

The experience gained from the numerical analyses of the previous chapter indicates that steps ③ and ② of Fig. 5.1 (in this order) are the most time-consuming. This experience is based on the analysis of aquifers initially discretized at tens of thousands of cells, then scaled-up to a few hundred blocks. It is apparent that steps ③ and ② will always be the most costly even though the order may change for larger

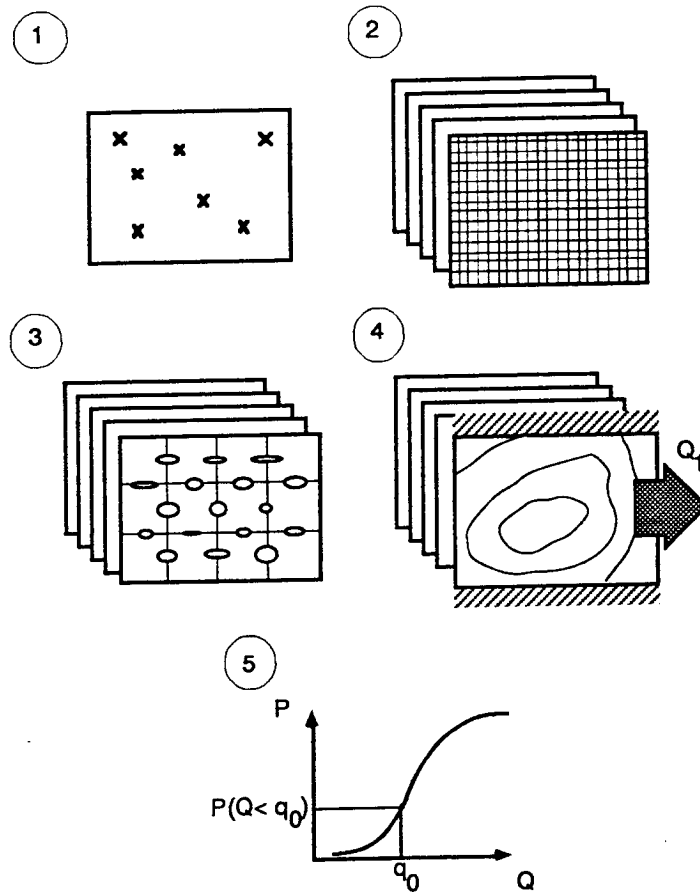


Figure 5.1: **Typical Monte-Carlo analysis of aquifer responses.** ① Collection of data and statistical analysis; ②  $N$  realizations of hydraulic conductivities at the macroscale are generated, each with possibly millions of nodes; ③ the macroscale conductivities are scaled-up into interface conductivities; ④ the solution of the flow problem is obtained on each scaled-up realization, and the response variable(s) is retrieved; ⑤ a statistical analysis is performed on the response variable(s) resulting in a probability distribution for each response variable.



discretizations and/or different scale-up ratios. Step ④ that is, the flow simulation could be the most expensive depending on the type of flow modeling, particularly if complex multiphase flow simulation is required.

This chapter presents two new techniques for reducing the time involved in the first two steps in Fig 5.1. By combining them, conditional realizations of scaled-up values are generated directly. Both techniques are extensions of the analytical and numerical scaling-up techniques presented in the previous chapter and are, therefore, limited by the same constitutive assumptions.

## 5.1 The Principle

The basic principle of these two new techniques is depicted by the flow chart in Fig. 5.2. The idea is to go from the conditioning macroscale data to the megascale interface conductivities in a single step instead of the two steps required in Fig. 5.1.

The same stochastic approach used to generate macroscale conductivity fields is used to generate megascale conductivity fields. Unfortunately, unlike macroscale conductivities, there are no megascale conductivity data; therefore, the random function model associated with the interface conductivities cannot be inferred directly from data.

If inference of a statistical model for interface conductivities were possible, together with the inference of the joint distribution of interface conductivities and macroscale conductivities, a simulation algorithm such as described in section 3.2 (joint simulation of multiGaussian variables) could be employed for the direct generation of interface conductivities. This direct generation would require knowledge of the expected values of each variable, the covariances (or variograms) of both, the variable being simulated, and of the conditioning data; and the cross-covariances (or cross-variograms) between these variables. The objective of this chapter is to discuss ways to obtain these covariances and cross-covariances.

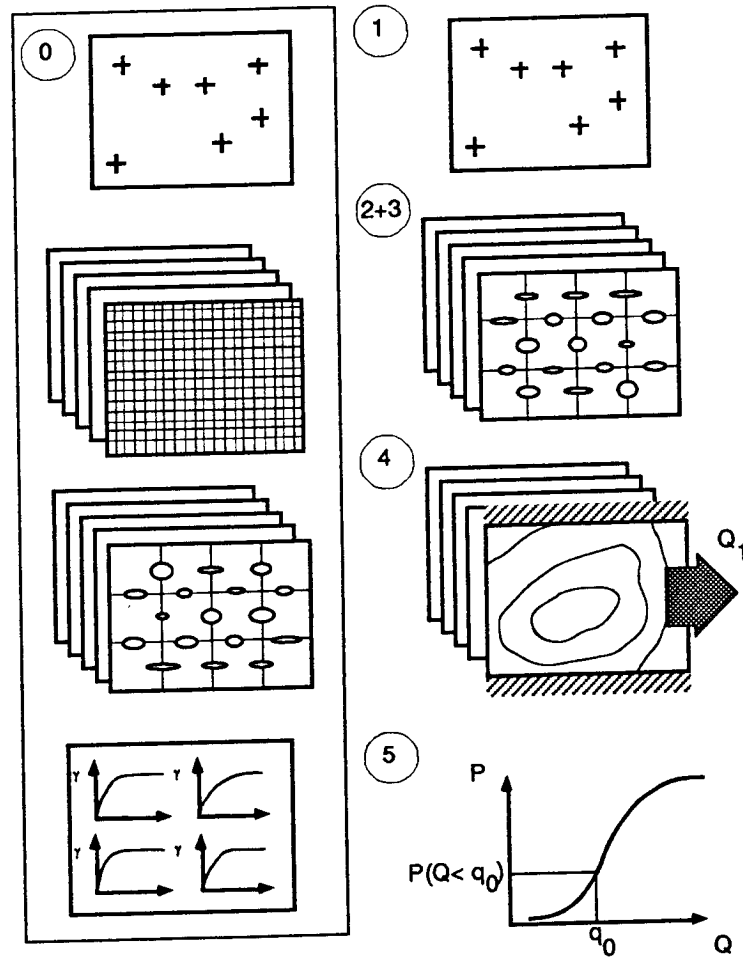


Figure 5.2: **Proposed Monte-Carlo analysis of aquifer responses.** ① Prior to the Monte-Carlo analysis itself, the data is collected and analyzed and some realizations of hydraulic conductivities at the macroscale are generated over a few thousand nodes, these realizations are scaled-up and the interface conductivities then serve as a training image to obtain the variograms and cross-variograms required for the direct simulation of interface conductivities conditioned to the measured values; ②+③  $N$  realizations of the components of the interface conductivities are generated directly at the megascale conditioned upon the macroscale data; ④ the solution of the flow problem is obtained on each scaled-up realization, and the response variable(s) is retrieved; ⑤ a statistical analysis is performed on the response variable(s) resulting in a probability distribution for each response variable.

## 5.2 Analytical Approach

This section expands the analytical development presented in section 4.2; therefore, all constitutive assumptions used in that section apply here. This section follows closely the paper by Rubin and Gómez-Hernández (1990).

In section 4.2 a closed-form expression for the value of block conductivities was derived. The block conductivity was assumed isotropic to flow and therefore represented by a scalar ( $K_V$ ). The expression of  $K_V$  is repeated here

$$K_V = K_g \left[ 1 + \overline{Y'} + \frac{\overline{Y'^2}}{2} + \frac{1}{j_a} \left( \overline{Y' j'_x} - \overline{Y'} \overline{j'_x} \right) \right] \quad (5.1)$$

where  $K_g$  is the geometric average of  $K$  over the block, the overbar indicates spatial average over the block,  $Y'$  is the fluctuation of log-conductivity about its arithmetic average,  $j_a$  is the modulus of the arithmetic average of the gradient vector, and  $j'_x$  is the  $x$ -component of the fluctuation of the gradient vector about its arithmetic average ( $\mathbf{j}_a$ ) when the  $x$  cartesian axis is aligned with  $\mathbf{j}_a$ .

Derivation of expression (5.1) was based on the exhaustive knowledge of the hydraulic conductivities over the entire aquifer, without any probabilistic interpretation. In this section we will model the log-conductivities in (5.1) as a realization of an ergodic and multiGaussian random function. Then, the block value ( $K_V$ ) becomes a random function denoted  $\widetilde{K}_V$ . (A tilde will be used to distinguish the random variables from their realizations or their deterministic counterparts.) The objective of this section is to derive the statistics of this new random function.

The stochastic version of (5.1) relating the random functions  $\widetilde{K}_V(\mathbf{x})$ ,  $\widetilde{Y}(\mathbf{x})$  and  $\widetilde{j}_x(\mathbf{x})$  is written

$$\widetilde{K}_V = K_g \left[ 1 + \overline{\widetilde{Y}} + \frac{\overline{\widetilde{Y}^2}}{2} + \frac{1}{j_a} \left( \overline{\widetilde{Y} \widetilde{j}_x} - \overline{\widetilde{Y}} \overline{\widetilde{j}_x} \right) \right] \quad (5.2)$$

Thanks to ergodicity, the average values in the previous expression can be exchanged by expected values. In this way,  $K_g$  and  $j_a$  represent geometric and arithmetic averages computed through the ensemble. Likewise, the fluctuations  $Y'$  and  $j'_x$  are redefined about the expected values of  $\widetilde{Y}$  and  $\widetilde{j}$ .

Taking the expected value on both sides of (5.2) results in

$$\begin{aligned} E\{\widetilde{K}_V\} &= K_g \left( 1 + \overline{E\{\widetilde{Y}'\}} + \frac{\overline{E\{\widetilde{Y}'^2\}}}{2} + \frac{1}{j_a} \left( \overline{E\{\widetilde{Y}'\widetilde{j}'_x\}} - \overline{E\{\widetilde{Y}'\}} \overline{E\{\widetilde{j}'_x\}} \right) \right) \\ &= K_g \left( 1 + \frac{\sigma_Y^2}{2} + \frac{1}{j_a} \left( \sigma_{Y,j_x}^2 - \overline{C}_{Y,j_x} \right) \right) \end{aligned} \quad (5.3)$$

where  $\sigma_Y^2$  is the stationary variance of the log-conductivity random function ( $\widetilde{Y}$ ),  $\sigma_{Y,j_x}^2$  is the stationary cross-variance between the random functions  $\widetilde{Y}$  and  $\widetilde{j}_x$ , and  $\overline{C}_{Y,j_x}$  is the average of the cross-covariance between  $\widetilde{Y}$  and  $\widetilde{j}_x$  when both end points of the separation vector  $\mathbf{r} = \mathbf{x} - \mathbf{x}'$  sweep the block  $V$

$$\overline{C}_{Y,j_x} = \frac{1}{V^2} \int_V \int_V C_{Y,j_x}(\mathbf{x} - \mathbf{x}') d\mathbf{x} d\mathbf{x}'$$

Relation (5.3) shows that  $E\{\widetilde{K}_V\}$  is a function of (1) the log-conductivity mean; (2) the log-conductivity variance; (3) the size of the block  $V$ ; and (4) the flow conditions as expressed through the cross-covariance between  $\widetilde{Y}$  and  $\widetilde{j}_x$ .

The value of the cross-covariance  $C_{Y,j_x}$  can be obtained as the partial derivative of the cross-covariance between log-conductivity and hydraulic heads  $C_{Y,h}(\mathbf{r})$ , with respect to the  $x$ -component of the vector  $\mathbf{r}$

$$C_{Y,j_x}(\mathbf{r}) = \frac{\partial C_{Y,h}}{\partial r_x}$$

Integral expressions for  $C_{Y,h}$  as well as closed-form expressions for specific log-conductivity covariances have been derived by Dagan and his co-workers. A thorough description of how these expressions are obtained is found in (Dagan, 1989, sec. 3.7). For the sake of completeness, the integral expression for  $C_{Y,h}$  for statistically isotropic log-conductivities and steady, uniform flow in unbounded formations, is reproduced here

$$C_{Y,h}(\mathbf{r}) = - \frac{\mathbf{j}_a \cdot \mathbf{r}}{|\mathbf{r}|} \left( \frac{1}{|\mathbf{r}|^{N-1}} \int_0^{|\mathbf{r}|} |\mathbf{r}'|^{N-1} C_Y(r') dr' \right) \quad (5.4)$$

where the dot indicates inner product,  $|\cdot|$  denotes modulus,  $N$  is the space number of dimensions, and  $C_Y(r')$  is the isotropic log-conductivity covariance as a function

only of the modulus of the separation vector ( $r' = |\mathbf{r}'|$ ). Substituting the expression of  $C_Y$  in (5.4) and taking the derivative of  $C_{Y,h}$  with respect to  $r_x$  after aligning the  $x$ -axis with the vector  $\mathbf{j}_a$  yields a closed-form expression for  $C_{Y,j_x}$ .

The covariance of  $\widetilde{K}_V$  is equal to the expected value of  $\widetilde{K}'_V(\mathbf{x})\widetilde{K}'_V(\mathbf{x} + \mathbf{r})$ , with  $\widetilde{K}'_V = \widetilde{K}_V - E\{\widetilde{K}_V\}$ . An expansion of  $\widetilde{K}'_V$  can be obtained from (5.2) and (5.3). All of the terms but one in this expansion yield terms of order larger than two when computing the covariance. Thus, we limit the expansion of  $\widetilde{K}'_V$  to the first-order terms,

$$\widetilde{K}'_V = K_g \widetilde{Y}'. \quad (5.5)$$

Due to the resulting linear relationship between  $\widetilde{Y}'$  and  $\widetilde{K}'_V$ , the block conductivity covariance is straightforwardly written as

$$C_{K_V}(\mathbf{r}) = K_g^2 \overline{C}_Y(V, V_{+\mathbf{r}}), \quad (5.6)$$

where  $V_{+\mathbf{r}}$  is the translation of block  $V$  by a vector  $\mathbf{r}$ , and  $\overline{C}_Y(V, V_{+\mathbf{r}})$  is the average log-conductivity covariance when one end point of the separation vector sweeps block  $V$  and the other sweeps block  $V_{+\mathbf{r}}$ .

$$\overline{C}_Y(V, V_{+\mathbf{r}}) = \frac{1}{V^2} \int_V \int_{V_{+\mathbf{r}}} C_Y(\mathbf{x}, \mathbf{x}') d\mathbf{x} d\mathbf{x}'$$

Values for  $\overline{C}_Y(V, V_{+\mathbf{r}})$  for  $\mathbf{r} = \mathbf{0}$  have been tabulated, for example, by Journal and Huijbregts (1978). Values for  $\overline{C}_Y(V, V_{+\mathbf{r}})$  for any arbitrary vector  $\mathbf{r}$  can be computed using the Gauss-Cauchy algorithm (see Journal and Huijbregts, 1978).

From (5.6),  $C_{K_V}$  is found to be linearly proportional to the square of  $K_g$  and inversely proportional to the square of the volume  $V$ .

Similarly, the cross-covariance between  $\widetilde{K}_V$  and  $\widetilde{Y}$  is obtained as  $E\{\widetilde{K}'_V \widetilde{Y}'\}$ , a second-order expansion of which is

$$C_{K_V, Y}(V, \mathbf{r}) = K_g \overline{C}_Y(V, \mathbf{r}) \quad (5.7)$$

where  $C_{K_V, Y}(V, \mathbf{r})$  represents the cross-covariance between point log-conductivity and block conductivity when the point is separated from the center of the block  $V$  by a

vector  $\mathbf{r}$ . The value  $\overline{C}_Y(V, \mathbf{r})$  is the average of the log-conductivity covariance when one end point of the vector sweeps volume  $V$  and the other remains fixed at a distance  $\mathbf{r}$  from the block center ( $\mathbf{x}$ ).

$$\overline{C}_Y(V, \mathbf{r}) = \frac{1}{V} \int_V C_Y(\mathbf{x}', \mathbf{x} + \mathbf{r}) d\mathbf{x}'$$

**Validation.** The previous analytical values for the expected value of  $\widetilde{K}_V$  and its variance were validated by a Monte-Carlo technique in two dimensions. Since expressions (5.3) and (5.6) were obtained by a second-order perturbation approach, the objective of that validation was to determine the corresponding level of error.

Monte-Carlo realizations of multi-lognormal hydraulic conductivities with an expected value of  $\ln K$  equal to  $-4.0$ , different variances, and exponential isotropic variogram<sup>1</sup>

$$\gamma_Y(\mathbf{r}) = \sigma_Y^2 \left(1 - \exp\left(-\frac{3|h|}{a}\right)\right)$$

were generated for an area  $2.2a$  by  $2.2a$  divided into cells  $0.03a$  by  $0.03a$ . The boundary conditions imposed were those shown in Fig. 2.3, that is, no flow along the boundaries parallel to the  $x$  (horizontal) axis, and prescribed head in each of the boundaries parallel to the  $y$  (vertical) axis. A sensitivity analysis was carried out to verify that the final results for  $K_V$  were independent of both the magnitude of the head gradient and the aquifer size. The flow simulator used in this case is the USGS two-dimensional code by Trescott *et al.* (1976).

Since the process is isotropic, the traditional method for scaling-up described in the previous chapter could be used instead of the more expensive method proposed in this dissertation. Blocks of different sizes were delineated around the center of the aquifer and their block conductivities computed. The mean and variance of the block conductivities were obtained by averaging over 200 realizations.

Figures 5.3 and 5.4 compare the theoretical values and numerical results of the ratio  $E\{\widetilde{K}_V\}/K_g$  (see Eq. (5.3)) for various block side lengths and variances of point

---

<sup>1</sup>of practical range  $a$

conductivity  $\sigma_Y^2$ . Note that although the approach is formally limited to  $\sigma_Y^2 < 1$ , it appears robust for much higher  $\sigma_Y^2$  as long as the averaging volume  $V$  is sufficiently large, because then one gets closer to ergodicity. For small blocks, the numerical results indicate that the expected value of  $\widetilde{K}_V$  could be almost three times as large as the geometric average.

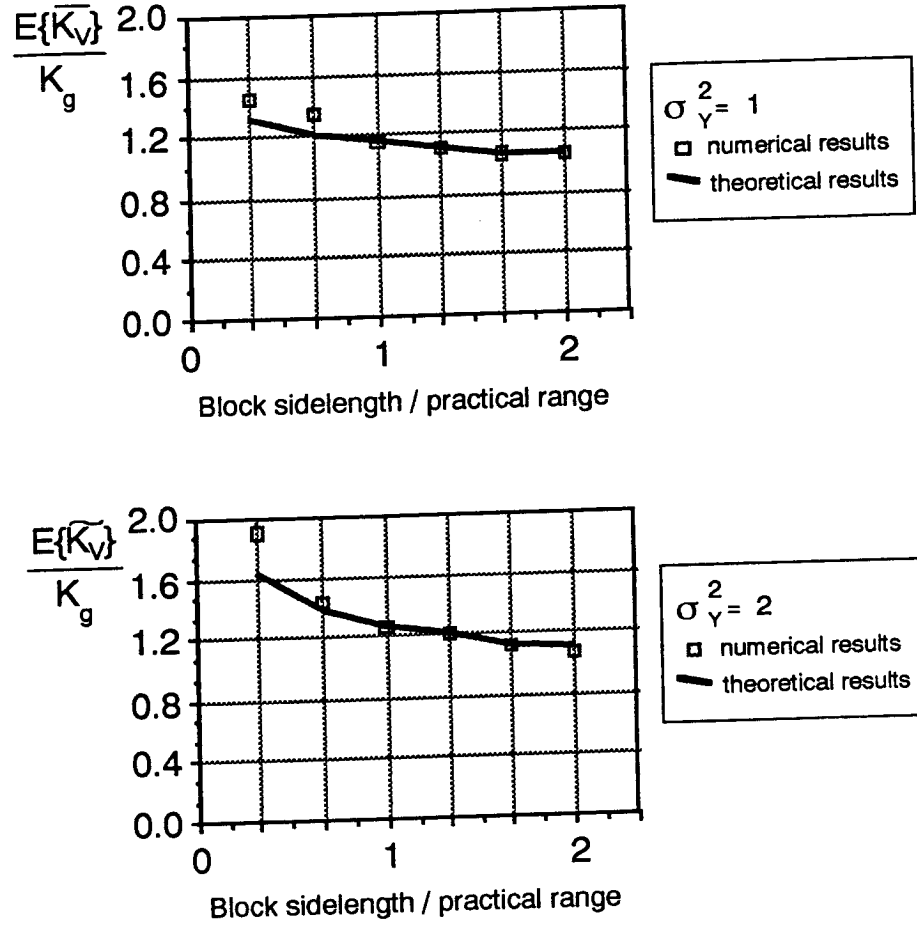


Figure 5.3: Expected value of the block conductivity for different variances of point conductivity. The theoretical values were computed using Eq. (5.3); the numerical ones correspond to the ensemble average of 200 numerical simulations

The theoretical variance  $\overline{C}_{K_V}(V, V)$  (see Eq. 5.6) for various block side lengths and  $\sigma_Y^2$  are compared with numerical results in Fig. 5.5 and 5.6. For  $\sigma_Y^2 = 1$  and  $\sigma_Y^2 = 2$ , good agreement is obtained between the simulated and theoretical variances

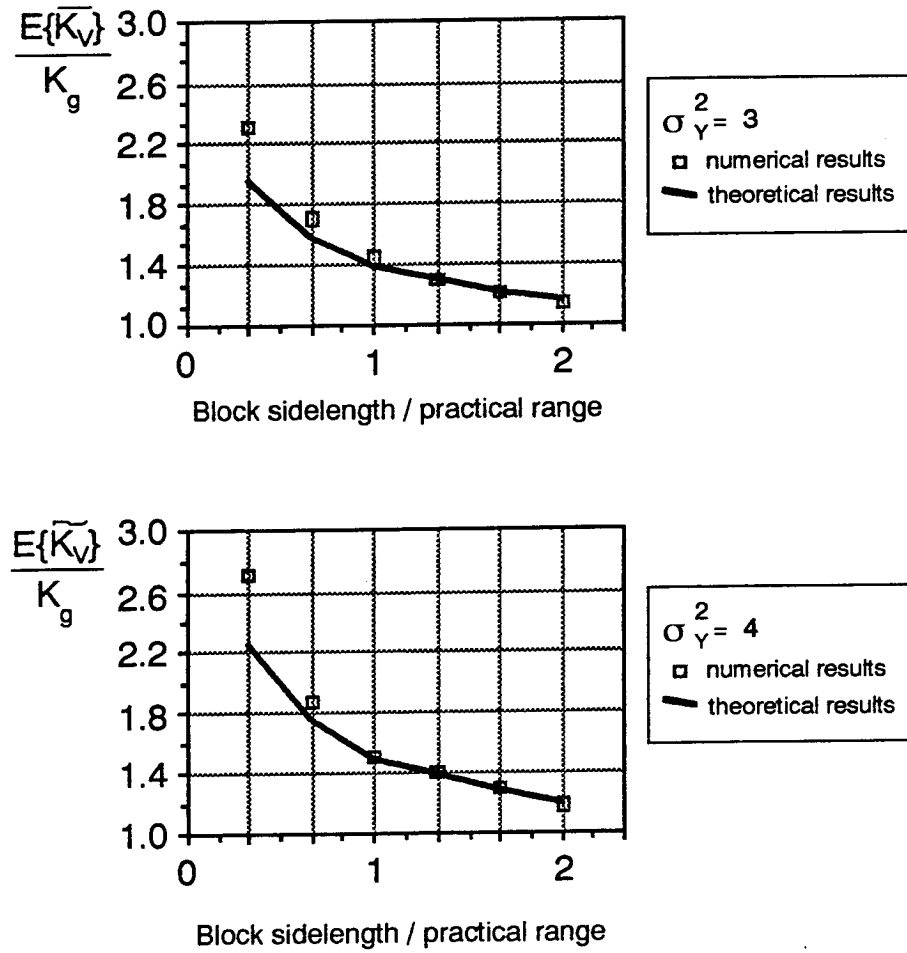


Figure 5.4: Expected value of the block conductivity for different variances of point conductivity. The theoretical values were computed using Eq. (5.3); the numerical ones correspond to the ensemble average of 200 numerical simulations



for practically all block sizes. For  $\sigma_Y^2$  larger than 2, a good agreement between theoretical and numerical results is obtained for blocks with side lengths larger than  $0.6a$ , again because of ergodicity.

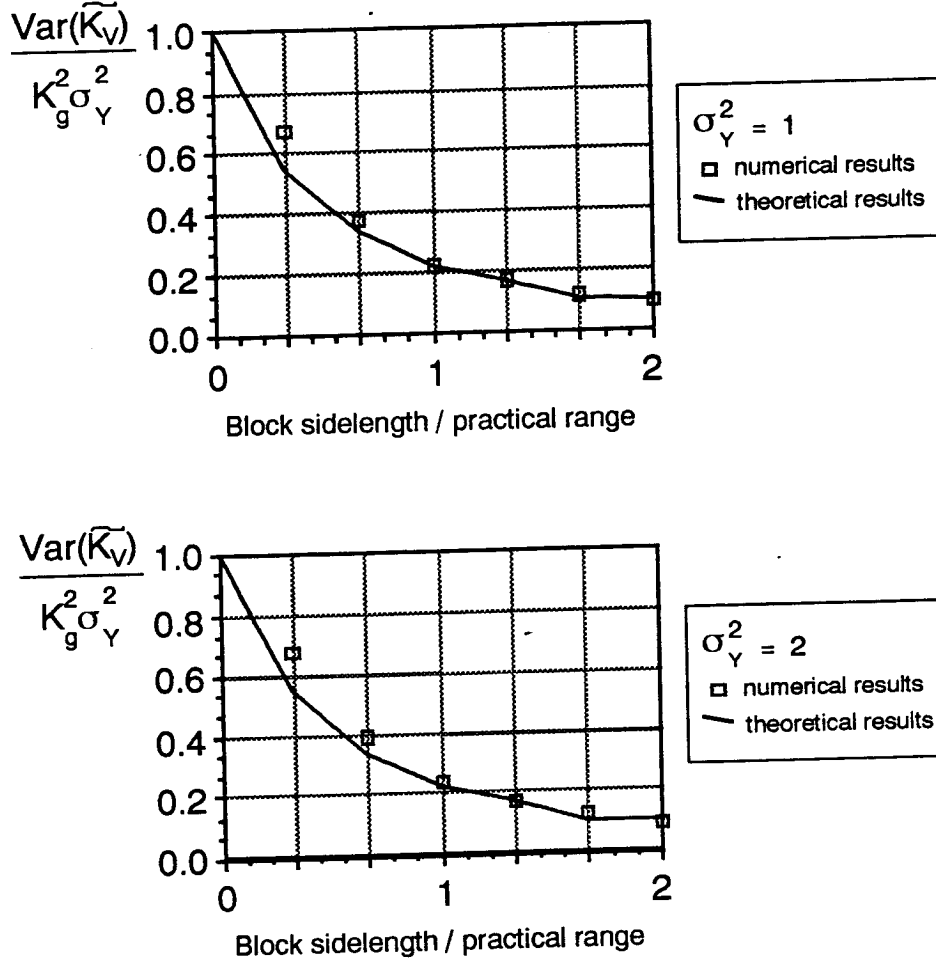


Figure 5.5: Variance of the block conductivity for different variances of point conductivity. The theoretical variances were computed using Eq. (5.6); the numerical ones correspond to the ensemble average of 200 numerical simulations

The sequential simulation algorithm for the generation of two jointly multiGaussian random functions can now be used, since the necessary stochastic models are fully specified:

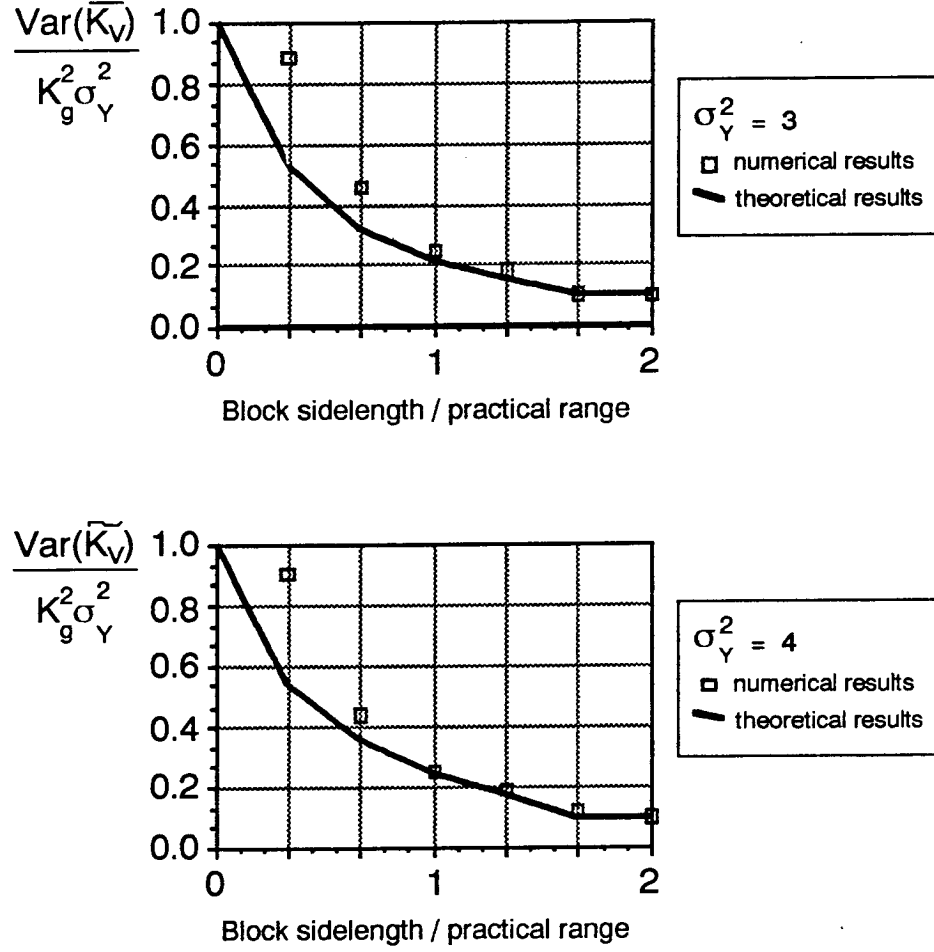


Figure 5.6: Variance of the block conductivity for different variances of point conductivity. The theoretical variances were computed using Eq. (5.6); the numerical ones correspond to the ensemble average of 200 numerical simulations

- The random function  $\tilde{Y}$  is multiGaussian with known mean and covariance
- Because of the small variability of  $\tilde{Y}$ ,  $\tilde{K}_V$  can be seen as a quasi-linear combination of  $\tilde{Y}'$  (see (5.2)). This quasi-linearity makes  $\tilde{K}_V$  multiGaussian as well.
- The expected value of  $\tilde{K}_V$  is given by (5.3)
- The covariance of  $\tilde{K}_V$  is given by (5.6)
- The cross-covariance between  $\tilde{Y}$  and  $\tilde{K}_V$  is given by (5.7)

Given these statistics, the normal system of linear equations (3.4) can be solved, and all required conditional pdfs can be derived. The sequential simulation algorithm can then be applied for the generation of realizations of  $\tilde{K}_V$  conditioned on the  $\tilde{Y}$  data.

Note that although the previous numerical validation was carried out with square blocks, the derivation only required the  $x$ -axis to be aligned with the average gradient vector without any implicit assumption on the block shape (as long as it remains constant).

## Discussion

A Gaussian-related analytical approach for the joint stochastic characterization of  $K_V$  and  $Y$  has been presented. This technique is limited to statistically isotropic media yielding block conductivities which are isotropic to flow. If the assumptions underlying the development of that approach are met, the results are very powerful in the sense that they provide closed-form expressions for the expected values, covariances and cross-covariances of block conductivities for blocks of any constant shape. Once expected values, covariances and cross-covariances are known, a multivariate conditional sequential simulation could be used for the direct generation of block conductivities as input to a numerical simulator.

### 5.3 Numerical Approach

A numerical technique for the inference of the statistics of the interface conductivities is now proposed in order to relax the assumptions required by the previous analytical development. The numerical scaling-up technique presented in the previous chapter is used as the basis for the following development.

The basic idea is to create a small synthetic training image of interface conductivities by scaling-up a simulated map of macroscale conductivities. The expected values, covariances and cross-covariances of interface conductivities are inferred directly from that training image.

The only requirement for the synthetic training image is that it should be large enough (in size and number of nodes) so that interface conductivity covariances can be inferred accurately. According to Journel and Huijbregts (1978) the size of this training image should be at least twice as large as the practical range of the interface conductivity covariance in the direction considered. A good estimate of the practical range is given by  $a + l$ , where  $a$  is the practical range of the macroscale conductivities and  $l$  is the size of the megascale blocks. Note that the training image size is usually much smaller than the aquifer size.

The numerical approach, as presented in this section, is limited to the stochastic characterization of interface conductivities for square blocks of a single size. The extension of this approach to rectangular blocks of a single size is straightforward. However, the extension of this technique to a mixture of rectangular blocks of different size would be tedious, if not unwieldy.

The stochastic characterization of interface conductivities consists of the following steps. First, generate a conditional simulation of macroscale conductivities over an area at least as large as twice the practical range of the macroscale conductivities plus the block side in each direction and containing at least a few hundred cells (Fig. 5.7a). Second, use the method for scaling-up proposed in the previous chapter (or any other method that produces of interface conductivity values) to obtain estimates of the conductivity coefficients at the block interfaces (Fig 5.7b). And third, use both the map of interface conductivities and the map of macroscale conductivities to infer

numerically the expected values, the covariances of the interface conductivity and the cross-covariances between interface conductivities and macroscale conductivities.

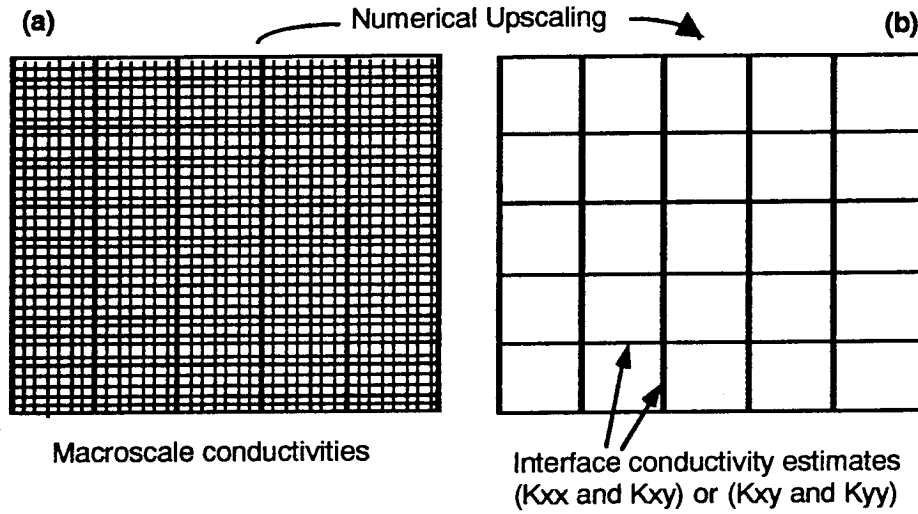


Figure 5.7: **Inferring the statistical model for interface conductivities.** A realization of macroscale conductivities is numerically scaled-up to obtain estimates of the interface conductivity coefficients. These estimates are used as a training image to infer a statistical model for their spatial variability.

## An Example

The step-by-step procedure for stochastic characterization of interface conductivities is now presented through an example. Due to personal preference, these stochastic characterizations will be carried out in terms of variograms and cross-variograms instead of covariances and cross-covariances, with the understanding that for weak second-order stationary stochastic processes with finite variance, the relation between variograms and covariances and between cross-variograms and cross-covariances is unique and given by

$$\gamma_Z(\mathbf{r}) = \sigma_Z^2 - C_Z(\mathbf{r})$$

$$\gamma_{YZ}(\mathbf{r}) = \sigma_{YZ}^2 - \frac{1}{2}(C_{YZ}(+\mathbf{r}) + C_{YZ}(-\mathbf{r}))$$

where  $\sigma_Z^2$  is the stationary variance of  $Z$ , and  $\sigma_{YZ}^2$  is the stationary cross-variance between  $Y$  and  $Z$ . We will further assume that the cross-covariance  $C_{YZ}$  is symmetric about  $\mathbf{r}$ , i.e.,  $C_{YZ}(+\mathbf{r}) = C_{YZ}(-\mathbf{r})$ .

Consider that conductivity data has been collected from an aquifer and the log-conductivity is modeled by a two-dimensional multiGaussian second-order stationary and ergodic random function model ( $\tilde{Y}$ ). The statistics of  $\tilde{Y}$  are: mean  $m_Y = 0$ , variance  $\sigma_Y^2 = 2.0$  and a variogram with anisotropic nugget effect (0 in the  $x$ -direction and 0.4 in the  $y$ -direction) plus an anisotropic spherical component with range in the  $x$ -direction  $a_x = 3l$  and range in the  $y$ -direction  $a_y = 0.3l$ , where  $l$  is the size of the megascale block. The analytical expression of this variogram is

$$\gamma(\mathbf{r}) = 0.4 \times \text{Sph} \left( \sqrt{\left(\frac{r_x}{3l}\right)^2 + \left(\frac{r_y}{\epsilon}\right)^2} \right) + 1.6 \times \text{Sph} \left( \sqrt{\left(\frac{r_x}{3l}\right)^2 + \left(\frac{r_y}{0.3l}\right)^2} \right)$$

where  $\text{Sph}(\mathbf{r})$  is defined as

$$\text{Sph}(r) = \begin{cases} \frac{3}{2}|r| - \frac{1}{2}|r|^3, & \text{if } |r| < 1 \\ 1, & \text{otherwise} \end{cases},$$

and  $\epsilon$  is a very small quantity so that  $\text{Sph}(r/\epsilon)=1$  for all  $r_y > \epsilon$ .

The aquifer is a square of size  $20l$  by  $20l$ . Each block contains 10 by 10 cells; thus the aquifer contains 200 by 200 macroscale cells. There are 1444 block interfaces at which the megafloes are computed and there are 38 cross-sections at which the total crossing flow is obtained.

An unconditional realization of  $\tilde{Y}$  was generated over an area of 200 by 200 cells using GSIM3D (Fig. 5.8). The minimum area recommended by Journel and Huijbregts (1978) for inferring reliable estimates of the variograms is  $2(a+l)$  which, for the largest practical range of the  $\tilde{Y}$  covariance, is equal to  $6l$ . The actual realization is  $20l$  by  $20l$  which is more than 3 times the recommended value. Also, after scaling-up, this area will contain almost 1500 hundred interface conductivities evenly distributed over that area. Therefore, both in terms of size and number of points, stable estimates of

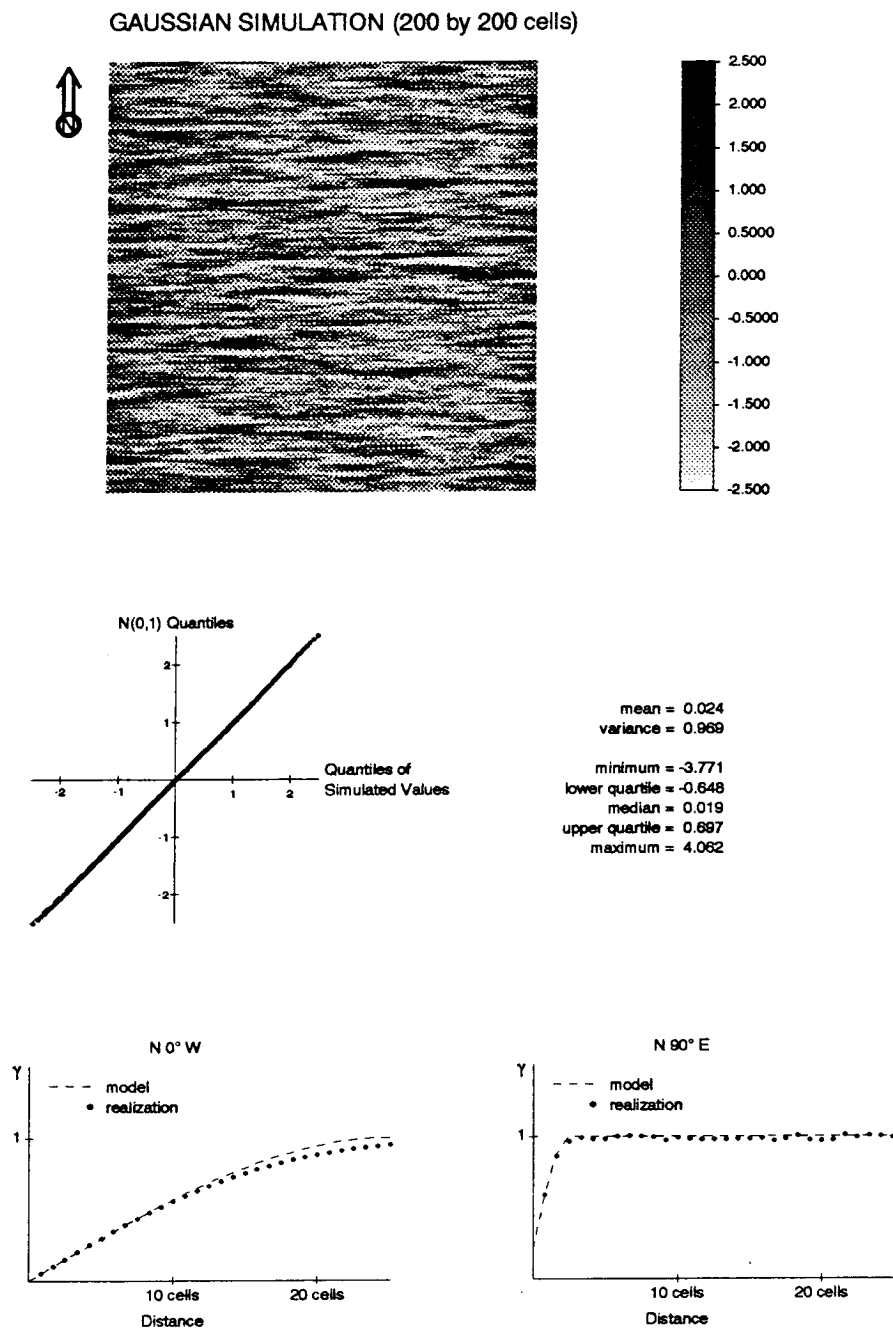


Figure 5.8: **Macroscale unconditional realization of standardized log-conductivities** used to build a training image of interface conductivities. Top: Grayscale map of the simulation, Center: quantile-quantile plot of the simulated values versus normal deviates, Bottom: reproduction of the input variograms

the variograms and cross-variograms should be obtained from this training image. If this is not the case, more training images can be generated and used.

The scaling-up technique proposed earlier in this dissertation (section 4.3) was applied to the realization in Fig. 5.8. The scaling-up was carried out with four different discretizations, each offset by half a block from the other. That is, if the first discretization has origin at  $(0,0)$ , the other three discretizations have their origin at  $(0, 0.5l)$ ,  $(0.5l, 0.5l)$  and  $(0.5l, 0)$  respectively. In this way, the variograms of the interface conductivities can be inferred for a distance as small as half a block. During the scale-up process it was observed that the  $K_{V,xy}$  coefficients were less than 1% the diagonal terms and were thus discarded. The reason for the small magnitude of these terms is the alignment of the major anisotropy axes of the  $\tilde{Y}$  covariance with the cartesian axes.

After discarding the  $K_{V,xy}$  coefficients, a 38 by 38 training image of the estimates of the interface conductivities  $K_{V,xx}$  (Fig. 5.9) and  $K_{V,yy}$  (Fig. 5.10) is obtained.

The first analysis carried out on these megascale training images was to check their univariate distributions. Figures 5.11 and 5.12 give normal and lognormal probability plots of  $K_{V,xx}$  and  $K_{V,yy}$ , which show that the interface conductivities are approximately log-normally distributed.

The lognormal character of the interface conductivities suggests that a multi-Gaussian model may be appropriate for the joint behavior of the logarithm of macroscale and megascale conductivities. Thus, the co-simulation technique presented in chapter 3 can be applied to the co-simulation of the interface log-conductivities  $\tilde{Y}_{V,xx}$  and  $\tilde{Y}_{V,yy}$  conditioned upon the macroscale log-conductivities  $\tilde{Y}$ .

The statistics required for such co-simulation are: the expected values and variogram of  $\tilde{Y}$ ,  $\tilde{Y}_{V,xx}$ , and  $\tilde{Y}_{V,yy}$ , the cross-variograms between  $\tilde{Y}$  and  $\tilde{Y}_{V,xx}$ ,  $\tilde{Y}$  and  $\tilde{Y}_{V,yy}$ , and between  $\tilde{Y}_{V,xx}$  and  $\tilde{Y}_{V,yy}$ . These statistics were inferred directly from the three training images of Fig. 5.8 to 5.10. The resulting experimental variograms along with the positive definite models used to fit them are displayed in Fig. 5.13 and 5.14.

Now that step ① of Fig. 5.2 is completed, we can proceed to the direct generation of conditional simulations of interface conductivities.



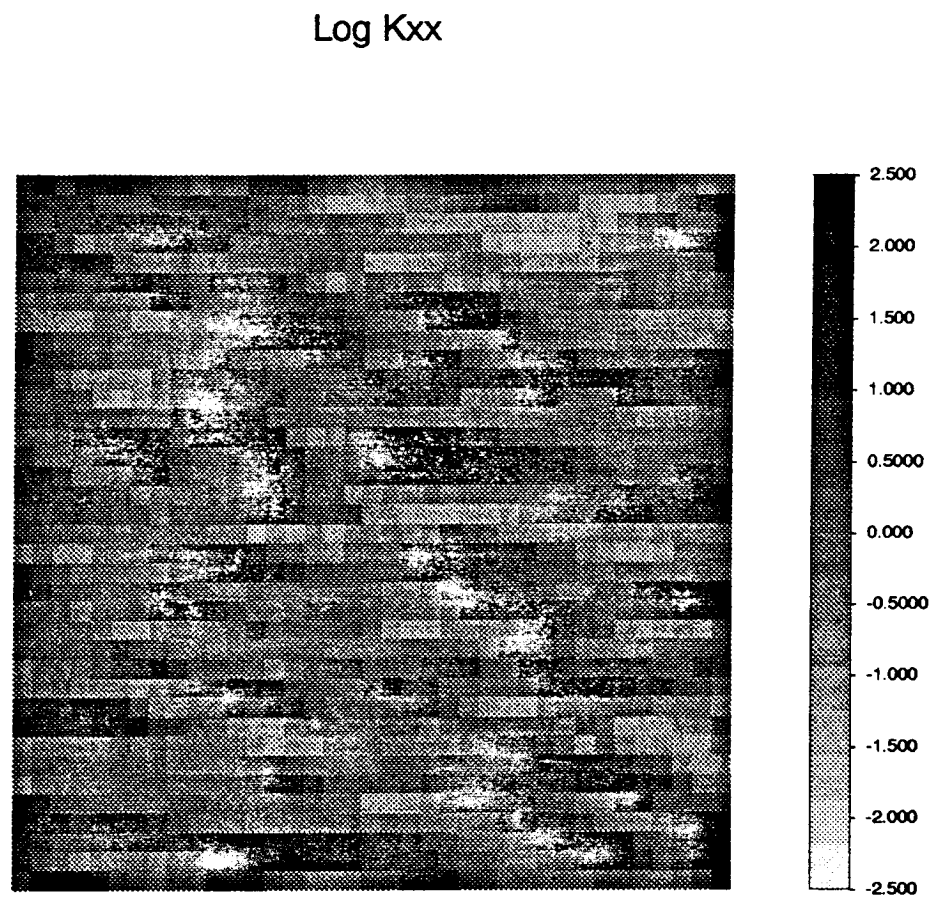


Figure 5.9: Training image for the horizontal interface log-conductivities.

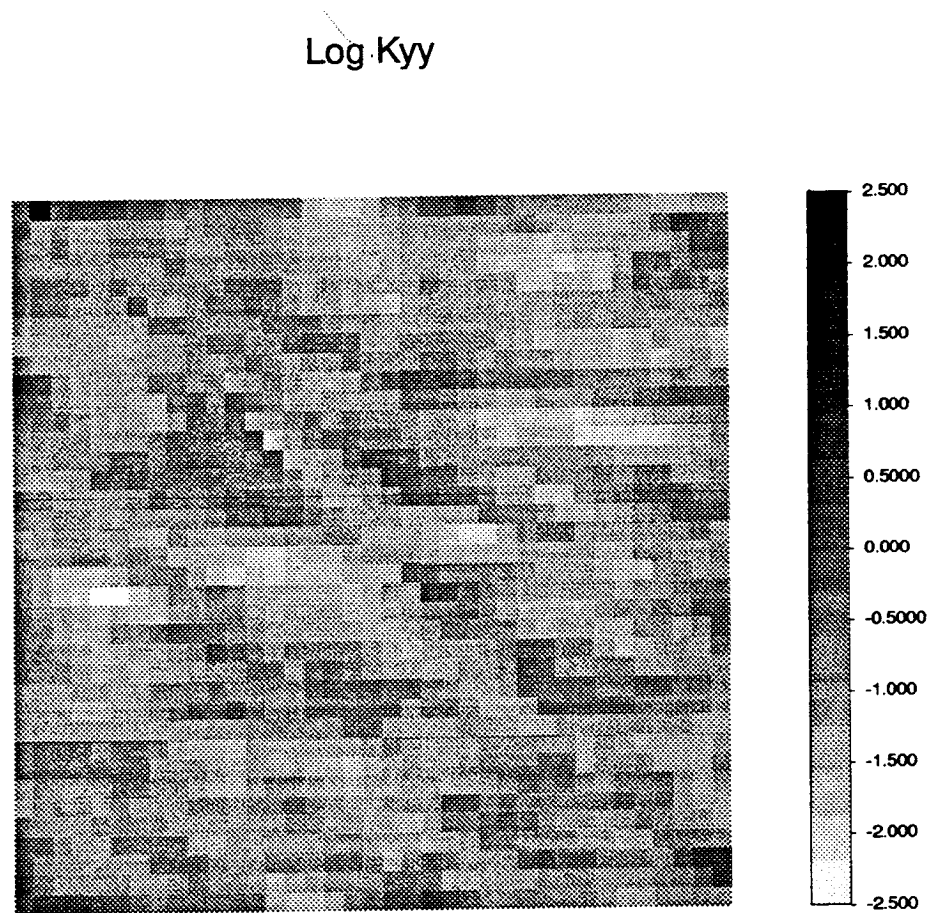


Figure 5.10: Training image for the vertical interface log-conductivities.

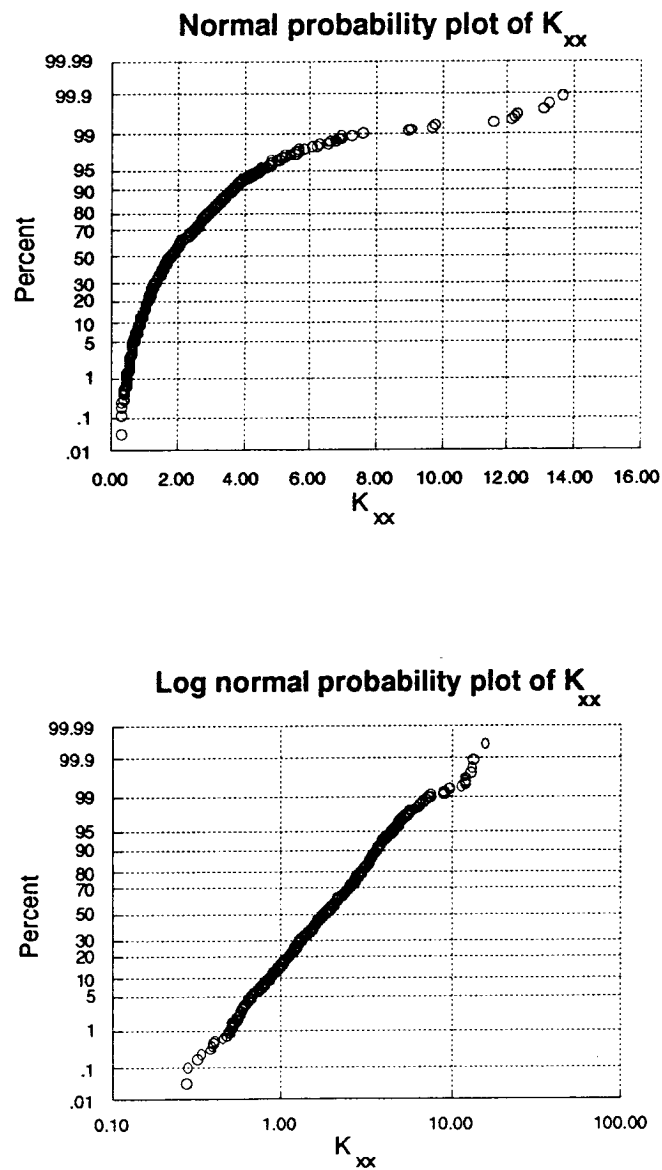


Figure 5.11: Normal and lognormal probability plots of the interface conductivities  $K_{V,xx}$ .

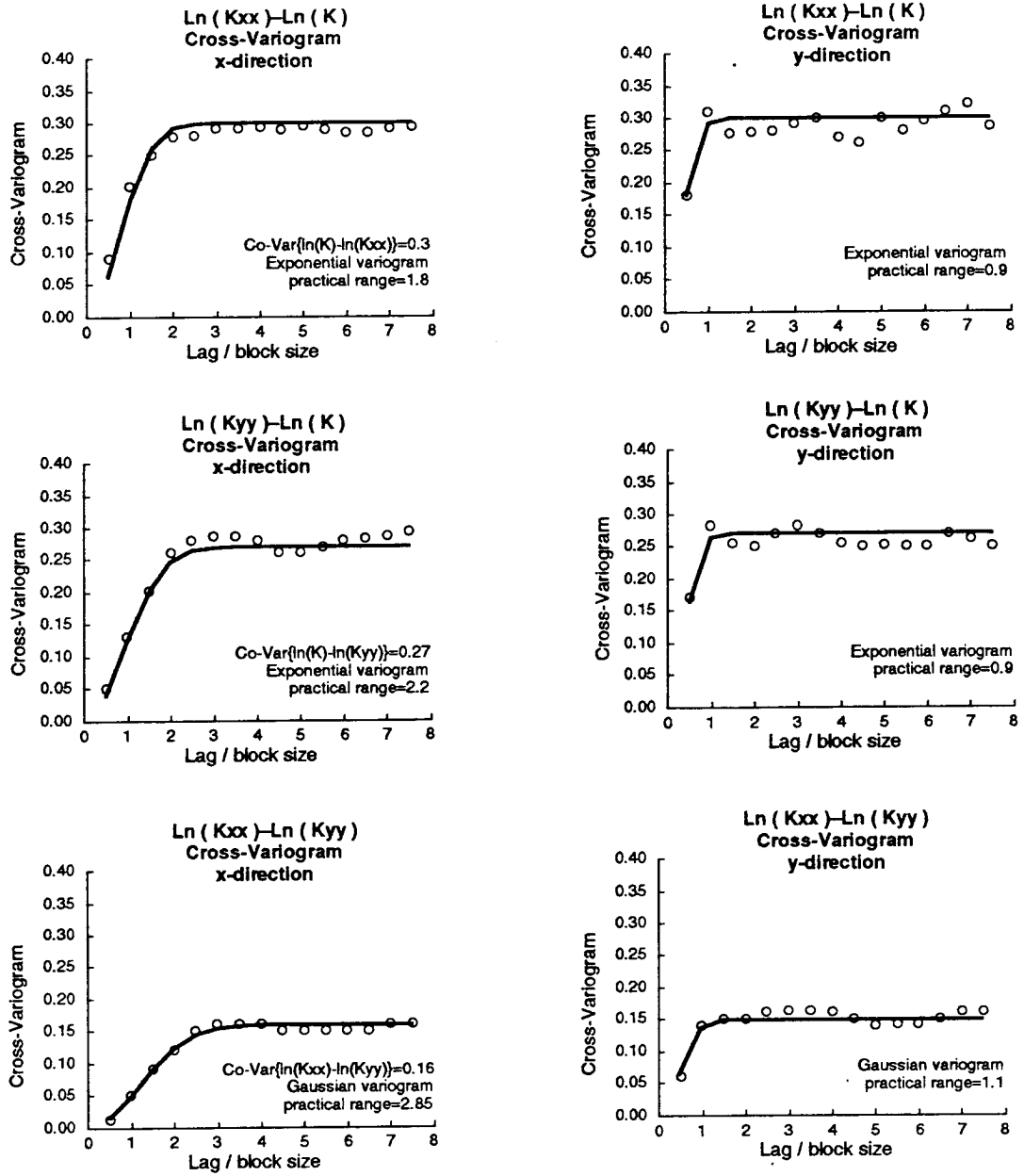


Figure 5.14: Input parameters for the co-simulation of interface conductivities. The expected values, variances and cross-variances, and variograms and cross-variograms for the three random functions involved in the co-simulation of  $Y_{V,xx}$  and  $Y_{V,yy}$  conditioned upon  $Y$  values are given.

## Validation

The previous stochastic modeling of interface conductivities is validated by performing the Monte-Carlo analysis described in Fig 5.2, and comparing the results to those obtained with the analysis carried out using the approach described in Fig 5.1, that is, without shortcutting the scaling-up of each block.

Realizations of interface conductivities are generated for an aquifer with 11 by 11 blocks, each block containing 10 by 10 cells. A total of 42 macroscale conditioning data were considered. The location of these data is shown in Fig 5.15 with their values given in Table 5.1.

$x/l$	$y/l$	$\ln K$	$x/l$	$y/l$	$\ln K$
0.5	0.5	2.629	10.5	0.5	-0.617
0.5	1.0	0.676	10.5	1.0	0.861
0.5	1.5	-0.477	10.5	1.5	0.237
0.5	2.0	0.066	10.5	2.0	-0.520
0.5	2.5	-0.229	10.5	2.5	-0.679
0.5	3.0	0.375	10.5	3.0	-0.390
0.5	3.5	0.827	10.5	3.5	0.605
0.5	4.0	-0.638	10.5	4.0	-3.291
0.5	4.5	0.581	10.5	4.5	-1.560
0.5	5.0	-0.969	10.5	5.0	0.525
0.5	5.5	0.250	10.5	5.5	2.128
0.5	6.0	0.745	10.5	6.0	-1.534
0.5	6.5	-2.697	10.5	6.5	-2.135
0.5	7.0	2.459	10.5	7.0	1.192
0.5	7.5	-0.882	10.5	7.5	-2.921
0.5	8.0	-0.376	10.5	8.0	3.033
0.5	8.5	-2.015	10.5	8.5	1.315
0.5	9.0	0.041	10.5	9.0	-1.896
0.5	9.5	0.996	10.5	9.5	-1.477
0.5	10.0	1.281	10.5	10.0	0.752
0.5	10.5	3.016	10.5	10.5	-1.813

Table 5.1: Conditioning data for Monte-Carlo analysis

Three sets of 200 conditional simulations of conductivities each were generated.

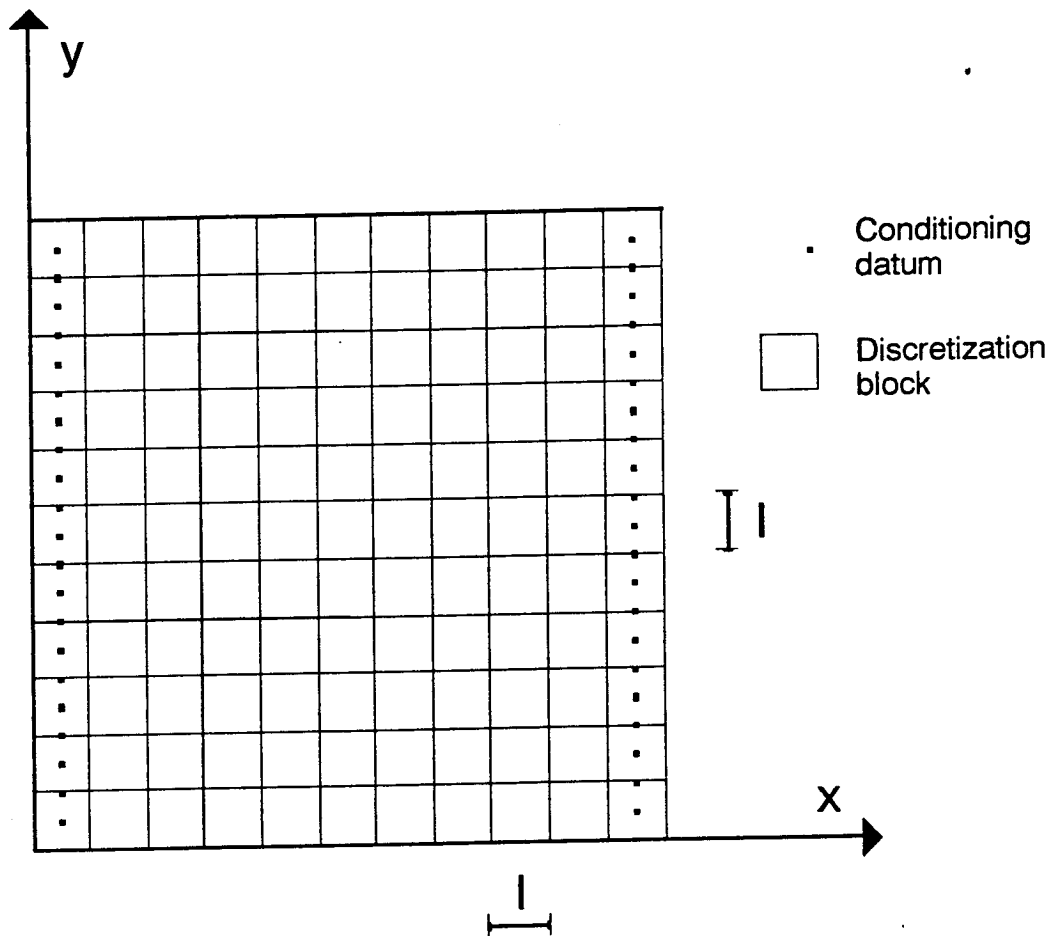


Figure 5.15: **Conditioning data.** The location of the 42 conditioning data used for the Monte-Carlo analysis are shown. The size of the tiny black square representing the datum is at scale with respect to the block size

The first set corresponds to log-conductivity realizations generated at the macroscale over a 110 by 110 cell discretization using GSIM3D. The previous realizations are scaled-up, using the method proposed in section 4.3, to obtain interface conductivities over an 11 by 11 block discretization: this constitutes the second set of 200 simulations. The third set corresponds to interface conductivities generated directly using GCOSIM3D and the statistical model previously inferred from the training images.

All three sets of 200 conditional simulations were subjected to flow modeling using a finite-difference method with prescribed head boundaries on the perimeter as described in Fig 4.10. These boundary conditions force an overall flow at a 45° from the aquifer boundaries. The total flows crossing the 10 vertical cross-sections and the 10 horizontal cross-sections aligned with the block interfaces were computed for each of the 200 realizations.

From each set of 200 realizations a frequency distribution of the total flow crossing the 20 cross-sections is obtained. This frequency distribution is conditional to the log-conductivity data and to the statistical description of the joint variability of macro- and megascale conductivities. The frequency distribution obtained from direct solution of flow over the first set of 200 macroscale realizations is considered as the reference. The very goal of this dissertation is to reproduce this reference frequency distribution, yet without the expensive process of scaling-up or solving flow at the macroscale.

Figures 5.16 and 5.17 show a comparison of these three sets of frequency distributions. The reference cumulative frequency distribution is the bold line, the distribution obtained with the full Monte-Carlo approach of Fig. 5.1 is the dashed line, and that obtained with the proposed faster Monte-Carlo approach (Fig. 5.2) is the dotted line. The dashed line and the bold line are difficult to distinguish; indeed, they were computed using exactly the same macroscale conductivity realizations, hence any discrepancy is only due to inaccuracies in the scale-up process. From a practical point of view, the dashed line is the best one could hope to have, since actual reference values are never available.

The proposed method (dotted line) does not reproduce the reference values as well

as the traditional approach (dashed line); however, given the tremendous savings in time, that reproduction is considered satisfactory. Best reproduction of the reference frequency distribution by the proposed method is within the inter-quartile range. In particular, median flows are well reproduced for most cross-sections. Outside this inter-quartile range, the proposed method produces a larger spread of the horizontal flows, i.e., those flows parallel to the major direction of continuity. The total flows orthogonal to the major direction of continuity are better reproduced although with a small bias.

The loss of accuracy in reproducing the different reference pdfs is overcome by the fact that the proposed Monte-Carlo analysis using direct simulation of interface conductivities is computationally feasible. Some execution times for each of the steps in Fig. 5.1 and Fig 5.2 and for the specific configuration considered are given in Table 5.2. According to these CPU times, the technique proposed in this dissertation, outperforms the more traditional approach. The traditional approach involves the generation of macroscale log-conductivities (9,000 s), computation of the interface conductivities for the block model which involves a small flow simulation for each interface (60,000 s), and simulation at the megascale (80 s) for a total of 69,080 s. On the other hand, the technique proposed requires the direct simulation of interface conductivities (460 s) and the simulation of flow at the megascale (80 s), for a total of 540 s. Therefore, once the block conductivities have been statistically characterized the method proposed in this dissertation can analyze 200 realizations when the traditional approach could analyze only 1.6.

Clayton Deutsch, in a personal communication, points out that the approach taken in this dissertation would be about 20 times faster than a power average approach , (Journel *et al.*, 1986; Deutsch, 1987, 1989; see also page 27).

The CPU time required for the inference of the stochastic models for interface log-conductivities was 1500 s, 200 of which were required for the generation of the 200 by 200 macroscale training image (Fig 5.8). and the remaining 1300 s for the scale-up of the interface conductivities. Additional time was required for the analysis and modeling of the variograms and cross-variograms. Since a manual analysis was preferred to an automatic one, this time is difficult to quantify.



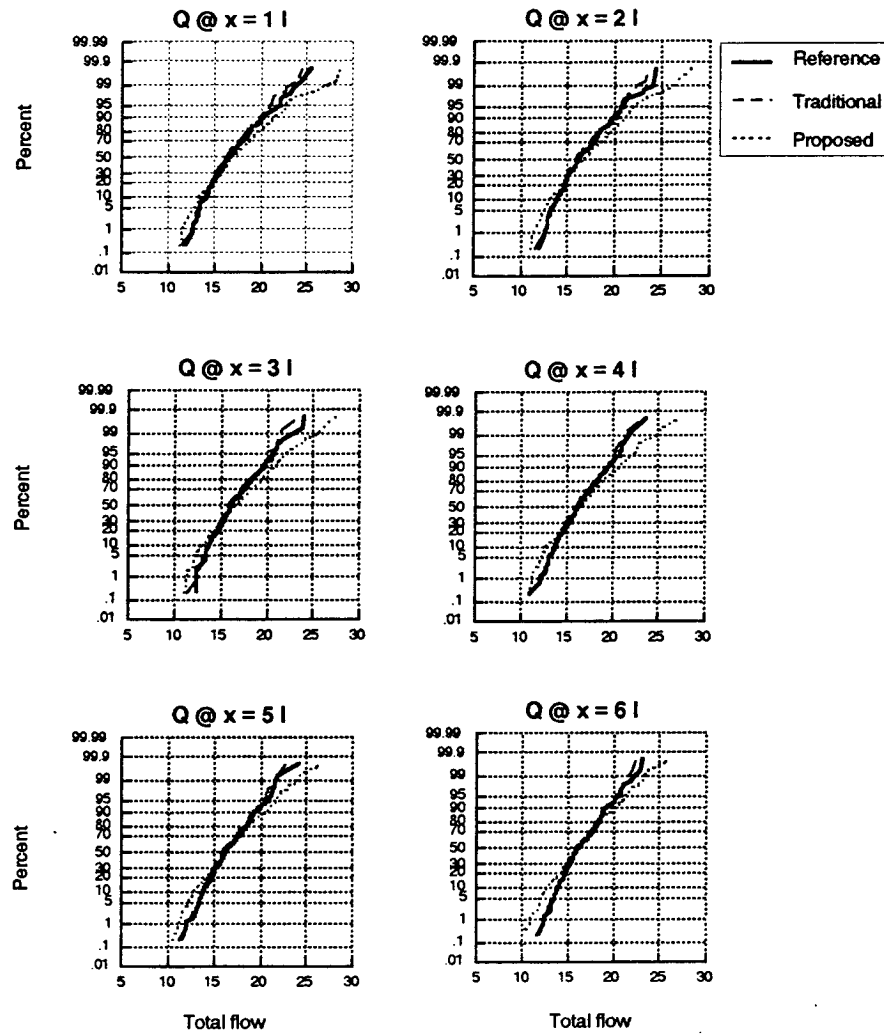


Figure 5.16: **Monte-Carlo analysis of horizontal flows.** The probability distributions of the total flow crossing vertical cross-sections are given. The solid line is the reference cdf, the dashed line corresponds to the traditional Monte-Carlo approach described in Fig. 5.1, and the dotted line corresponds to the proposed approach described in Fig. 5.2

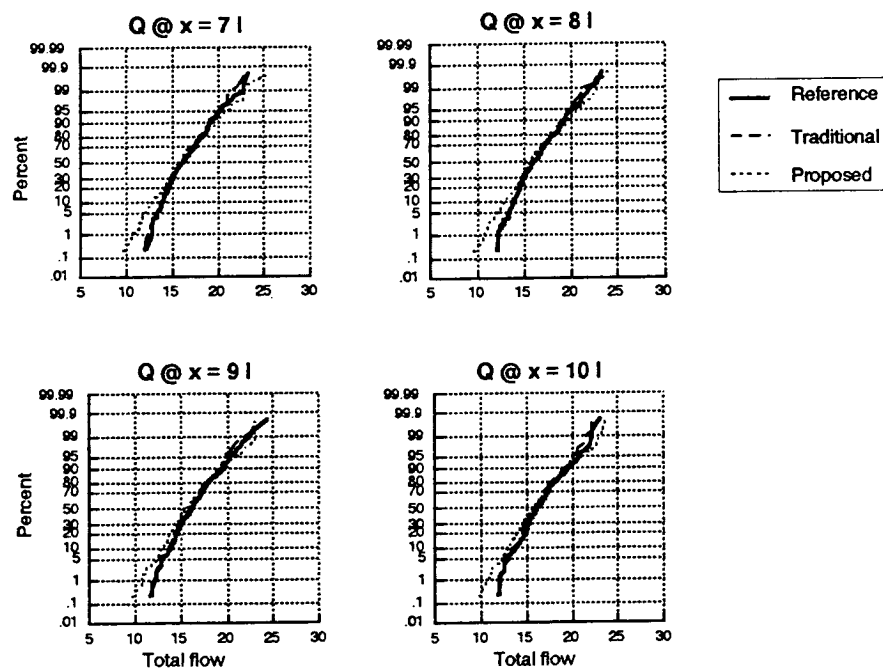


Figure 5.16: Monte-Carlo analysis of horizontal flows (cont.).

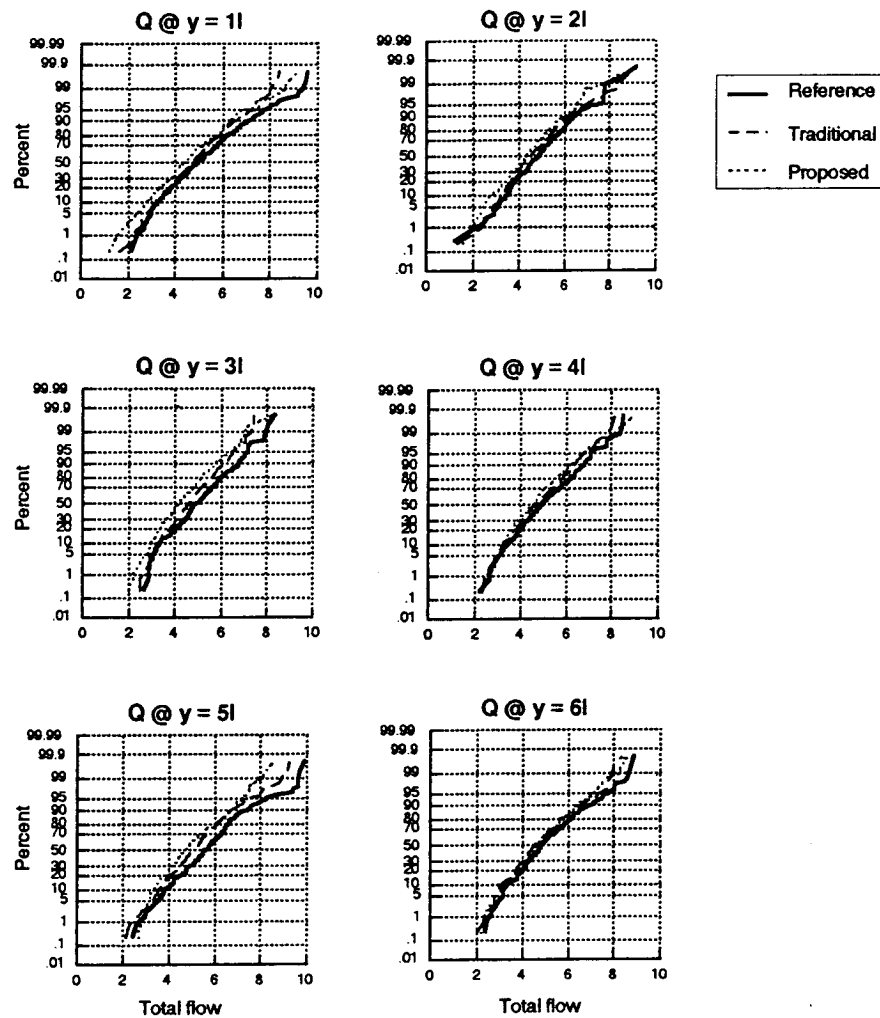


Figure 5.17: **Monte-Carlo analysis of vertical flows.** The probability distributions of the total flow crossing the horizontal cross-sections are given. The solid line is the reference cdf, the dashed line correspond to the traditional Monte-Carlo approach described in Fig. 5.1, and the dotted line corresponds to the proposed approach described in Fig. 5.2. Note the different scale on the  $x$ -axis with respect to the previous figure

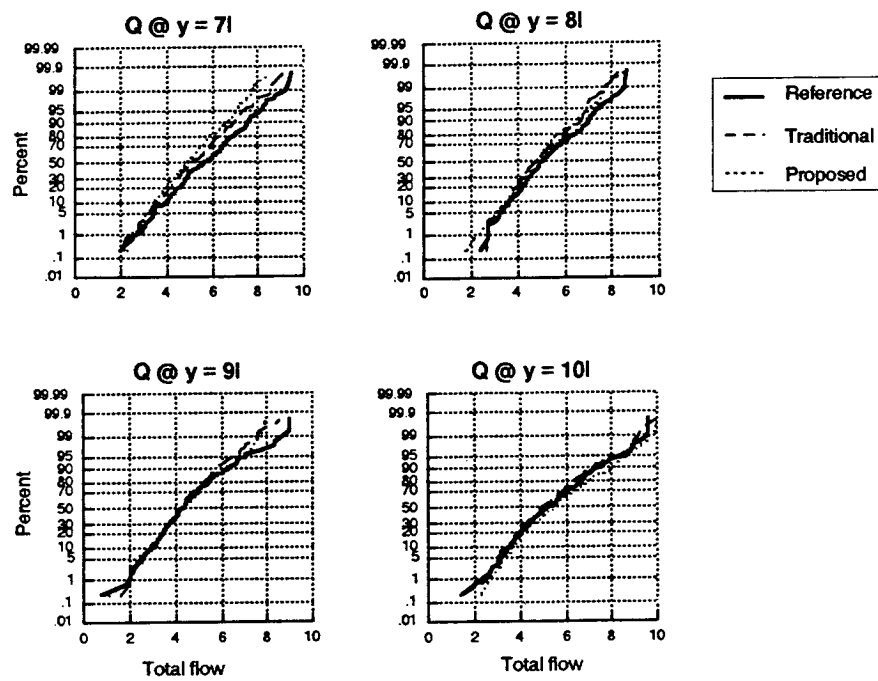


Figure 5.17: Monte-Carlo analysis of vertical flows (cont.).

Step	CPU (in seconds)
Generation of 200 110 by 110 cell realizations using GSIM3D	9,000
Scaling-up each one of the 24,000 block interfaces using the proposed method of Chapter 4	60,000
Direct generation of 200 realizations of interface conductivities on 11 by 11 blocks using GCOSIM3D	460
Simulation of flow on 200 11 by 11 block discretization	80

Table 5.2: Apollo DN10000 CPU times required by the various steps of the Monte-Carlo analyses (200 realizations)

These estimates could change for other discretizations and scale-up ratios.

## Discussion

A numerical technique for inference of a stochastic model for interface conductivities has been proposed. This numerical technique is not limited by the magnitude of the spatial variability of hydraulic conductivity as is the analytical technique presented in section 5.2.

An example has been given of how the numerical analysis would proceed starting from the simulation of macroscale conductivities and ending in a Monte-Carlo analysis of aquifer responses. This analysis has been limited to an aquifer discretized into square blocks of a single size for which the coefficients  $K_{V,xy}$  are negligible. Accounting for these limitations, the numerical method proposed in this dissertation is clearly faster than other more traditional methods. The price to pay for such increase in speed appears to be a minor loss of accuracy in the reproduction of the

frequency distributions of the response variables. Further research is required to determine whether this loss of accuracy could be reduced further by carrying out a more extensive analysis of the synthetic training images.

The proposed technique can be readily extended to rectangular blocks of a single size. The extension to rectangular blocks of different sizes although theoretically possible would be tedious and unwieldy: at the block scale, there will be as many random functions as possible pairs of blocks of different sizes sharing an interface. Inference of the joint behavior of all these random functions will quickly become unfeasible for more than two or three different block sizes.

The limitation to blocks of a single size is serious for practical applications. Note though, that this limitation is shared by all analytical methods. The proposed method lacks flexibility in the choice of the block shapes to better account for the geometry of both the flow units and the flow patterns: flow units of a very irregular shape are difficult to discretize with blocks of a single size; localized flow patterns with high concentration of streamlines (as is the case of flow near a well) are better reproduced using a higher density of smaller blocks where the concentration of streamlines occurs.

The extension of the proposed technique to blocks of a single size with non-negligible  $K_{V,xy}$  coefficients would require further research. As a first approximation, the coefficients  $K_{V,xy}$  could be treated as another random function requiring its own stochastic modeling. This approximation may pose problems because the relation between the different coefficients  $K_{V,xx}$ ,  $K_{V,xy}$  and  $K_{V,yy}$  is likely to be stronger than the one provided by a measure of mere linear correlation. Reproduction of the different variograms and cross-variograms may not be enough to generate plausible sets of these three coefficients.

## Chapter 6

### Conclusions

The objective of this dissertation is to provide tools that allow performing Monte-Carlo analyses of aquifer response variables within a reasonable CPU-time. As described in the introduction (see Fig. 1.1, repeated here as Fig. 6.1) the ideal Monte-Carlo analysis, in which flow is repeatedly simulated at the scale of the measurements is presently unattainable. The first improvement consists of the development of very fast techniques for the generation of hydraulic conductivity fields at the scale of the measurements and conditioned to the data. The first part of this dissertation (chapter 3) is devoted to this objective. The second improvement consists of developing a technique for the change of scale from the scale of the measurements into a scale that can be easily handled by current numerical flow simulators. The second part of this dissertation (chapter 4) is devoted to this objective. Then the approach represented by the second row in Fig. 6.1 becomes feasible. Finally, a third improvement consists of merging the fast generation of hydraulic conductivity fields with the change of scale techniques into the direct generation of hydraulic conductivities at the scale of the numerical simulator gridblocks. The third part of this dissertation (chapter 5) develops this latter algorithm.

Regarding techniques for the fast generation of hydraulic conductivity fields, the

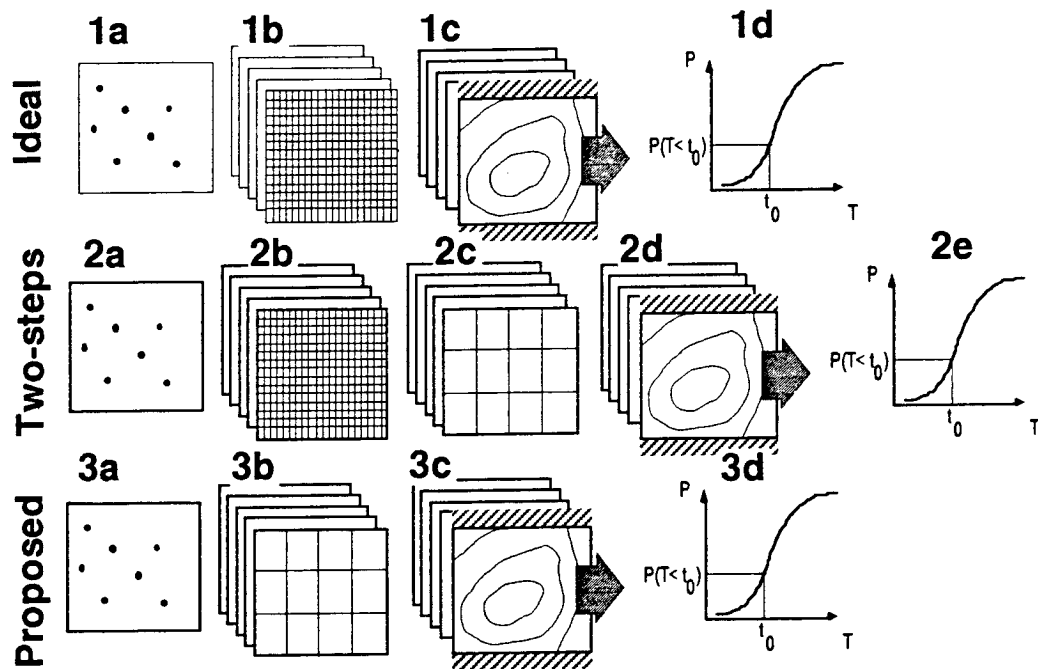


Figure 6.1: **Three Monte-Carlo approaches.** 1) An ideal approach: fields of hydraulic conductivities are generated at the measurement scale (1b) conditioned to the data (1a), groundwater flow is simulated at that scale (1c) and a frequency distribution of the response variables is built (1d). 2) A two-steps approach: fields of hydraulic conductivities are generated at the measurement scale (2b) conditioned to the data (2a), hydraulic conductivity values are scaled-up so that the number of resulting gridblocks can be easily handled by current numerical simulators (2c), groundwater flow is simulated at the gridblock scale (2d) and a frequency distribution of the response variable is built (2e). 3) Proposed approach: fields of hydraulic conductivities are directly generated at the gridblock scale (3b) conditioned to data measured at a smaller scale (3a), groundwater flow is simulated at the gridblock scale (3c) and a frequency distribution of the response variable is built (3d)



sequential simulation technique proposed by Journel (1985), is studied in depth resulting in the first full implementation of the sequential simulation algorithm for the generation of both Gaussian and non-Gaussian random fields with direct conditioning to local data. This algorithm is also applied for the first time to the co-simulation of several variables with a joint Gaussian multivariate distribution. Two important implementation decisions are taken, one regarding the search procedure (p. 54) the other regarding the computation of the covariances (p. 55). The solutions adopted minimize CPU time at the cost of increased memory requirements. Another important implementation decision relates whether ordinary kriging or simple kriging should be used in the modeling of the conditional probability distributions (p. 56).

Regarding the scale-up of conductivities, two new techniques are proposed and validated, one is analytical and the other is numerical. The analytical technique results in a closed-form expression for the value of the megascale conductivity (Eq. 4.6). The two most important requirements needed to obtain this analytical expression are: i) small variability of log-conductivity (variance of  $\ln K$  below 2) and ii) the block conductivities must be isotropic to flow, so that the block conductivity tensor is reduced to a scalar. An important consequence of Eq. (4.6) is that the block conductivity is dependent on the boundary conditions existing at the sides of the block. The numerical technique is more flexible than the analytical one since it is not limited by the variability of log-conductivity nor is there a requirement that the block values be isotropic. The novel aspects of the proposed technique are: i) the use of a "skin" surrounding the interface whose conductivity is sought (see Fig. 4.9), and ii) the solution of flow within this "skin" for a set of boundary conditions that drive the groundwater flow in several directions within the "skin" (see Fig. 4.11). These two innovations attempt to reduce the impact of using unrealistic boundary conditions on the calculation of the interface conductivity values (see discussion in p. 78 and following).

Finally, sequential stochastic simulation and the proposed scale-up techniques are combined in a single step allowing for the direct generation of interface conductivities conditioned on data measured at a smaller scale. This combination requires knowledge

of the expected value and covariance of the megascale conductivities and of the cross-covariances between microscale and megascale conductivities. Two techniques are proposed to obtain these statistics, again one is analytical and the other is numerical. The analytical technique develops the stochastic version of (4.6) to reach closed-form expressions for the above mentioned statistics (Eq. 5.3, 5.6 and 5.7). It is limited by the same assumptions as required to obtain (4.6). The numerical technique is based on the generation of a training image (Fig. 5.7): a realization—much smaller than the aquifer size—of macroscale conductivities is numerically scaled-up to obtain estimates of the interface conductivities. These estimates along with the macroscale realization are used as training images to infer numerically a statistical model for their joint spatial variability. The single major limitation of this numerical approach is that it can handle only blocks of a single size.

All algorithms proposed were tested on synthetic data sets with specific statistical properties, and all demonstrated positive results. The proposed Monte-Carlo analysis (third row in Fig. 6.1) of total flow crossing an aquifer is 125 times faster (CPU-wise) than a similar Monte-Carlo analysis carried out with the two-steps approach (second row in Fig. 6.1). This large gain of computer time is obtained at the cost of minor loss of accuracy.

## 6.1 Suggestions for Further Research

### Simulation of Random Fields

Sequential simulation appears to be a very efficient algorithm for the generation of conditional realizations of random fields, whether Gaussian or not, whether single variable or with multiple dependent variables.

Some important implementation solutions were proposed in this dissertation. However, the following issues still deserve further research:

- Relocation of the conditioning data values. Presently, the conditioning data are relocated to the nearest grid nodes prior to the beginning of the simulation. This

relocation has a minimum impact on the final realization if the average distance between data points is large compared to the grid node spacing. However, when simulating directly block values at a scale larger than the data, the data spacing could be small with respect to the block size; moreover, there could be several data within a grid block. In such a case, it would be necessary to account for all the conditioning data at their exact original locations. This is not a problem in theory, but could result in less efficient coding.

- Search. More efficient search algorithms should be considered. The extent of the search neighborhood should decrease gradually as the sequential simulation progresses, being largest in the beginning when only a few nodes have been simulated and much smaller at the end. Similarly, the procedure for selecting both original data and previously simulated values within the neighborhood could vary as the sequential simulation progresses.
- Linear system solvers. The kriging systems of linear equations are presently solved using a generic lower-upper decomposition of the matrix of coefficients. Other solvers, such as Cholesky decomposition or Gauss elimination without pivoting, should be considered and some may be faster. For instance, in those cases where simple kriging is used to obtain the conditional probability distribution, the kriging matrix is symmetric and positive definite, thus a Cholesky decomposition could be used. Another case concerns the generation of realizations of non-Gaussian random fields using several threshold values. This case requires the solution, at each simulated node, of as many systems of linear equations as there are different indicator variables. If the data configuration for each threshold value is the same, and since the indicator covariances do not, in general, vary drastically from one threshold to the next, one can expect that the solutions of the systems of equations will not be very different from one threshold to the next. Consequently, one could derive a solving algorithm in which the solution for the first threshold is obtained using a direct method and the solutions for the remaining thresholds are obtained by an iterative method using for initial guess the solution for the previous threshold.

- Drawing from the conditional probability distribution. Presently, the conditional probability distribution is built first and then a random value is drawn from it. In the non-Gaussian case, one might draw first a random number between 0 and 1 and then start solving the systems of indicator kriging until two consecutive thresholds provide estimates of the conditional probability distribution that are above and below that random value. The simulated value for that node will be in the class delimited by those two thresholds.

### Scaling-up of conductivities

The analytical results should be extended to the case of statistically anisotropic point conductivities with arbitrary orientation of the major direction of continuity. Similarly, the case of point conductivity anisotropic to flow should be considered.

The present restriction for the variance of log-conductivity to be lesser than two should be relaxed.

The numerical technique, as proposed, should work for any block size and any level of variability of the point conductivities as long as the boundary conditions used to determine the flows crossing the interfaces are similar to the boundary conditions prevailing in the actual aquifer. Presently, only constant head boundaries along the four sides of a “skin” surrounding the interface are considered; in some instances, these boundary conditions may be inadequate and alternatives should be proposed. For instance, a block extracted from a perfectly stratified aquifer subject to flow orthogonal to the direction of stratification should be modeled with no flow boundaries on the faces parallel to the flow direction.

The problem of which boundary conditions to use would disappear if a “skin” as large as the entire aquifer could be used. Since this is numerically unrealistic, further research should be carried in order to determine how large the skin should be so that the resulting estimates of the interface conductivity tensors are close to the estimates that would have been obtained, had the entire aquifer been used as skin.

Conversely, one could attempt to identify the most appropriate boundary conditions that should be applied to a particular skin as a function of the skin size relative to the point conductivity correlation length and aquifer size.

## Stochastic Modeling of Block Conductivities

The analytical approach has been developed for multiGaussian, isotropic, point log-conductivities with small variability; it provides closed-form expressions for all the auto- and cross-covariances required for the direct generation of block conductivities. Extension of this work to statistically anisotropic point conductivities, possibly also anisotropic to flow, and with large variances requires further research. An even more challenging problem would be the extension to non-Gaussian point log-conductivities, such as bimodal distributions (sand/shale, pay/non-pay).

The numerical approach is not limited by previous restrictions; however, in practice—although not in theory—it is limited to blocks of a single size. More research is needed to extend these results to blocks of different sizes. Blocks of different sizes are needed for a better match of both the geometry of the flow units and that of the flow patterns (as is required for better approximation of converging flow). Ideally, closed-form expressions similar to those obtained in the analytical approach should be pursued.

The problem of direct generation of realizations including the coefficient  $K_{V,xy}$  was not addressed in this dissertation. In the example given in section 5.3, these coefficients, as obtained from the training image, happen to be negligible with respect to both  $K_{V,xx}$  and  $K_{V,yy}$ ; as a result, only the joint characterization of the spatial variability of  $K_{V,xx}$  and  $K_{V,yy}$  was required. As a first approximation the coefficients  $K_{V,xy}$  could be treated as another random function to be jointly characterized with the other two random variables. However, the relation of the three coefficients  $K_{V,xx}$ ,  $K_{V,yy}$  and  $K_{V,xy}$  is likely to be stronger than the one provided by the linear correlation of a cross-variogram.



## Appendix B

# Finite Differences Formulation Of A Groundwater Flow Problem With Full-Tensor Conductivities

This Appendix presents the finite-difference formulation of the two-dimensional groundwater flow equation for the generic case in which the principal components of the hydraulic conductivity tensor are not aligned with the cartesian axes. No external sinks or sources are considered.

### B.1 Numerical formulation

The partial differential equation governing flow in two dimensions is written as

$$\frac{\partial}{\partial x} \left( K_{xx} \frac{\partial h}{\partial x} + K_{xy} \frac{\partial h}{\partial y} \right) + \frac{\partial}{\partial y} \left( K_{xy} \frac{\partial h}{\partial x} + K_{yy} \frac{\partial h}{\partial y} \right) = 0$$

where  $x$  and  $y$  are the cartesian coordinates,  $h$  is the hydraulic head and  $K_{xx}$ ,  $K_{xy}$ ,  $K_{yy}$  are the components of the hydraulic conductivity tensor.

If this equation is discretized on the grid shown in Fig. B.1 using central differences the following equation results

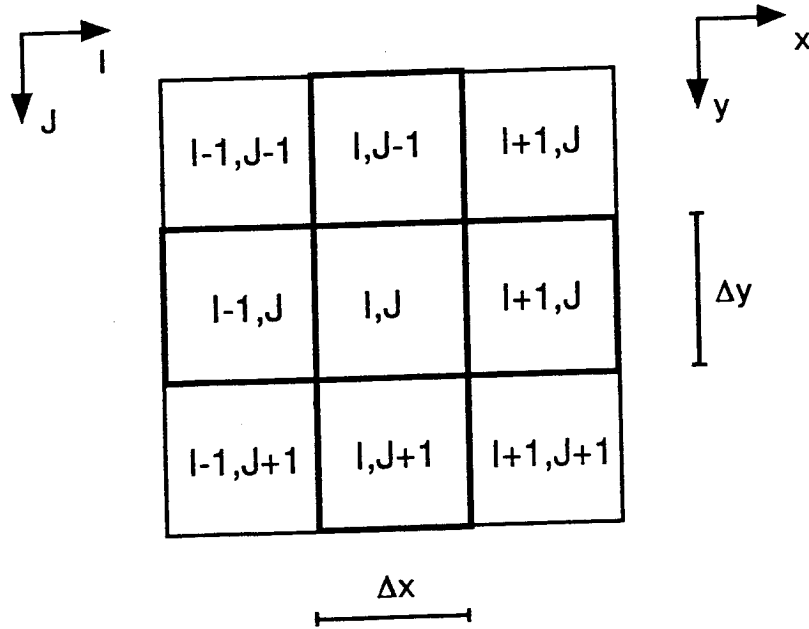


Figure B.1: Finite differences discretization. Nine point scheme

$$\begin{aligned} & \frac{1}{\Delta x} \left( K_{xx} \frac{\partial h}{\partial x} + K_{xy} \frac{\partial h}{\partial y} \Big|_{I+1/2, J} - K_{xx} \frac{\partial h}{\partial x} + K_{xy} \frac{\partial h}{\partial y} \Big|_{I-1/2, J} \right) \\ & + \frac{1}{\Delta y} \left( K_{xy} \frac{\partial h}{\partial x} + K_{yy} \frac{\partial h}{\partial y} \Big|_{I, J+1/2} - K_{xy} \frac{\partial h}{\partial x} + K_{yy} \frac{\partial h}{\partial y} \Big|_{I, J-1/2} \right) = 0 \quad (B.1) \end{aligned}$$

The partial derivatives of the hydraulic head are approximated using central differences as follows

$$\begin{aligned} \frac{\partial h}{\partial x} \Big|_{I+1/2, J} &= \frac{h_{I+1, J} - h_{I, J}}{\Delta x} \\ \frac{\partial h}{\partial y} \Big|_{I+1/2, J} &= \frac{1}{2} \left( \frac{h_{I+1, J+1} - h_{I-1, J+1}}{2\Delta y} + \frac{h_{I+1, J} - h_{I-1, J}}{2\Delta y} \right) \end{aligned}$$



$$\begin{aligned}
\left. \frac{\partial h}{\partial x} \right|_{I-1/2,J} &= \frac{h_{I,J} - h_{I-1,J}}{\Delta x} \\
\left. \frac{\partial h}{\partial y} \right|_{I-1/2,J} &= \frac{1}{2} \left( \frac{h_{I+1,J} - h_{I-1,J}}{2\Delta y} + \frac{h_{I+1,J-1} - h_{I-1,J-1}}{2\Delta y} \right) \\
\left. \frac{\partial h}{\partial x} \right|_{I,J+1/2} &= \frac{1}{2} \left( \frac{h_{I+1,J} - h_{I-1,J}}{2\Delta x} + \frac{h_{I+1,J+1} - h_{I-1,J+1}}{2\Delta x} \right) \\
\left. \frac{\partial h}{\partial y} \right|_{I,J+1/2} &= \frac{h_{I,J+1} - h_{I,J}}{\Delta y} \\
\left. \frac{\partial h}{\partial x} \right|_{I,J-1/2} &= \frac{1}{2} \left( \frac{h_{I+1,J} - h_{I-1,J}}{2\Delta x} + \frac{h_{I+1,J-1} - h_{I-1,J-1}}{2\Delta x} \right) \\
\left. \frac{\partial h}{\partial y} \right|_{I,J-1/2} &= \frac{h_{I,J} - h_{I,J-1}}{\Delta y}
\end{aligned}$$

Substitution in B.1 and multiplying both sides by  $\Delta x \Delta y$  results in

$$\begin{aligned}
& K_{xx;I+1/2,J} \frac{\Delta y}{\Delta x} (h_{I+1,J} - h_{I,J}) \\
& + K_{xy;I+1/2,J} \frac{1}{4} (h_{I+1,J+1} - h_{I-1,J+1} + h_{I+1,J} - h_{I-1,J}) \\
& + K_{xx;I-1/2,J} \frac{\Delta y}{\Delta x} (-h_{I,J} + h_{I-1,J}) \\
& + K_{xy;I-1/2,J} \frac{1}{4} (-h_{I+1,J} + h_{I-1,J} - h_{I+1,J-1} + h_{I-1,J-1}) \\
& + K_{yy;I,J+1/2} \frac{\Delta x}{\Delta y} (h_{I,J+1} - h_{I,J}) \\
& + K_{xy;I,J+1/2} \frac{1}{4} (h_{I+1,J} - h_{I-1,J} + h_{I+1,J+1} - h_{I-1,J+1}) \\
& + K_{yy;I,J-1/2} \frac{\Delta x}{\Delta y} (-h_{I,J} + h_{I,J-1}) \\
& + K_{xy;I,J-1/2} \frac{1}{4} (-h_{I+1,J} + h_{I-1,J} - h_{I+1,J-1} + h_{I-1,J-1}) = 0
\end{aligned}$$

Rearranging terms, the following nine-point scheme results

$$\begin{aligned}
& A h_{I-1,J-1} + B h_{I,J-1} + C h_{I+1,J-1} + \\
& D h_{I-1,J} + E h_{I,J} + F h_{I-1,J} + \\
& G h_{I-1,J+1} + H h_{I,J+1} + I h_{I+1,J+1} = 0
\end{aligned} \tag{B.2}$$

where

$$\begin{aligned}
 A &= \frac{1}{4}(K_{xy;I-1/2,J} + K_{xy;I,J-1/2}) \\
 B &= \frac{\Delta x}{\Delta y}K_{yy;I,J-1/2} + \frac{1}{4}(-K_{xy;I+1/2,J} + K_{xy;I-1/2,J}) \\
 C &= \frac{1}{4}(K_{xy;I+1/2,J} + K_{xy;I,J-1/2}) \\
 D &= \frac{\Delta y}{\Delta x}K_{xx;I-1/2,J} + \frac{1}{4}(-K_{xy;I,J+1/2} + K_{xy;I,J-1/2}) \\
 E &= \frac{\Delta y}{\Delta x}(-K_{xx;I+1/2,J} - K_{xx;I-1/2,J}) + \frac{\Delta x}{\Delta y}(-K_{yy;I,J+1/2} - K_{yy;I,J-1/2}) \\
 F &= \frac{\Delta y}{\Delta x}K_{xx;I+1/2,J} + \frac{1}{4}(K_{xy;I,J+1/2} - K_{xy;I,J-1/2}) \\
 G &= \frac{1}{4}(-K_{xy;I-1/2,J} - K_{xy;I,J+1/2}) \\
 H &= \frac{\Delta x}{\Delta y}K_{yy;I,J+1/2} + \frac{1}{4}(K_{xy;I+1/2,J} + K_{xy;I-1/2,J}) \\
 I &= \frac{1}{4}(K_{xy;I+1/2,J} + K_{xy;I,J+1/2})
 \end{aligned}$$

Equation (B.2) is written for all nodes within the aquifer, except for those for which the head is given, resulting in a set of linear equations that is solved using an iterative method based on a successive overrelaxation (SOR) scheme.

On each iteration, the heads at all nodes are updated. Then, an intermediate value  $\hat{h}_{I,J}$  is computed using the most recently updated head values, these heads could be from the previous iteration if they have not been updated in this iteration yet, or the heads just updated during the present iteration.

$$\begin{aligned}
 \hat{h}_{I,J} &= \frac{1}{E}(-A h_{I-1,J-1} - B h_{I,J-1} - C h_{I+1,J-1} - D h_{I-1,J} \\
 &\quad - F h_{I+1,J} - G h_{I-1,J+1} - H h_{I,J+1} - I h_{I+1,J+1})
 \end{aligned}$$

The updated head value for iteration  $m + 1$  is given by

$$h_{I,J}^{m+1} = h_{I,J}^m + \omega(\hat{h}_{I,J} - h_{I,J}^m)$$

where the coefficient  $\omega$  is the relaxation coefficient. We talk of overrelaxation if  $\omega$  is larger than 1 and of underrelaxation if it is smaller than 1. For  $\omega = 1$  the iterative scheme is the standard Gauss-Seidel algorithm. Iterations are stopped when the maximum absolute head change over all aquifer nodes is smaller than a prespecified closure value. (This value was set to  $1e-8$  for all runs in this dissertation.)

All aquifers for which flow was solved using full hydraulic conductivity tensors were small (maximum of 21 by 21 blocks). For this reason, the convergence of the solution was very fast for a wide range of the parameter  $\omega$ . As a consequence a value of  $\omega = 1$  was used for all runs.

The boundary conditions used for all problems were constant head boundaries at the outermost rows and columns of the aquifer. For this reason, no special care had to be taken in the computer code to account for boundary conditions. The handling of the boundary conditions amounts to not updating the nodes for which the head is prescribed.

## B.2 Computer code

The C code according to the ANSI standard follows

```
#include "stdio.h"
#include "math.h"

/* #define OS Unix */
#define OS Mac
#if OS==Mac
#include "stdlib.h"
#elif OS==Unix
    typedef unsigned size_t;
    char    *malloc();
#endif
#define CONVERGENCE      1
#define NO_CONVERGENCE   0
#define PARAMETER_FILE   "kxy_parm"
```

```

#define DEBUG 1
#ifndef DEBUG
#define DEBUG 0
#endif

float  **cc,**cr,**ccxy,**cryx,**a,**b,**c,**d,
      **e,**f,**g,**h,**l;
float  **head,**head_fluctuation,**qxx,
      **qyy,average_qx=0,average_qy=0;
float  accl,closure,dx,dy,max_head_change,jx,jy;
int     **ibound,ncol,nrow,max_iter;
char    kxx_file[80],kxx_format[80],kyy_file[80],
      kyy_format[80], head_file[80],head_format[80],
      Head_file[80],Head_format[80],
      qxx_file[80],qxx_format[80],qyy_file[80],
      qyy_format[80];
FILE    *fpdebug;

main()
{
  read_parameters();
  initialize();
  read_permeabilities();
  set_boundary_conditions1();
  compute_abc();
  if (iterate() == CONVERGENCE) print_results();
  else printf ("Max Iteration achieved with no convergence!!\n");
  #if DEBUG >= 1
    check_flows();
    print_coefficients();
    print_conductances();
  #endif
}
initialize()
{
  int i,j;
  float **matrix();
  int    **imatrix();

  /* allocate matrices */

```

```

cc =matrix(0,ncol,0,nrow); cr =matrix(0,ncol,0,nrow);
ccxy=matrix(0,ncol,0,nrow); cryx=matrix(0,ncol,0,nrow);
a=matrix(0,ncol,0,nrow); f=matrix(0,ncol,0,nrow);
b=matrix(0,ncol,0,nrow); g=matrix(0,ncol,0,nrow);
c=matrix(0,ncol,0,nrow); h=matrix(0,ncol,0,nrow);
d=matrix(0,ncol,0,nrow); l=matrix(0,ncol,0,nrow);
e=matrix(0,ncol,0,nrow);
ibound=imatrix(0,ncol,0,nrow);
head=matrix(0,ncol+1,0,nrow+1);
head_fluctuation=matrix(0,ncol+1,0,nrow+1);
qxx=matrix(0,ncol,0,nrow);
qyy=matrix(0,ncol,0,nrow);

/* initialize cc, cr, ccxy, crxy and head */

for(i=0;i<=ncol;i++) for(j=0;j<=nrow;j++) {
cc[i][j]=cr[i][j]=ccxy[i][j]=cryx[i][j]=qxx[i][j]=qyy[i][j]=0.;
ibound[i][j]=1;
if(i==1 || i==ncol || j==1 || j==nrow)
    head[i][j]=dx*(i-1)*jx+dy*(j-1)*jy;
else head[i][j]=0.;
}
#ifdef DEBUG >=1
if ( (fpdebug=fopen(DEBUG_FILE,"w"))==NULL) {
printf("Error opening debug file\n");
exit(30);
}
#endif
}
read_parameters()
{

FILE *fp;

if( (fp=fopen(PARAMETER_FILE,"r")) == NULL) {
printf ("Error opening parameter file\n");
exit(20);
}
if(fscanf(fp,"%d%d%s",&ncol,&nrow)!=2 ||
fscanf(fp,"%f%f%s",&dx,&dy) !=2 ||
fscanf(fp,"%f%f%s",&jx,&jy) !=2 ||

```

```

fscanf(fp,"%f%f%d%s",&accl,&closure,&max_iter)!=3 ||
fscanf(fp,"%s%s%s",kxx_file,kxx_format)!=2 ||
fscanf(fp,"%s%s%s",kyy_file,kyy_format)!=2 ||
fscanf(fp,"%s%s",Head_file)!=1 ||
fscanf(fp,"%s%s",head_file)!=1 ||
fscanf(fp,"%s%s",qxx_file)!=1 ||
fscanf(fp,"%s%s",qyy_file)!=1
) {
    printf ("Error reading parameter file\n");
    exit(21);
}
fclose(fp);
}
read_permeabilities()
{
/* we will assume that the permeability file has been created
   by 'extractt' and therefore the values of Kxx for the first
   and last rows and the values of Kyy for the first and last
   columns are zeroes, what is OK for constant heads in the outer
   perimeter */

FILE *fp;
int i,j;

if( (fp=fopen(kxx_file,"r")) ==NULL) {
    printf("Error openning Kxx file \n");
    exit(22);
}

/* reading by rows */

for(j=2;j<=nrow-1;j++) for(i=1;i<=ncol-1;i++) {
    if( fscanf(fp,kxx_format,&(cc[i][j]),&(ccxy[i][j]))!=2) {
        printf("Error reading Kxx\n");
        exit (23);
    }
}
fclose(fp);

if( (fp=fopen(kyy_file,"r")) ==NULL) {
    printf("Error openning Kyy file \n");

```

```

    exit(24);
}

/* reading by rows */

for(j=1;j<=nrow-1;j++) for(i=2;i<=ncol-1;i++) {
    if( fscanf(fp,kyy_format,&(cryx[i][j]),&(cr[i][j])) !=2 ) {
        printf("Error reading Kyy\n");
        exit(25);
    }
}
fclose(fp);

#ifdef DEBUG>=1
    print_conductances();
#endif

/* if the values read are permeabilities instead of conductances,
   also called transmissibilities, apply the correction factors */

for(j=1;j<=nrow;j++) for(i=1;i<=ncol;i++) {
    cc[i][j] *= (dy/dx);
    cr[i][j] *= (dx/dy);
}

#ifdef DEBUG>=1
    print_conductances();
#endif

}

set_boundary_conditions1()
{
    int i,j;

/* boundary conditions in this case are constant head boundaries
   all around the perimeter of the field. We need to set the
   ibound flag to -1 and the conductance between adjacent
   constant head cells equal to zero */

    for (i=1;i<=ncol;i++) {
        cc[i][1]=ccxy[i][1]=cc[i][nrow]=ccxy[i][nrow]=0.;
    }
}

```

```

    ibound[i][1]=ibound[i][nrow]=-1;
}
for (j=1;j<=nrow;j++) {
    cr[1][j]=cryx[1][j]=cr[ncol][j]=cryx[ncol][j]=0.;
    ibound[1][j]=ibound[ncol][j]=-1;
}
}
set_boundary_conditions2()
{
    int i,j;

    /* boundary conditions in this case are constant head boundaries
       at parallel sides and on flow boundaries the other two
       ibound flag to -1 and the conductance between adjacent
       constant head cells equal to zero */

    for (j=1;j<=nrow;j++) {
        cr[1][j]=cryx[1][j]=cr[ncol][j]=cryx[ncol][j]=0.;
        ibound[1][j]=ibound[ncol][j]=-1;
    }
}
compute_abc()
{
    int i,j;

    /* computing the coefficients of the finite difference equation for
       the Laplace equation (no external stresses) */

    for (i=1;i<=ncol;i++) for(j=1;j<=nrow;j++) {
        a[i][j]=.25*(ccxy[i-1][j]+cryx[i][j-1]);
        b[i][j]=.25*(-ccxy[i][j]+ccxy[i-1][j])+cr[i][j-1];
        c[i][j]=.25*(-ccxy[i][j]-cryx[i][j-1]);
        d[i][j]=cc[i-1][j]+.25*(-cryx[i][j]+cryx[i][j-1]);
        e[i][j]= -cc[i][j]-cc[i-1][j]-cr[i][j]-cr[i][j-1];
        f[i][j]=cc[i][j]+.25*(cryx[i][j]-cryx[i][j-1]);
        g[i][j]=.25*(-ccxy[i-1][j]-cryx[i][j]);
        h[i][j]=.25*(ccxy[i][j]-ccxy[i-1][j])+cr[i][j];
        l[i][j]=.25*(ccxy[i][j]+cryx[i][j]);
    }
}
#endif DEBUG >=1

```



```

print_coefficients();
#endif
}
iterate()
{
int i;

for(i=1;i<=max_iter;i++) {
fill_outside_ring();
if( one_iteration() == CONVERGENCE ) break;
}
if(i>=max_iter) return (NO_CONVERGENCE);
else return (CONVERGENCE);
}
fill_outside_ring()
{
/* rows 0 and nrow+1 and columns 0 and ncol+1 are filled with
the same values as in row 1, row nrow, column 1 and column ncol,
respectively in order to simulate no flow boundaries around
the edge of the field. Because of the way the tangential pressure
gradients are computed at the faces of the blocks, there has not
been yet accounted for the possibility of having inactive nodes
within the field */

int i,j;

head[0][0]=head[1][1];
head[0][nrow+1]=head[1][nrow];
head[ncol+1][0]=head[ncol][1];
head[nrow+1][ncol+1]=head[nrow][ncol];

for(i=1; i<= ncol; i++) {
head[i][0]=head[i][1];
head[i][nrow+1]=head[i][nrow];
}
for(j=1; j<= nrow; j++) {
head[0][j]=head[1][j];
head[ncol+1][j]=head[ncol][j];
}
}
one_iteration()

```

```

{
/* this subroutine performs one Gauss-Seidel iteration with
   over-relaxation. At the end of the iteration makes a closure
   check by comparing the maximum head change in the iteration
   with the maximum difference allowed */

int i,j;
float intermediate_h,increment;

max_head_change=0.;

for(i=1;i<=ncol;i++) for(j=1;j<=nrow;j++)
if (ibound[i][j] == 1) {
intermediate_h = (-a[i][j]*head[i-1][j-1]
                  -b[i][j]*head[i][j-1]
                  -c[i][j]*head[i+1][j-1]
                  -d[i][j]*head[i-1][j]
                  -f[i][j]*head[i+1][j]
                  -g[i][j]*head[i-1][j+1]
                  -h[i][j]*head[i][j+1]
                  -l[i][j]*head[i+1][j+1]
                  ) / e[i][j];
increment= intermediate_h - head[i][j];
if (fabs(increment) >= max_head_change)
    max_head_change=fabs(increment);
head[i][j]=head[i][j]+accl*increment;
}
if(max_head_change <= closure) return (CONVERGENCE);
else return(NO_CONVERGENCE);
}

print_results()
{
compute_flows();
print_flows();
print_head();
compute_head_fluctuation();
print_head_fluctuation();
}

compute_flows()
{
int i,j;

```

```

fill_outside_ring();

for(i=1;i<=ncol;i++) for(j=1;j<=nrow;j++) {
qxx[i][j]= -cc[i][j]*(head[i+1][j]-head[i][j])
            -ccxy[i][j]*(head[i+1][j+1]-head[i+1][j-1]
                        +head[i][j+1]-head[i][j-1])/4.;
qyy[i][j]= -cr[i][j]*(head[i][j+1]-head[i][j])
            -cryx[i][j]*(head[i+1][j+1]-head[i-1][j+1]
                        +head[i+1][j]-head[i-1][j])/4.;
}
}
print_flows()
{
int i,j,counter=0;
FILE *fp;

if( (fp=fopen(qxx_file,"w")) == NULL) {
printf("Error opening qxx file\n");
exit(26);
}

/* writing by rows */
for (j=1;j<=nrow;j++) {
counter=0;
for (i=1;i<=ncol;i++) {
fprintf(fp,"%15.4e",qxx[i][j]);
average_qx+=qxx[i][j];
if (++counter % 5 == 0) fprintf(fp,"\n");
}
fprintf(fp,"\n");
}
fprintf(fp,"\n\nAverage qx --->%f/%d\n",average_qx,counter);
fclose(fp);

if( (fp=fopen(qyy_file,"w")) == NULL) {
printf("Error opening qyy file\n");
exit(27);
}

```

```

/* writing by rows */
for (j=1;j<=nrow;j++) {
    counter=0;
    for (i=1;i<=ncol;i++) {
        fprintf(fp,"%15.4e",qyy[i][j]);
        average_qy+=qyy[i][j];
        if (++counter % 5 == 0) fprintf(fp,"\n");
    }
    fprintf(fp,"\n");
}
fprintf(fp,"\n\nAverage qy --->%f/%d\n",average_qy,counter);
fclose(fp);
}
print_head()
{
    int i,j,counter;
    FILE *fp;

    if( (fp=fopen(Head_file,"w")) == NULL) {
        printf("Error openning head file\n");
        exit(28);
    }

    /* writing by rows */
    for (j=1;j<=nrow;j++) {
        counter=0;
        for (i=1;i<=ncol;i++) {
            fprintf(fp,"%8.2f",head[i][j]);
            if (++counter % 8 == 0) fprintf(fp,"\n");
        }
        fprintf(fp,"\n");
    }
    fclose(fp);
}
compute_head_fluctuation()
{
    int i,j;

    for(i=1;i<=ncol;i++) for(j=1;j<=nrow;j++)
        head_fluctuation[i][j]=head[i][j]-dx*(i-1)*jx-dy*(j-1)*dy;
}

```

```

print_head_fluctuation()
{
FILE *fp;
int i,j,counter;

if( (fp=fopen(head_file,"w")) == NULL) {
printf("Error opening head fluctuation file\n");
exit(29);
}

/* writing by rows */
for (j=1;j<=nrow;j++) {
    counter=0;
    for (i=1;i<=ncol;i++) {
        fprintf(fp,"%8.2f",head_fluctuation[i][j]);
        if (++counter % 8 == 0) fprintf(fp,"\n");
    }
    fprintf(fp,"\n");
}
fclose(fp);
}

check_flows()
{
int i,j;
float qtot;

    fprintf(fpdebug,"Col Row      Head      qxx[i][j] qxx[i-1][j]");
    fprintf(fpdebug,"qyy[i][j] qyy[i][j-1] qtot\n");
for(j=1;j<=nrow;j++) for(i=1;i<=ncol;i++) {
    qtot= qxx[i][j]-qxx[i-1][j]+qyy[i][j]-qyy[i][j-1];
    fprintf(fpdebug,
        "%3d %3d %10.4f %10.4f %10.4f %10.4f %10.4f %10.4f\n",
        i,j,head[i][j],qxx[i][j],qxx[i-1][j],qyy[i][j],qyy[i][j-1],
        qtot);
}
}

print_coefficients()
{
int i,j;

    fprintf(fpdebug,"\n(i,j)      a      b      c      d      e");

```

```

    fprintf(fpdebug,"      f      g      h      l\n");
    for(i=1;i<=ncol;i++) for(j=1;j<=ncol;j++) {
        fprintf(fpdebug,"(%3d,%3d) %7.2f %7.2f %7.2f %7.2f",
            i,j,a[i][j],b[i][j],c[i][j],d[i][j]);
        fprintf(fpdebug,"%7.2f %7.2f %7.2f %7.2f %7.2f\n",
            e[i][j],f[i][j],g[i][j],h[i][j],l[i][j]);
    }
    fprintf(fpdebug,"\n\n");
}
print_conductances()
{
    int i,j;

    fprintf(fpdebug,"Column to column conductances... Kxx \n");
        for(j=0;j<=nrow;j++) {
    for(i=0;i<=ncol;i++) {
        fprintf(fpdebug,"%8.2f ",cc[i][j]);
    }
        fprintf(fpdebug,"\n");
    }
    fprintf(fpdebug,"Column to column conductances... Kxy \n");
        for(j=0;j<=nrow;j++) {
    for(i=0;i<=ncol;i++) {
        fprintf(fpdebug,"%8.2f ",ccxy[i][j]);
    }
        fprintf(fpdebug,"\n");
    }
    fprintf(fpdebug,"Row to row conductances... Kyy \n");
        for(j=0;j<=nrow;j++) {
    for(i=0;i<=ncol;i++) {
        fprintf(fpdebug,"%8.2f ",cr[i][j]);
    }
        fprintf(fpdebug,"\n");
    }
    fprintf(fpdebug,"Row to row conductances... Kyx \n");
        for(j=0;j<=nrow;j++) {
    for(i=0;i<=ncol;i++) {
        fprintf(fpdebug,"%8.2f ",cryx[i][j]);
    }
        fprintf(fpdebug,"\n");
    }
}

```

}

### B.3 Example input files

Three files are required, a parameter file and the two files containing the interface conductivities for the horizontal interfaces and for the vertical interfaces.

#### Parameter file

```

7          7          -----ncolumns.....nrows
1.         1.         -----deltax.....deltay
1.         0.         -----gradx.....grady
1.         1e-9      10000 -----accel.param...closure.....maxiter
kxx        %f%f       -----kxx.file.....kxx.format
kyy        %f%f       -----kyy.file.....kyy.format
head       -----Head.file
head_fluct -----head.fluctuation.file
qxx        -----qxx.file
qyy        -----qyy.file

```

#### Column to column interface conductivities

```

5      1
3      1
4      0
2      .1
5      .3
4.1    1.1

3.1    1.2
3      1
4      0
3.2    0.4
5      .3
4.1    1.1

5      1
3      1
2      .3

```

2 .1  
5 .3  
2 .3

5 1  
1.1 .1  
4 0  
2 .1  
1.2 2  
4.1 1.1

5 1  
3 1  
4 0  
2 .1  
5 .3  
4.1 1.1

#### Row to row interface conductivities

1. 0.1  
2. 0.2  
3. 0.3  
4. 1.  
4. 0.5

2. 0.2  
2. 0.2  
1. 0.1  
4. 1.  
4. 0.5

2. 0.2  
1. 0.2  
2. 0.2  
4. 1.  
4. 0.5

5. 0.1



2. 0.2  
3. 0.5  
1. 0.  
1. 0.5

2. 0.3  
2. 0.2  
3. 0.3  
4. 0.4  
2. 0.1

1. 0.1  
1. 0.2  
3. 0.3  
1. 0.1  
3. 0.5

1. 0.1  
2. 0.2  
3. 0.3  
3. 0.6  
4. 0.5



## Appendix C

### Least Squares Formulation

Obtaining the coefficients  $K_{V,xx}$  and  $K_{V,xy}$  in Eq. (4.11) requires the solution of an overdetermined system of linear equations. The solution of such system is obtained by standard linear least squares. The least squares procedure is described below for the sake of completeness, it closely follows Press *et al.* (1988, p.109 and following).

Consider the set of linear equations:

$$\sum_{j=1}^M a_{ij}x_j = b_i \quad i = 1, \dots, N \quad (\text{C.1})$$

where  $M$  is the number of unknowns,  $N$  is the number of equations, and  $N > M$ . Let  $\mathbf{A}$  be the matrix whose  $N$  by  $M$  components are  $a_{ij}$ ,  $\mathbf{b}$  be a vector whose  $N$  components are  $b_i$ , and  $\mathbf{x}$  be the vector of  $M$  unknowns  $x_j$ . The unknowns  $x_j$  are obtained by minimizing the sum of the square differences between the left and right hand side in C.1

$$\chi^2 = \sum_{i=1}^N \left[ b_i - \sum_{j=1}^M a_{ij}x_j \right]^2$$

The minimum occurs when the derivative of  $\chi^2$  with respect to all  $M$  unknowns vanishes

$$\frac{\partial \chi^2}{\partial x_k} = 0 \quad k = 1, \dots, M$$

that is,

$$\sum_{i=1}^N \left( \sum_{j=1}^M a_{ij} x_j - b_i \right) a_{ik} = 0 \quad k = 1, \dots, M$$

interchanging the summations

$$\sum_{j=1}^M \left( \sum_{i=1}^N a_{ij} a_{ik} x_j \right) - \sum_{i=1}^N a_{ik} b_i = 0 \quad k = 1, \dots, M$$

which can be written in matricial notation as

$$(\mathbf{A}^T \cdot \mathbf{A}) \cdot \mathbf{x} = \mathbf{A}^T \cdot \mathbf{b}, \quad (\text{C.2})$$

from which the values of  $x_j$  that minimize  $\chi^2$  are obtained as

$$\mathbf{x} = (\mathbf{A}^T \cdot \mathbf{A})^{-1} \cdot \mathbf{A}^T \cdot \mathbf{b}$$

The equations (C.2) are known as normal equations.

# Bibliography

- Ababou, R., Gelhar, L. W., and McLaughlin, D. (1988). Three-dimensional flow in random porous media. Technical Report no. 318 of the Ralph M. Parsons Laboratory, Department of Civil Engineering, Massachusetts Institute of Technology.
- Alabert, F. G. (1987a). The practice of fast conditional simulations through the lu decomposition of the covariance matrix. *Math. Geology*, 19(5):369–387.
- Alabert, F. G. (1987b). Stochastic imaging of spatial distributions using hard and soft data. Master's thesis, Stanford University, Branner Earth Sciences Library.
- Anderson, T. W. (1984). *Multivariate statistical analysis*. Wiley, New York.
- Aris, R. (1956). On the dispersion of a solute in a fluid flowing through a tube. *Proc. R. Soc. London. Ser. A*, 235:67–77.
- Bachu, S. and Cuthiell, D. (1990). Effects of core-scale heterogeneity on steady state and transient fluid flow in porous media: numerical analysis. *Water Resources Research*, 26(5):863–874.
- Bakr, A. A., Gelhar, L. W., Gutjahr, A. L., and MacMillan, J. R. (1978). Stochastic analysis of spatial variability in subsurface flow, 1, Comparison of one- and three-dimensional flows. *Water Resources Research*, 14(2):263–271.
- Bear, J. (1979). *Hydraulics of Groundwater*. Mc Graw-Hill, New York.

- Begg, S. H., Carter, R. R., and Dranfield, P. (1989). Assigning effective values to simulator gridblock parameters for heterogeneous reservoirs. *SPE Reservoir Engineering*, pages 455–463.
- Begg, S. H., Chang, D. M., and Haldorsen, H. H. (1985). A simple statistical method of calculating the effective vertical permeability of a reservoir containing discontinuous shales. *SPE* 14271.
- Begg, S. H. and King, P. R. (1985). Modelling the effects of shales on reservoir performance: calculation of effective vertical permeability. *SPE* 13529.
- Black, T. C. and Freyberg, D. L. (1990). Simulation of one-dimensional correlated fields using a matrix-factorization moving average approach. *Math. Geology*, 22(1):39–62.
- Borgman, L. E., Taheri, M., and Hagan, R. (1984). Three-dimensional, frequency-domain simulations of geological variables. In Verly, G., David, M., Journel, A. G., and Marechal, A., editors, *Geostatistics for Natural Resources Characterization*. D. Reidel Publishing.
- Bouwer, H. (1969). Planning and interpreting soil permeability measurements. *Journal of the Irrigation and Drainage Division of the A.S.C.E.*, IR(3):391–402.
- Bratley, P., Fox, B. L., and S., L. E. (1983). *A Guide to Simulation*. Springer-Verlag, New York.
- Brenner, H. (1980). Dispersion resulting from flow through spatially periodic porous media. *Philos. Trans. R. Soc. London, Ser. A*, 297(1498):81–133.
- Brooker, P. (1985). Two-dimensional simulations by turning bands. *Math. Geology*, 17(1).
- Chirlin, G. R. and Dagan, G. (1980). Theoretical head variograms for steady flow in statistically homogeneous aquifers. *Water Resources Research*, 16(6):1001–1015.

- Clifton, P. M. and Neuman, S. P. (1982). Effects of kriging and inverse modeling on conditional simulation of the Avra Valley aquifer in Southern California. *Water Resources Research*, 16(6):1215-1234.
- Dagan, G. (1979). Models of groundwater flow in statistically homogeneous porous formations. *Water Resources Research*, 15(1):47-63.
- Dagan, G. (1981). Analysis of flow in heterogeneous random aquifers by the method of embedding matrix. 1. Steady flow. *Water Resources Research*, 17(1):107-121.
- Dagan, G. (1982a). Analysis of flow through heterogeneous random aquifers, 2, Unsteady flow in confined formations. *Water Resources Research*, 18(5):1571-1585.
- Dagan, G. (1982b). Stochastic modeling of groundwater flow by unconditional and conditional probabilities, 1, Conditional simulation and the direct problem. *Water Resources Research*, 18(4):813-833.
- Dagan, G. (1985). Stochastic modeling of groundwater flow by unconditional and conditional probabilities, 2, The inverse problem. *Water Resources Research*, 21(4):573-578.
- Dagan, G. (1986). Statistical theory of groundwater flow and transport: Pore to laboratory, laboratory to formation, and formation to regional scale. *Water Resources Research*, 22(9):120S-134S.
- Dagan, G. (1989). *Flow and Transport in Porous Formations*. Springer-Verlag.
- Dagan, G. and Rubin, Y. (1988). Stochastic identification of recharge, transmissivity and storativity in aquifer unsteady flow: a quasi-steady approach. *Water Resources Research*, 24(10):1698-1710.
- Davis, M. W. (1987). Production of conditional simulations via the LU triangular decomposition of the covariance matrix. *Math Geol*, 19(2):91-98.
- Delhomme, J. P. (1979). Spatial variability and uncertainty in groundwater flow parameters: A geostatistical approach. *Water Resources Research*, 15(2):269-280.

- Desbarats, A. J. (1987a). Numerical estimation of effective permeability in sand-shale formations. *Water Resources Research*, 23(2):273-286.
- Desbarats, A. J. (1987b). *Stochastic Modeling of Flow in Sand-Shale Sequences*. PhD thesis, Stanford University, Branner Earth Sciences Library.
- Desbarats, A. J. (1988). Estimation of effective permeabilities in the Lower Stevens formation of the Paloma field, San Joaquin Valley, California. *SPE Reservoir Engineering*, pages 1301-1307.
- Desbarats, A. J. (1989). Support effects and the spatial averaging of transport properties. *Mathematical Geology*, 21(3):383-389.
- Deutsch, C. V. (1987). A probability approach to estimate effective absolute permeability. Master's thesis, Stanford University, Branner Earth Sciences Library.
- Deutsch, C. V. (1989). Calculating effective absolute permeability in sand-shale sequences. *SPE Formation Evaluation*, 4(3):343-348.
- El-Kadi, A. I. and Brutsaert, W. (1985). Applicability of effective parameters for unsteady flow in nonuniform aquifers. *Water Resources Research*, 21(2):183-198.
- Freeze, R. A. (1975). A stochastic-conceptual analysis of one-dimensional groundwater flow in nonuniform heterogeneous media. *Water Resources Research*, 11(5):725.
- Freeze, R. A. and Cherry, J. A. (1978). *Groundwater*. Prentice-Hall.
- Gelhar, L. W. (1974). Stochastic analysis of phreatic aquifers. *Water Resources Research*, 10(3):539-545.
- Gelhar, L. W. and Axness, C. L. (1983). Three dimensional stochastic analysis of macrodispersion in aquifers. *Water Resources Research*, 19(1):161-180.
- Gómez-Hernández, J. J. (1989). Indicator conditional simulation of the architecture of hydraulic conductivity fields: application to a sand-shale sequence. In Sahuquillo,



- A., Andréu, J., and O'Donnell, T., editors, *Groundwater Management: Quantity and Quality* IAHS publication no. 188, pages 41–51. IAHS, IAHS Press.
- Gómez-Hernández, J. J. (1990a). Simulation of block effective permeabilities conditioned upon data measured at a different scale. In Kovac, editor, *Calibration and Reliability in Groundwater*, Oxfordshire, UK. IAHS, IAHS Press
- Gómez-Hernández, J. J. (1990b). The impact of the multiGaussian hypothesis on the generation of hydraulic conductivity fields with significant connectivity of extreme values. In *Proc. of the NEA workshop on flow heterogeneity*. Nuclear Energy Agency..
- Gómez-Hernández, J. J. (1991). A case study of three-dimensional multiple indicator conditional simulation: Florida's Jay oil field. submitted for publication to *JPT*.
- Gómez-Hernández, J. J. and Gorelick, S. M. (1988). Influence of spatial variability of aquifer and recharge properties in determining effective parameter values. In Peck, A. et al., editors, *Consequences of Spatial Variability in Aquifer Properties and Data Limitations for Groundwater Modelling Practice* IAHS publication no. 175, pages 217–272, Oxfordshire, UK. IAHS, IAHS Press.
- Gómez-Hernández, J. J. and Gorelick, S. M. (1989). Effective groundwater model parameter values: Influence of spatial variability of hydraulic conductivity, leakage and recharge. *Water Resources Research*, 25(3):405–419.
- Gómez-Hernández, J. J. and Journel, A. G. (1989). Conditional simulation of the Wilmington sand-shale sequence, Los Angeles basin. In Ports, M. A., editor, *Hydraulic Engineering*, NY. American Society of Civil Engineers.
- Gómez-Hernández, J. J. and Journel, A. G. (1990). Stochastic characterization of grid-block permeabilities: from point values to block tensors. In *Proceedings of the 2nd European conference on the mathematics of oil recovery*.
- Gómez-Hernández, J. J. and Rubin, Y. (1990). Spatial averaging of statistically anisotropic point conductivities. In *Optimizing the Resources of Water Management*, pages 566–571. ASCE.

- Gómez-Hernández, J. J. and Srivastava, R. M. (1990). ISIM3D: An ANSI-C three dimensional multiple indicator conditional simulation program. *Computer and Geosciences*, 16(4):395–440.
- Gutjahr, A. L. and Gelhar, L. W. (1981). Stochastic models of subsurface flow: Infinite versus finite domains and stationarity. *Water Resources Research*, 17(2):337–350.
- Gutjahr, A. L., Gelhar, L. W., Bakr, A. A., and MacMillan, J. R. (1978). Stochastic analysis of spatial variability in subsurface flows. 2. Evaluation and application. *Water Resources Research*, 14(5):953–959.
- Haldorsen, H. H. (1986). Simulation parameters assignment and the problem of scale in reservoir engineering. In Lake, L. W. and Carroll, H. B., editors, *Reservoir Characterization*, pages 293–340. Academic Press.
- Haldorsen, H. H. and Chang, D. M. (1986). Notes on stochastic shales; from outcrop to simulation model. In Lake, L. W. and Carroll, H. B., editors, *Reservoir Characterization*, pages 445–485. Academic Press.
- Haldorsen, H. H. and Lake, L. W. (1982). A new approach to shale management in field scale simulation models. *SPE 10976*.
- Hoeksema, R. J. and Kitanidis, P. K. (1984). An application of the geostatistical approach to the inverse problem in two-dimensional groundwater modeling. *Water Resources Research*, 20(7):1003–1020.
- Hoeksema, R. J. and Kitanidis, P. K. (1985a). Analysis of the spatial structure of properties of selected aquifers. *Water Resources Research*, 21(4):563–572.
- Hoeksema, R. J. and Kitanidis, P. K. (1985b). Comparison of Gaussian conditional mean and kriging estimation in the geostatistical solution of the inverse problem. *Water Resources Research*, 21(6):825–836.

- Isaaks, E. H. (1990). *The Application of Monte-Carlo Methods to the Analysis of Spatially Correlated Data*. PhD thesis, Stanford University, Branner Earth Sciences Library.
- Journal, A. G. (1974). Geostatistics for conditional simulation of ore bodies. *Economic Geology*, 69(5):673-687.
- Journal, A. G. (1987). *Geostatistics for the Environmental Sciences*. Report of EPA project no. CR811893.
- Journal, A. G. (1979). Geostatistical simulation: Methods for exploration and mine planning. *Engineering and Mining Journal*, 180(12):86-91.
- Journal, A. G. (1983a). Non-parametric estimation of spatial distributions. *Math. Geology*, 5(3):445-468.
- Journal, A. G. (1983b). The place of non-parametric geostatistics. In Verly, G., David, M., Journal, A. G., and Marechal, A., editors, *Geostatistics for Natural Resources Characterization*. Proceedings of the NATO Advanced Study Institute, South Lake Tahoe, California, September 6-17, D. Reidel, Dordrecht, Holland.
- Journal, A. G. (1985). Sequential simulation. Unpublished notes, Stanford University.
- Journal, A. G. (1986). Constrained interpolation and qualitative information, the soft kriging approach. *Math. Geology*, 18(1):119-140.
- Journal, A. G. (1989). Imaging of spatial uncertainty: A non-Gaussian approach. In Buxton, B., editor, *Geostatistical, Sensitivity, and Uncertainty Methods for Ground-Water Flow and Radionuclide Transport Modeling*. DOE/AECL, Batelle Press.
- Journal, A. G. and Alabert, F. G. (1988). Focusing on spatial connectivity of extreme-valued attributes: Stochastic indicator models of reservoir heterogeneities. *SPE* 18324.

- Journal, A. G. and Alabert, F. G. (1989). Non-Gaussian data expansion in the earth sciences. *Terra Nova*, 1(2):123–134.
- Journal, A. G. and Alabert, F. G. (1990). New method for reservoir mapping. *JPT*, pages 212–218.
- Journal, A. G., Deutsch, C. V., and Desbarats, A. J. (1986). Power averaging for block effective permeability. *SPE 15128*.
- Journal, A. G. and Gómez-Hernández, J. J. (1989a). Stochastic imaging of the Wilmington clastic sequence. *SPE 19857*.
- Journal, A. G. and Gómez-Hernández, J. J. (1989b). Topics in advanced geostatistics. Unpublished class notes.
- Journal, A. G. and Huijbregts, C. J. (1978). *Mining Geostatistics*. Academic Press, London.
- Journal, A. G. and Rossi, M. (1989). Do we need kriging with a trend? *Math. Geology*, 21(7).
- Kasap, E. and Lake, L. W. (1989). An analytical method to calculate the effective permeability tensor of a grid block and its application in an outcrop study. *SPE 18434*.
- King, P. R. (1987). The use of field theoretic methods for the study of flow in a heterogeneous porous medium. *J. Phys. A: Math. Gen.*, 20:3935–3947.
- King, P. R. (1988). The use of renormalization for calculating effective permeability. *Transport in Porous Media*, 4(1):37–58.
- Kirkpatrick, S. (1973). Percolation and conduction. *Reviews of Modern Physics*, 45(4):574–588.
- Kitanidis, P. K. (1990). Effective hydraulic conductivity for gradually varying flow. *Water Resources Research*, 26(6):1197–1208.

- Lasseter, T. J., Waggoner, J. R., and Lake, L. W. (1986). Reservoir heterogeneities and their influence on ultimate recovery. In Lake, L. W. and Carroll, H. B., editors, *Reservoir Characterization*, pages 545–559. Academic Press.
- Long, J. C. S., Remer, J. S., Wilson, C., and Witherspoon, P. A. (1982). Porous media equivalents for networks of discontinuous fractures. *Water Resour. Res.*, 18(3):645–658.
- Long, J. C. S. and Witherspoon, P. A. (1985). The relationship of the degree of interconnection to permeability in fracture networks. *J. Geophys. Res.*, 90(B4):3087–3098.
- Luenberger, D. L. (1969). *Optimization by Vector Space Methods*. Wiley and Sons, NY.
- Luster, G. (1985). *Raw Materials for Portland Cement: Applications of Conditional Simulation of Coregionalization*. PhD thesis, Stanford University.
- Mantoglou, A. (1987). Digital simulation of multivariate two and three-dimensional stochastic processes with a spectral turning bands method. *Math. Geology*, 19(2):129–149.
- Mantoglou, A. and Wilson, J. L. (1981). Simulation of random fields with the turning band method. Technical Report no. 264 of the Ralph M. Parsons Laboratory, Department of Civil Engineering, Massachusetts Institute of Technology.
- Mantoglou, A. and Wilson, J. L. (1982). The turning bands method for simulation of random fields using line generation by a spectral method. *Water Resources Research*, 18:1379–1394.
- Matern, B. (1960). Spatial variation. *Meddelanden Fran Statens Skogsforskningsinstitut, Stockholm*, 49(5):144.
- Matheron, G. (1967). *Éléments pour une Théorie des Milieux Poreux*. Mason et Cie.

- Matheron, G. (1973). The intrinsic random functions and their applications. *Adv. Appl. Probabilities*, 5:439–458.
- Matheron, G. (1984). L'émergence de la loi de Darcy. *Annales des Mines*, 5/6:11–16.
- McDonald, M. G. and Harbaugh, A. W. (1984). A modular three-dimensional finite-difference ground-water flow model. Open-file report 83-875, U.S. Geological Survey.
- Mizell, S. A., Gutjahr, A. L., and Gelhar, L. W. (1982). Stochastic analysis of spatial variability in two-dimensional steady groundwater flow assuming stationary and nonstationary heads. *Water Resources Research*, 18(4):845–860.
- Myers, D. E. (1989). To be or not to be ... stationary? That is the question. *Math. Geology*, 21(2):347–362.
- Naff, R. L. and Vecchia, A. V. (1986). Stochastic analysis of three-dimensional flow in a bounded domain. *Water Resources Research*, 22(5):645–704.
- Naff, R. L. and Vecchia, A. V. (1987). Depth-averaging effects on hydraulic head for media with stochastic hydraulic conductivity. *Water Resources Research*, 23(4):561.
- Papoulis, A. (1986). *Probability, Random Variables and Stochastic Processes*. McGraw-Hill, New York, 2nd edition.
- Poley, A. D. (1988). Effective permeability and dispersion in locally heterogeneous aquifers. *Water Resources Research*, 24(11):1921–1926.
- Press, W. H., Flannery, B. P., Teukolsky, S. A., and Vetterling, W. T. (1988). *Numerical recipes in C*. Cambridge University Press, Cambridge.
- Rubin, Y. and Dagan, G. (1987a). Stochastic identification of transmissivity and effective recharge in steady groundwater flow, 1, Theory. *Water Resources Research*, 23(7):1185–1191.

- Rubin, Y. and Dagan, G. (1987b). Stochastic identification of transmissivity and effective recharge in steady groundwater flow, 2, Case study. *Water Resources Research*, 23(7):1192-1200.
- Rubin, Y. and Dagan, G. (1988). Stochastic analysis of boundary effects on head spatial variability in heterogeneous aquifers, 1, Constant head boundary. *Water Resources Research*, 24(10):1689-1697.
- Rubin, Y. and Dagan, G. (1989). Stochastic analysis of boundaries effects on head spatial variability in heterogeneous aquifers, 2, Impervious boundary. *Water Resources Research*, 25(4):707-712.
- Rubin, Y. and Gómez-Hernández, J. J. (1990). A stochastic approach to the problem of upscaling of conductivity in disordered media, Theory and unconditional numerical simulations. *Water Resources Research*, 26(4):691-701.
- Rubin, Y., Gómez-Hernández, J. J., and Journel, A. G. (in press, 1991). Analysis of upscaling and effective properties in disordered media. In Lake, L. W. and Carroll, H. B., editors, *Reservoir Characterization II*.
- Sáez, A. E., Otero, C. J., and Rusinek, I. (1989). The effective homogeneous behavior of heterogeneous porous media. *Transport in Porous Media*, 4:213-238.
- Shinozuka, M. and Jan, C. M. (1972). Digital simulation of random processes and its applications. *Journal of Sound and Vibration*, 25(1):111-128.
- Smith, L. (1981). Spatial variability of flow parameters in a stratified sand. *Math. Geology*, 13(1):1-21.
- Smith, L. and Freeze, R. A. (1979a). Stochastic analysis of steady state groundwater flow in a bounded domain, 1, One-dimensional simulations. *Water Resources Research*, 15(3):521-528.
- Smith, L. and Freeze, R. A. (1979b). Stochastic analysis of steady state groundwater flow in a bounded domain, 2, Two-dimensional simulations. *Water Resources Research*, 15(6):1543-1559.

- Sudicky, E. A. (1986). A natural gradient experiment on solute transport in a sand aquifer: Spatial variability of hydraulic conductivity and its role in the dispersion process. *Water Resources Research*, 22(13):2069–2082.
- Sullivan, J. (1984). *Non-parametric Estimation of Spatial Distribution*. PhD thesis, Stanford University, Branner Earth Sciences Library.
- Thompson, A. F. B., Ababou, R., and Gelhar, L. W. (1989). Implementation of the three-dimensional turning bands random field generator. *Water Resources Research*, 25(10):2227–2244.
- Trescott, P. C., Pinder, G. F., and Larson, S. P. (1976). Finite-difference model for aquifer simulation in two dimensions with results of numerical experiments. In *Techniques of Water-Resources Investigations of the United States Geological Survey*. U.S. Gov. Printing Office.
- Vanmarcke, E. (1983). *Random Fields, Analysis and Synthesis*.
- Wagner, B. and Gorelick, S. M. (1989). Reliable aquifer remediation in the presence of spatially variable hydraulic conductivity: from data to design. *Water Resources Research*, 25(10):2211–2226.
- Warren, J. E. and Price, H. S. (1961). Flow in heterogeneous porous media. *Society of Petroleum Engineering Journal*, 1:153–169.
- White, C. D. (1987). *Representation of Heterogeneity for Numerical Reservoir Simulation*. PhD thesis, Stanford University, Branner Earth Sciences Library.
- White, C. D. and Horne, R. N. (1987). Computing absolute transmissibility in the presence of fine-scale heterogeneity. *SPE 16011*.